

General Disclaimer

One or more of the Following Statements may affect this Document

- This document has been reproduced from the best copy furnished by the organizational source. It is being released in the interest of making available as much information as possible.
- This document may contain data, which exceeds the sheet parameters. It was furnished in this condition by the organizational source and is the best copy available.
- This document may contain tone-on-tone or color graphs, charts and/or pictures, which have been reproduced in black and white.
- This document is paginated as submitted by the original source.
- Portions of this document are not fully legible due to the historical nature of some of the material. However, it is the best reproduction available from the original submission.



(NASA-CR-168057) WAVE PROPAGATION IN
GRAPHITE/EPOXY LAMINATES DUE TO IMPACT
Interim Report (Purdue Univ.) 171 p
HC A08/MF A01

N 83-22325

CSCL IID

Unclass

G3/24

03376

COMPOSITE MATERIALS LABORATORY



PURDUE UNIVERSITY
School of Aeronautics and Astronautics
West Lafayette, Indiana 47907

CML 82-5

NASA CR 168057

WAVE PROPAGATION IN GRAPHITE/EPOXY
LAMINATES DUE TO IMPACT

by

T.M. Tan and C.T. Sun

December, 1982

1. Report No. NASA CR-168057	2. Government Accession No.	3. Recipient's Catalog No.	
4. Title and Subtitle WAVE PROPAGATION IN GRAPHITE/EPOXY LAMINATES DUE TO IMPACT		5. Report Date December 1982	
		6. Performing Organization Code	
7. Author(s) T. M. Tan and C. T. Sun		8. Performing Organization Report No.	
9. Performing Organization Name and Address Purdue University School of Aeronautics and Astronautics West Lafayette, IN 47907		10. Work Unit No.	
		11. Contract or Grant No. NSG 3185	
12. Sponsoring Agency Name and Address National Aeronautics & Space Administration Washington, DC 20546		13. Type of Report and Period Covered Interim Report	
		14. Sponsoring Agency Code	
15. Supplementary Notes Project Monitor: C. C. Chamis, Structures & Mechanical Technologies Div. NASA Lewis Research Center, M.S. 49-6 21000 Brookpark Road Cleveland, OH 44135			
16. Abstract The low velocity impact response of graphite/epoxy laminates is investigated theoretically and experimentally. A 9-node isoparametric finite element in conjunction with an empirical contact law was used for the theoretical investigation. Flat laminates subjected to pendulum impact were used for the experimental investigation. Theoretical results are in good agreement with strain gage experimental data. The collective results of the investigation indicate that the theoretical procedure describes the impact response of the laminate up to about 150 in/sec. impact velocity.			
ORIGINAL PAGE IS OF POOR QUALITY			
17. Key Words (Suggested by Author(s)) Impact fiber composites, laminates contact law, finite element, stress waves		18. Distribution Statement Unclassified, Unlimited	
19. Security Classif. (of this report) Unclassified	20. Security Classif. (of this page) Unlimited	21. No. of Pages 130	22. Price*

* For sale by the National Technical Information Service, Springfield, Virginia 22161

ORIGINAL PAGE IS
OF POOR QUALITY

TABLE OF CONTENTS

	Page
TABLE OF CONTENTS	III
LIST OF TABLES	v
LIST OF FIGURES	vi
LIST OF SYMBOLS	ix
CHAPTER 1 - INTRODUCTION	1
CHAPTER 2 - STRESS WAVE IN A LAMINATED PLATE	5
2.1 Laminate Theory with Transverse shear effects	6
2.1.1 Lamina Constitutive Equations	6
2.1.2 Plate Strain-Displacement Relations	9
2.1.3 Stress-Resultants and Laminate Constitutive Equations	12
2.1.4 Plate Equations of Motion	16
2.2 Propagation of Harmonic Waves	18
2.3 Propagation of Wave Front	23
2.3.1 Kinematic Conditions of Compatibility on the Wave Front	25
2.3.2 Dynamical Conditions on the Wave Front	27
2.3.3 Propagation Velocity of the Wave Front	32
2.3.4 Wave Surface and Ray	35
CHAPTER 3 - STATICAL INDENTATION LAWS	48
3.1 Specimens and Experimental Procedure	52
3.2 Experimental Results	53
3.2.1 Loading Curves	53
3.2.2 Unloading Curves	57
3.2.3 Reloading Curves	71

3.3 Discussion	71
CHAPTER 4 - IMPACT EXPERIMENTS	80
4.1 Experimental Procedure	81
4.2 Calibration of Impact-Force Transducer	84
4.3 Finite Element Analysis	94
4.3.1 Plate Finite Element	94
4.3.2 Modeling of Projectile	97
4.4 Results and Discussion	100
CHAPTER 5 - SUMMARY AND CONCLUSION	113
LIST OF REFERENCES	116
APPENDIX: COMPUTER PROGRAM AND USER INSTRUCTIONS	119

LIST OF TABLES

Table	Page
3.1 Contact coefficient k of loading law $F = k\alpha^{1.6}$	60
4.1 Specifications for Model 200A05 Impact-Force Transducer.....	85

LIST OF FIGURES

Figure	Page
2.1 Lamina reference axes and laminate reference axes.....	8
2.2 Laminate displacement components for a cross-section perpendicular to the y-axis.....	10
2.3 Stress-resultants and geometry of a typical N-layer laminate.....	14
2.4 Dispersion curves for plane harmonic waves propagating in the 0° - 45° - and 90° - directions.....	22
2.5 Frequency curves for flexural waves propagating in the 0° - 45° - and 90° - directions.....	24
2.6 A deformed volume V divided by a travelling surface Ω	29
2.7 Normal velocities of in-plane wave fronts.....	36
2.8 Normal velocities of flexural wave fronts.....	37
2.9 Wave front positions at different times and rays for in-plane extensional mode.....	43
2.10 Wave front positions at different times and rays for in-plane shear mode.....	44
2.11 Wave front positions at different times and rays for bending mode.....	45
2.12 Wave front positions at different times and rays for twisting mode.....	46
3.1 Schematical diagram for the indentation test set-up.....	54
3.2 Loading curve of $[0^\circ/45^\circ/0^\circ/-45^\circ/0^\circ]_{2s}$ specimens with 0.5 inch indenter ($n=3/2$).....	55

3.3 Loading curve of $[90^\circ/45^\circ/90^\circ/-45^\circ/90^\circ]_{2s}$ specimens with 0.5 inch Indenter ($n=3/2$).....	56
3.4 Loading curve of $[0^\circ/45^\circ/0^\circ/-45^\circ/0^\circ]_{2s}$ specimens with 0.75 inch Indenter ($n=3/2$).....	58
3.5 Loading curve of $[90^\circ/45^\circ/90^\circ/-45^\circ/90^\circ]_{2s}$ specimens with 0.75 inch Indenter ($n=3/2$).....	59
3.6 Relation between permanent indentation and maximum indentation.....	61
3.7 Unloading curves of $[0^\circ/45^\circ/0^\circ/-45^\circ/0^\circ]_{2s}$ specimens with 0.5 inch Indenter ($q=2.2$).....	63
3.8 Unloading curves of $[90^\circ/45^\circ/90^\circ/-45^\circ/90^\circ]_{2s}$ specimens with 0.5 inch Indenter ($q=2.2$).....	64
3.9 Unloading curves of $[0^\circ/45^\circ/0^\circ/-45^\circ/0^\circ]_{2s}$ specimens with 0.75 inch Indenter ($q=1.8$).....	65
3.10 Unloading curves of $[90^\circ/45^\circ/90^\circ/-45^\circ/90^\circ]_{2s}$ specimens with 0.75 inch Indenter ($q=1.8$).....	66
3.11 Unloading curves of $[0^\circ/45^\circ/0^\circ/-45^\circ/0^\circ]_{2s}$ specimens with 0.5 inch Indenter ($q=2.5$).....	67
3.12 Unloading curves of $[90^\circ/45^\circ/90^\circ/-45^\circ/90^\circ]_{2s}$ specimens with 0.5 inch Indenter ($q=2.5$).....	68
3.13 Unloading curves of $[0^\circ/45^\circ/0^\circ/-45^\circ/0^\circ]_{2s}$ specimens with 0.75 inch Indenter ($q=2.0$).....	69
3.14 Unloading curves of $[90^\circ/45^\circ/90^\circ/-45^\circ/90^\circ]_{2s}$ specimens with 0.75 inch Indenter ($q=2.0$).....	70
3.15 Reloading curve of $[0^\circ/45^\circ/0^\circ/-45^\circ/0^\circ]_{2s}$ specimen with 0.5 inch Indenter ($p=1.5$).....	72
3.16 Reloading curve of $[90^\circ/45^\circ/90^\circ/-45^\circ/90^\circ]_{2s}$ specimen with 0.5 inch Indenter ($p=1.5$).....	73
3.17 Reloading curve of $[0^\circ/45^\circ/0^\circ/-45^\circ/0^\circ]_{2s}$ specimen with 0.75 inch Indenter ($p=1.5$).....	74
3.18 Reloading curve of $[90^\circ/45^\circ/90^\circ/-45^\circ/90^\circ]_{2s}$ specimen with 0.75 inch Indenter ($p=1.5$).....	75
3.19 Unloading rigidity s as function of maximum Indentation.....	78
4.1 Lamine dimension and strain gage locations.....	82

4.2 Graphical illustration of impact projectile.....	82
4.3 Schematical diagram for the impact experimental set-up.....	83
4.4 Experimental set-up for the calibration of Impact-force transducer.....	86
4.5 Typical output voltages from transducer and accelerometer.....	88
4.6 Relation between V_F and V_a	88
4.7 Assumed exponential impulsive loading and the response history at the midpoint of the rod.....	90
4.8 Accelerations of rod for assumed exponential impulsive loading.....	92
4.9 Assumed sine-function impulsive loading and the response history at the midpoint of the rod.....	93
4.10 9-node isoparametric plate element.....	95
4.11 Finite element mesh for laminated plate and projectile.....	101
4.12 Strain response history at gage No.1.....	103
4.13 Strain response history at gage No.2.....	104
4.14 Strain response history at gage No.3.....	105
4.15 Strain response history at gage No.4.....	106
4.16 Strain response history at gage No.5.....	107
4.17 Strain response history at gage No.6.....	108
4.18 Transducer response and contact force histories from experimental and finite element results.....	109
4.19 Transducer response histories from experimental and finite element results up to 800 microseconds.....	111
4.20 Deformed configurations of laminated plate after impact.....	112

LIST OF SYMBOLS

A	Cross-sectional area of the projectile
A_{ij} , B_{ij} , D_{ij}	Laminate stiffnesses
E_s	Young's modulus of the steel indenter
E_1	Young's modulus of laminar in the fiber direction
E_2	Young's modulus of laminar in the transverse direction
F	Contact force
F_m	Maximum contact force
G	Shear modulus
$[K_p]$, $[K_r]$	Stiffness matrices
$[M_p]$, $[M_r]$	Mass matrices
M	Stress couples of laminate
N	Stress resultants of laminate
$\{P_p\}$, $\{P_r\}$	Assembled global load vectors
Q	Transverse shear force of laminate
Q_{ij}	Reduced stiffnesses
\bar{Q}_{ij}	Transformed reduced stiffnesses
R_s	Radius of steel indenter
S_i	Shape functions of plate element
V_F	Output voltage of the force transducer
V_a	Output voltage of the accelerometer

a	Acceleration
c	Phase velocity
c_a	Sensitivity of the accelerometer
c_F	Sensitivity of the impact-force transducer
c_n	Normal velocity of wave front
f_i	Shape functions of rod element
[f]	Discontinuity of f across wave front surface
h	Laminate thickness
k	Wave number
k	Contact coefficient
k_1	Reloading rigidity
$[k_p], [k_r]$	Element stiffness matrices
$[m_p], [m_r]$	Element mass matrices
n	Power index of loading law
n_i	Unit normal on the wave front
p	Power index of reloading law
p_i	Slowness vector
$\{p_p\}_e, \{p_r\}_e$	Element load vectors
q	Power index of unloading law
$\{q_p\}, \{q_r\}$	Assembled global displacement vectors
$\{q_p\}_e, \{q_r\}_e$	Element displacement vectors
s	Unloading rigidity
t	Time
t^*	Non-dimensional time
u, v, w	Displacement components of laminate
u^0, v^0, w^0	Midplane displacement components

x, y, z	Laminate coordinate system
x_1, x_2, x_3	Laminar coordinate system
Ω	Wave front surface
α	Indentation depth
α_0	Permanent Indentation
α_m	Maximum Indentation
α_{cr}, α_p	Critical indentations
γ	Shearing strain
ϵ	Normal strain
K_x, K_y, K_{xy}	Rotation gradients
λ	Wave length
ν	Poisson's ratio
ν_s	Poisson's ratio of the steel indenter
ξ, η	Normalized local coordinates of plate element
ρ	Mass density of laminate
σ	Normal stress
τ	Shearing stress
ϕ_x, ϕ_y	Rotations of cross-sections of laminate
ω	Frequency

ORIGINAL PAGE IS
OF POOR QUALITY

CHAPTER 1

INTRODUCTION

Advanced fiber-reinforced composite materials such as boron/epoxy and graphite/epoxy have been successfully employed as structural materials in aircrafts, missiles and space vehicles in recent years, and the performance of these composites has shown their superiority over metals in applications requiring high strength, high stiffness as well as low weight. The advantages of these composites, however, are overshadowed by their relatively poor resistance to the impact loadings, which has prevented the application of these materials to turbine fan blades. Many other reports dealing with the responses of advanced composites to various types of impact have further increased the need for a better understanding of the problem so that the survivability of these composites can be improved.

It is obvious that impact produces damage and consequently reduces the strength of composite materials. The damage modes usually include local permanent deformations, breakage of fibers, delaminations, etc.. While the cause of these damages are still unknown and may not be simple in nature, in general, the impact of a soft object could give a longer contact duration, and the dynamic

ORIGINAL PAGE IS
OF POOR QUALITY

response of the whole structure is of importance. The hard object impact usually gives a short contact time and results in the initial transmission of impact energy into a local region of the structure. This initial energy will propagate into the rest of the structure in the form of stress waves. Far field damage away from the impact area could result from the reflection of stress waves. It is generally agreed that the cause of the sudden failure must be examined from the point of transient wave propagation phenomena.

Flexural waves induced by dynamic loads in laminated composites are more complicated than those in homogeneous and isotropic plates due to the anisotropic and nonhomogeneous properties in the laminate. Moreover, because of the low transverse shear modulus in fiber composites, the effect of transverse shear deformation becomes significant and should be considered in the formulation. In Chapter 2, the laminate theory which includes the transverse shear deformation effect is reviewed, and harmonic waves in a graphite/epoxy laminated plate are studied. The propagation of wave front which, for a given time after impact, bound the stressed region surrounding the impact point, is also investigated.

A survey of wave propagation and impact in composite materials has been given by Moon [1]. Many analytical [2-5], numerical [6-7] and experimental [8-10] methods have been employed to study the transient impact problems. The

response of a laminated plate can be analyzed using these methods provided the applied load history is prescribed. However if the dynamic load results from an impact of an object on the laminated plate, then the resulting contact force must be determined first. An accurate account of the contact behavior becomes the most important step in analyzing the impact response problems.

A classical contact law between two elastic spheres was derived by Hertz [11]. When letting the radius of one of the spheres go to infinity, one obtains the contact law between an elastic sphere and an elastic half-space. Many authors have used the Hertzian contact law for the study of impact on metals and composites [12-13]. Recently, Yang and Sun [14] performed statical indentation tests on graphite/epoxy composite laminates using spherical steel indenters of different sizes and found that the Hertzian law of contact was not adequate. In particular, they found that significant permanent indentations existed and that the unloading paths were very different from the loading path. Noting that energy dissipation takes place during the process of impact, Yang and Sun [14] suggested that this energy is responsible for the local damage of the target materials. The unloading curves and permanent indentations obtained from the statical indentation tests may provide a useful information in estimating the amount of damage due to impact since this energy is simply the area enclosed by the

loading-unloading curves. In this study, similar statical indentation tests were conducted and the results are presented in Chapter 3.

Wang [15] has performed a number of impact tests on graphite/epoxy laminated beams and plates. It was shown that the strain responses calculated using finite element method and the statically determined contact laws from [14] agreed with the experimental measurements quite well. This indicates that the statical indentation law is reasonably adequate in the dynamical impact analysis. It was also suggested that the contact force should be measured experimentally to provide an additional basis for comparison with the finite element solution which could allow further evaluation the applicability of the contact laws in impact analysis. Chapter 4 describes an impact experiment on graphite/epoxy laminated plate using an impact-force transducer with a spherical steel cap as the impactor. The contact force history and strain responses at various points on the plate were measured by means of the transducer and surface strain gages, respectively, and were compared with the predictions of finite element analysis using the statically determined contact law.

Chapter 5 summarizes the results obtained in Chapter 2, 3 and 4.

ORIGINAL PAGE IS
OF POOR QUALITY

ORIGINAL PAGE IS
OF POOR QUALITY

CHAPTER 2

STRESS WAVE IN A LAMINATED PLATE

A laminated plate theory which includes the effects of transverse shear deformation and rotatory inertia was developed by Yang, Norris and Stavsky [16] in a way suggested by Mindlin [17] for homogeneous isotropic plates. It was shown that the frequency curves for the propagation of harmonic waves in an infinite two-layer isotropic plate in plane strain agreed with the predictions of the exact solution obtained from theory of elasticity very well. A similar laminated plate theory was developed by Whitney and Pagano [18] and was employed in the study of static bending and vibration for antisymmetric angle-ply composite plates with particular layer properties. It was found that the effect of shear deformation can be quite significant for composite plates with span-to-depth ratio as high as 20. Good agreement was also observed in numerical results for plate bending as comparing with exact solutions of elasticity. In this study, the laminate theory developed by Whitney and Pagano was used for its simplicity yet quite satisfactory in describing the harmonic wave propagation [19].

2.1 Laminate Theory with Transverse Shear Effects

2.1.1 Lamina Constitutive Equations

A laminated plate of constant thickness h consists of a number of thin laminae of unidirectionally fiber-reinforced composite perfectly bonded together. Each lamina, whose fiber may orient in any arbitrary direction, can be regarded as a homogeneous orthotropic solid. Consider a typical k -th lamina. A coordinate system (x_1, x_2, x_3) is chosen in such a way that the x_1-x_2 plane coincides with the midplane of lamina, and x_1 and x_2 axes are parallel and perpendicular to the fiber direction, respectively. If a state of plane stress parallel to the x_1-x_2 plane is assumed, then the in-plane stress-strain relations are given by

$$\begin{Bmatrix} \sigma_{11} \\ \sigma_{22} \\ \tau_{12} \end{Bmatrix}^k = \begin{bmatrix} Q_{11} & Q_{12} & 0 \\ Q_{12} & Q_{22} & 0 \\ 0 & 0 & Q_{66} \end{bmatrix} \begin{Bmatrix} \epsilon_{11} \\ \epsilon_{22} \\ \gamma_{12} \end{Bmatrix}^k \quad (2-1)$$

The transverse shear stress-strain relations are given by

$$\begin{Bmatrix} \tau_{23} \\ \tau_{13} \end{Bmatrix}^k = \begin{bmatrix} Q_{44} & 0 \\ 0 & Q_{55} \end{bmatrix} \begin{Bmatrix} \gamma_{23} \\ \gamma_{13} \end{Bmatrix}^k \quad (2-2)$$

in which

$$\begin{aligned}
 Q_{11} &= E_1 / (1 - \nu_{12} \nu_{21}) & \text{ORIGINAL PAGE IS} \\
 Q_{22} &= E_2 / (1 - \nu_{12} \nu_{21}) & \text{OF POOR QUALITY} \\
 Q_{12} &= \nu_{12} E_2 / (1 - \nu_{12} \nu_{21}) = \nu_{21} E_1 / (1 - \nu_{12} \nu_{21}) \\
 Q_{66} &= G_{12} & (2-3) \\
 Q_{44} &= G_{23} \\
 Q_{55} &= G_{13}
 \end{aligned}$$

are the so-called reduced stiffnesses, where E , G and ν are Young's modulus, shear modulus and Poisson's ratio, respectively, and subscripts 1 and 2 denote the directions parallel to x_1 and x_2 axes, respectively.

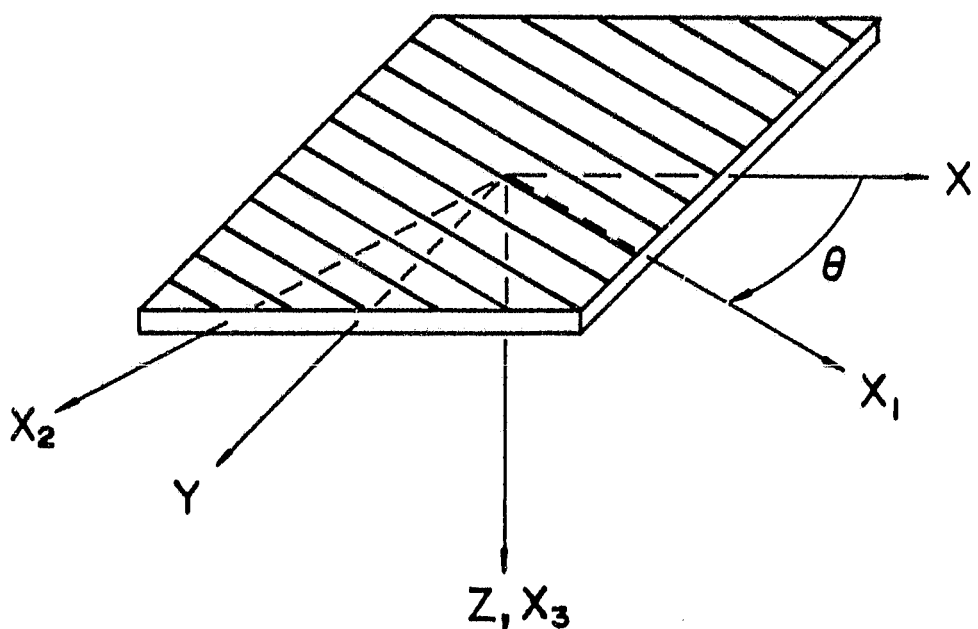
The coordinate system for an arbitrarily oriented lamina does not, in general, coincide with the reference axes (x, y, z) of laminated plate (see Figure 2.1). Using the coordinate transformation laws for stress and strain, we obtain the stress-strain relations in laminate reference system as

$$\begin{bmatrix} \sigma_{xx} \\ \sigma_{yy} \\ \tau_{xy} \\ \tau_{yz} \\ \tau_{xz} \end{bmatrix}^k = \begin{bmatrix} \bar{Q}_{11} & \bar{Q}_{12} & \bar{Q}_{16} & 0 & 0 \\ \bar{Q}_{12} & \bar{Q}_{22} & \bar{Q}_{26} & 0 & 0 \\ \bar{Q}_{16} & \bar{Q}_{26} & \bar{Q}_{66} & 0 & 0 \\ 0 & 0 & 0 & \bar{Q}_{44} & \bar{Q}_{45} \\ 0 & 0 & 0 & \bar{Q}_{45} & \bar{Q}_{55} \end{bmatrix} \begin{bmatrix} \epsilon_{xx} \\ \epsilon_{yy} \\ \gamma_{xy} \\ \gamma_{yz} \\ \gamma_{xz} \end{bmatrix}^k \quad (2-4)$$

in which \bar{Q}_{ij} are given by

$$\bar{Q}_{11} = Q_{11}m^4 + 2(Q_{12} + 2Q_{66})m^2n^2 + Q_{22}n^4$$

ORIGINAL PAGE VI
OF POOR QUALITY



(X_1, X_2, X_3) — Lamina Reference Axes

(X, Y, Z) — Laminate Reference Axes

Figure 2.1 Lamina reference axes and laminate reference axes

$$\begin{aligned}
 Q_{22} &= Q_{11}n^4 + 2(Q_{12} + 2Q_{66})m^2n^2 + Q_{22}m^4 \\
 Q_{12} &= (Q_{11} + Q_{22} - 4Q_{66})m^2n^2 + Q_{12}(m^4 + n^4) \\
 Q_{16} &= (Q_{11} - Q_{12} - 2Q_{66})m^3n + (Q_{12} - Q_{22} + 2Q_{66})mn^3 \\
 Q_{26} &= (Q_{11} - Q_{12} - 2Q_{66})mn^3 + (Q_{12} - Q_{22} + 2Q_{66})m^3n \\
 Q_{66} &= (Q_{11} + Q_{22} - 2Q_{12} - 2Q_{66})m^2n^2 + Q_{66}(m^4 + n^4) \\
 Q_{44} &= Q_{44}m^2 + Q_{55}n^2 \\
 Q_{45} &= (Q_{44} - Q_{55})mn \\
 Q_{55} &= Q_{44}n^2 + Q_{55}m^2
 \end{aligned} \tag{2-5}$$

where

$$m = \cos\theta \quad n = \sin\theta$$

and θ is the angle between x -axis and x_1 -axis measured from x to x_1 , counterclockwise as shown in Figure 2.1.

2.1.2 Plate Strain-Displacement Relations

The displacement components of the laminated plate are assumed to be of the form [16]

$$\begin{aligned}
 u(x, y, z) &= u^0(x, y) + z\phi_x(x, y) \\
 v(x, y, z) &= v^0(x, y) + z\phi_y(x, y) \\
 w(x, y, z) &= w^0(x, y) = w(x, y)
 \end{aligned} \tag{2-6}$$

where u^0 , v^0 and w^0 are the midplane displacement components in the x -, y - and z -directions, respectively, and ϕ_x and ϕ_y are rotations of cross-sections perpendicular to x - and y -axis, respectively (see Figure 2.2). In Equation (2.6) we

ORIGINAL PAGE IS
OF POOR QUALITY

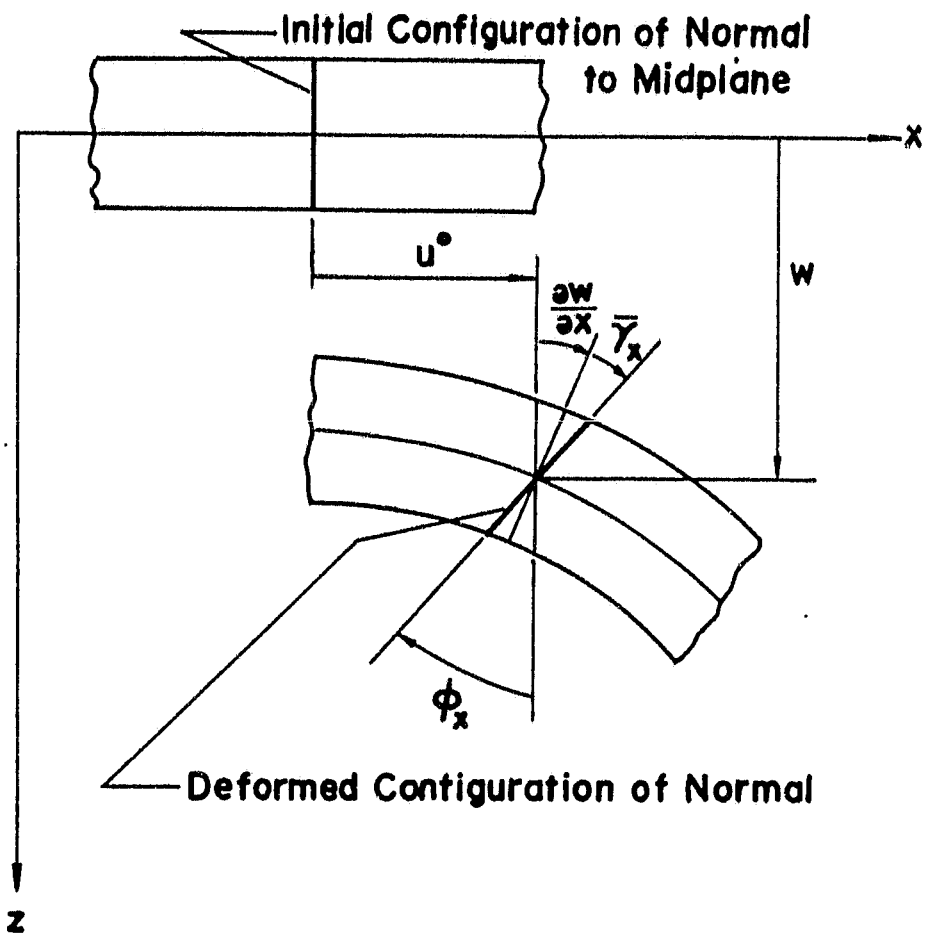


Figure 2.2 Laminate displacement components for a cross-section perpendicular to the y -axis

have assumed that u and v vary linearly in the thickness direction, while w is constant through the thickness.

The strain components for a point in k -th lamina of the laminated plate with a distance z from the midplane can be computed as

$$\begin{aligned}\epsilon_{xx}^k &= \epsilon_x^0 + zk_x \\ \epsilon_{yy}^k &= \epsilon_y^0 + zk_y \\ \gamma_{xy}^k &= \gamma_{xy}^0 + zk_{xy} \\ \gamma_{yz}^k &= \partial w / \partial y + \partial v / \partial z = \partial w / \partial y + \phi_y = \gamma_{yz}^0 \\ \gamma_{xz}^k &= \partial w / \partial x + \partial u / \partial z = \partial w / \partial x + \phi_x = \gamma_{xz}^0\end{aligned}\tag{2-7}$$

where

$$\begin{aligned}\gamma_x^0 &= \partial u^0 / \partial x \\ \gamma_y^0 &= \partial v^0 / \partial y \\ \gamma_{xy}^0 &= \partial u^0 / \partial y + \partial v^0 / \partial x\end{aligned}\tag{2-8}$$

are the in-plane strain components of midplane, and

$$\begin{aligned}\kappa_x &= \partial \phi_x / \partial x \\ \kappa_y &= \partial \phi_y / \partial x \\ \kappa_{xy} &= \partial \phi_x / \partial y + \partial \phi_y / \partial x\end{aligned}\tag{2-9}$$

are the rotation gradients.

In Equation (2-7), since w , ϕ_x and ϕ_y are independent of z , it follows that the transverse shear strains are constant through the thickness of the plate.

Equation (2-7) can be written in concise matrix form as

$$\begin{bmatrix} \epsilon \\ \gamma \end{bmatrix}^k = \begin{bmatrix} \epsilon_x \\ \epsilon_y \\ \gamma_{xy} \\ \gamma_{yz} \\ \gamma_{xz} \end{bmatrix} = \begin{bmatrix} \epsilon_x^0 \\ \epsilon_y^0 \\ \gamma_{xy}^0 \\ \gamma_{yz}^0 \\ \gamma_{xz}^0 \end{bmatrix} + z \begin{bmatrix} k_x \\ k_y \\ k_{xy} \\ 0 \\ 0 \end{bmatrix} = \begin{bmatrix} \epsilon \\ \gamma \end{bmatrix}^0 + z \begin{bmatrix} k \\ 0 \end{bmatrix} \quad (2-10)$$

Thus, the strain components at any point in the plate can be determined from the extensional strain components of the midplane, the rotation gradients of the plate and the distance z from the midplane.

2.1.3 Stress-Resultants and Laminate Constitutive Equations

Substitution of Equation (2-10) in Equation (2-4) gives the stress components for a point in the k -th lamina as:

$$\begin{bmatrix} \sigma_{xx} \\ \sigma_{yy} \\ \tau_{xy} \\ \tau_{yz} \\ \tau_{xz} \end{bmatrix}^k = \begin{bmatrix} Q_{11} & Q_{12} & Q_{16} & 0 & 0 \\ Q_{12} & Q_{22} & Q_{26} & 0 & 0 \\ Q_{16} & Q_{26} & Q_{66} & 0 & 0 \\ 0 & 0 & 0 & Q_{44} & Q_{45} \\ 0 & 0 & 0 & Q_{45} & Q_{55} \end{bmatrix} \begin{bmatrix} \epsilon_x^0 \\ \epsilon_y^0 \\ \gamma_{xy}^0 \\ \gamma_{yz}^0 \\ \gamma_{xz}^0 \end{bmatrix} + z \begin{bmatrix} k_x \\ k_y \\ k_{xy} \\ 0 \\ 0 \end{bmatrix} \quad (2-11)$$

The stress-resultants acting on a laminate can be obtained by integration of the stresses in each lamina through the laminate thickness. Specifically, the in-plane

ORIGINAL PAGE IS
OF POOR QUALITY

stress-resultants are given by

$$\begin{Bmatrix} N_x \\ N_y \\ N_{xy} \end{Bmatrix} = \int_{-h/2}^{h/2} \begin{Bmatrix} \sigma_{xx} \\ \sigma_{yy} \\ \gamma_{xy} \end{Bmatrix} dz = \sum_{k=1}^N \int_{h_{k-1}}^{h_k} \begin{Bmatrix} \sigma_{xx} \\ \sigma_{yy} \\ T_{xy} \end{Bmatrix} dz \quad (2-12)$$

the stress couples are given by

$$\begin{Bmatrix} M_x \\ M_y \\ M_{xy} \end{Bmatrix} = \int_{-h/2}^{h/2} \begin{Bmatrix} \sigma_{xx} \\ \sigma_{yy} \\ \gamma_{xy} \end{Bmatrix} zdz = \sum_{k=1}^N \int_{h_{k-1}}^{h_k} \begin{Bmatrix} \sigma_{xx} \\ \sigma_{yy} \\ T_{xy} \end{Bmatrix} zdz \quad (2-13)$$

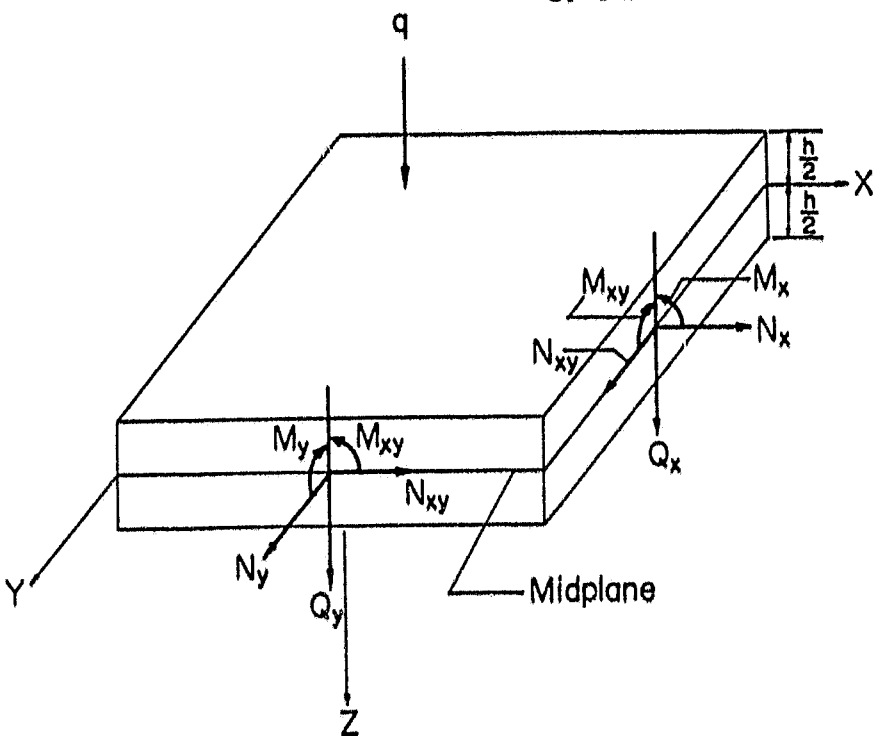
and the transverse shear forces are given by

$$\begin{Bmatrix} Q_y \\ Q_x \end{Bmatrix} = \int_{-h/2}^{h/2} \begin{Bmatrix} T_{yz} \\ T_{xz} \end{Bmatrix} dz = \sum_{k=1}^N \int_{h_{k-1}}^{h_k} \begin{Bmatrix} T_{yz} \\ T_{xz} \end{Bmatrix} dz \quad (2-14)$$

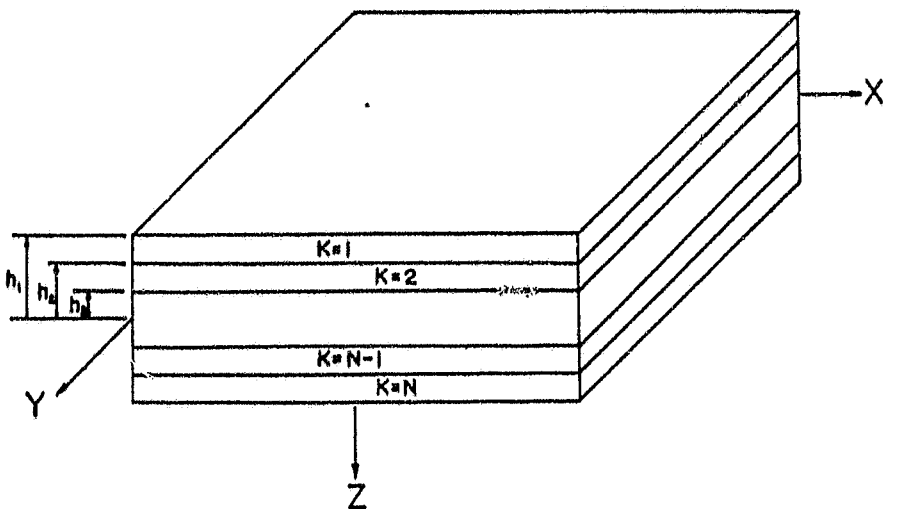
The sign convention for these stress-resultants along with the geometry of a typical N-layer laminated plate are shown in Figure 2.3.

Substituting Equation (2-11) into the right hand sides of the above three equations and performing the integrations, we obtain

ORIGINAL PAGE IS
OF POOR QUALITY



(a) STRESS RESULTANTS OF A LAMINATE



(b) GEOMETRY OF AN n -LAYER LAMINATE

Figure 2.3 Stress-resultants and geometry of a typical n -layer laminate

$$\begin{Bmatrix} N_x \\ N_y \\ N_{xy} \end{Bmatrix} = \begin{bmatrix} A_{11} & A_{12} & A_{16} \\ A_{12} & A_{22} & A_{26} \\ A_{16} & A_{26} & A_{66} \end{bmatrix} \begin{Bmatrix} \epsilon_x^0 \\ \epsilon_y^0 \\ \gamma_{xy}^0 \end{Bmatrix} + \begin{bmatrix} B_{11} & B_{12} & B_{16} \\ B_{12} & B_{22} & B_{26} \\ B_{16} & B_{26} & B_{66} \end{bmatrix} \begin{Bmatrix} K_x \\ K_y \\ K_{xy} \end{Bmatrix} \quad (2-15)$$

$$\begin{Bmatrix} M_x \\ M_y \\ M_{xy} \end{Bmatrix} = \begin{bmatrix} B_{11} & B_{12} & B_{16} \\ B_{12} & B_{22} & B_{26} \\ B_{16} & B_{26} & B_{66} \end{bmatrix} \begin{Bmatrix} \epsilon_x^0 \\ \epsilon_y^0 \\ \gamma_{xy}^0 \end{Bmatrix} + \begin{bmatrix} D_{11} & D_{12} & D_{16} \\ D_{12} & D_{22} & D_{26} \\ D_{16} & D_{26} & D_{66} \end{bmatrix} \begin{Bmatrix} K_x \\ K_y \\ K_{xy} \end{Bmatrix} \quad (2-16)$$

$$\begin{Bmatrix} Q_y \\ Q_x \end{Bmatrix} = \begin{bmatrix} A^{*44} & A^{*45} \\ A^{*45} & A^{*55} \end{bmatrix} \begin{Bmatrix} \gamma_{yz} \\ \gamma_{xz} \end{Bmatrix} \quad (2-17)$$

where

$$(A_{ij}, B_{ij}, D_{ij}) = \int_{-h/2}^{h/2} \bar{Q}_{ij}(1, z, z^2) dz \quad i, j = 1, 2, \dots \quad (2-18)$$

and

$$A^{*ij} = \int_{-h/2}^{h/2} \bar{Q}_{ij} dz \quad i, j = 4, 5 \quad (2-19)$$

Equations (2-15) through (2-17) are usually written symbolically as

$$\begin{Bmatrix} N \\ M \\ Q \end{Bmatrix} = \begin{bmatrix} A & B & 0 \\ B & D & 0 \\ 0 & 0 & A^* \end{bmatrix} \begin{Bmatrix} \epsilon^0 \\ \kappa \\ \gamma \end{Bmatrix} \quad (2-20)$$

which is the laminate constitutive equation with transverse shear effect included.

ORIGINAL PAGE IS
OF POOR QUALITY

2.1.4 Plate Equations of Motion

The stress-equations of motion for the k-th lamina are given by

$$\begin{aligned}\sigma_{xx,x} + \tau_{xy,y} + \tau_{xz,z} &= \rho\ddot{u} \\ \tau_{xy,x} + \sigma_{yy,y} + \tau_{yz,z} &= \rho\ddot{v} \\ \tau_{xz,x} + \tau_{yz,y} + \sigma_{zz,z} &= \rho\ddot{w}\end{aligned}\quad (2-21)$$

where ρ is the mass density. Integrating Equation (2-21) through the thickness of laminate and then substituting Equation (2-12), (2-14) and (2-6) in, we obtain

$$\begin{aligned}N_{x,x} + N_{xy,y} &= P\ddot{u}^0 + R\ddot{\phi}_x \\ N_{xy,x} + N_{y,y} &= P\ddot{v}^0 + R\ddot{\phi}_y \\ Q_{x,x} + Q_{y,y} + q &= P\ddot{w}\end{aligned}\quad (2-22)$$

where q is the normal traction on the plate. Multiplying the first two equations of Equation (2-21), integrating through the thickness of laminate and then substituting Equations (2-13), (2-14) and (2-5) in, we obtain

$$\begin{aligned}M_{x,x} + M_{xy,y} - Q_x &= R\ddot{u}^0 + I\ddot{\phi}_x \\ M_{xy,x} + M_{y,y} - Q_y &= R\ddot{v}^0 + I\ddot{\phi}_y\end{aligned}\quad (2-23)$$

in which P , R and I are defined as

$$(P, R, I) = \int_{-h/2}^{h/2} \rho(1, z, z^2) dz \quad (2-24)$$

Equations (2-22) and (2-23) are the plate equations of

motion. Substitution of Equation (2-20) and then the strain-displacement relations in these two equations yield the equations of motion in terms of midplane displacements and rotations of the plate.

A graphite/epoxy laminated plate provided by NASA Lewis Research Center was used throughout this study. This laminate is a $[0^\circ/45^\circ/0^\circ/-45^\circ/0^\circ]_{2s}$ graphite/epoxy composite with 0.0053 inch ply thickness and the following ply properties [15]:

$$E_1 = 17.5 \times 10^6 \text{ psi}.$$

$$E_2 = 1.15 \times 10^6 \text{ psi}.$$

$$G_{12} = G_{13} = G_{23} = 0.8 \times 10^6 \text{ psi}. \quad (2-25)$$

$$\nu_{12} = 0.30$$

$$\rho = 0.000148 \text{ lb-sec}^2/\text{in}^4$$

For symmetrically laminated composite plate, $B_{ij} = 0$ and $R = 0$. In addition, by choosing the x-axis of the laminate reference system to coincide with the 0° fiber direction, we obtain $A_{16} = A_{26} = 0$ and $D_{16} = D_{26}$. Further, in this study, we assume $G_{13} = G_{23} = G_{12}$, and consequently, $A^{*45} = 0$ and $A^{*44} = A^{*55}$. For this particular laminate, the displacement-equations of motion are given by

$$A_{11}\partial^2 u^0/\partial x^2 + A_{66}\partial^2 u^0/\partial y^2 + (A_{12} + A_{66})\partial^2 v^0/\partial x\partial y = P\ddot{u}^0$$

$$(A_{12} + A_{66})\partial^2 u^0/\partial x\partial y + A_{66}\partial^2 v^0/\partial x^2 + A_{22}\partial^2 v^0/\partial y^2 = P\ddot{v}^0$$

$$\begin{aligned}
 & D_{11} \frac{\partial^2 \phi_x}{\partial x^2} + 2D_{16} \frac{\partial^2 \phi_x}{\partial x \partial y} + D_{66} \frac{\partial^2 \phi_x}{\partial y^2} \\
 & + D_{16} (\frac{\partial^2 \phi_y}{\partial x^2} + \frac{\partial^2 \phi_y}{\partial y^2}) + (D_{12} + D_{66}) \frac{\partial^2 \phi_y}{\partial x \partial y} \\
 & - A^*_{44} (\partial w / \partial x + \phi_x) = I \ddot{\phi}_x
 \end{aligned} \tag{2-26}$$

$$\begin{aligned}
 & D_{16} (\frac{\partial^2 \phi_x}{\partial x^2} + \frac{\partial^2 \phi_x}{\partial y^2}) + (D_{12} + D_{66}) \frac{\partial^2 \phi_x}{\partial x \partial y} \\
 & + D_{66} \frac{\partial^2 \phi_y}{\partial x^2} + 2D_{16} \frac{\partial^2 \phi_y}{\partial x \partial y} + D_{22} \frac{\partial^2 \phi_y}{\partial y^2} \\
 & - A^*_{44} (\partial w / \partial y + \phi_y) = I \ddot{\phi}_y
 \end{aligned}$$

$$A^*_{44} (\frac{\partial^2 w}{\partial x^2} + \frac{\partial^2 w}{\partial y^2} + \partial \phi_x / \partial x + \partial \phi_y / \partial y) + q = p \ddot{w}$$

In Equation (2-26), the first two equations govern the in-plane motion while the last three equations govern the flexural motion.

2.2 Propagation of Harmonic Waves

Consider a infinitely large laminated plate governed by the equations of motion (2-26). We assume plane harmonic waves in the form

$$\begin{aligned}
 u^0 &= U \exp[ik(\eta - ct)] \\
 v^0 &= V \exp[ik(\eta - ct)] \\
 w &= W \exp[ik(\eta - ct)] \\
 \phi_x &= \Phi_x \exp[ik(\eta - ct)] \\
 \phi_y &= \Phi_y \exp[ik(\eta - ct)]
 \end{aligned} \tag{2-27}$$

propagating over the plate, where U , V , W , Φ_x and Φ_y are constant amplitudes, k is the wave number, c is the phase

velocity and η is given by

$$\eta = x \cos\alpha + y \sin\alpha$$

ORIGINAL PAGE IS
OF POOR QUALITY

(2-28)

In which α is the angle between the direction of wave propagation and x-axis.

Substitution of Equation (2-27) into Equation (2-26) with $q = 0$ yields a system of five homogeneous equations for the five constant amplitudes. In order to have a nontrivial solution, the determinant of the coefficient matrix is set equal to zero. Since the equations are uncoupled into two groups, the determinantal equation can be separated into two equations as

$$|a_{1j}| = 0 \quad (2-29)$$

for the in-plane extensional and in-plane shear waves, and

$$|b_{1j}| = 0 \quad (2-30)$$

for the flexural waves. In Equations (2-29) and (2-30) the coefficients a_{1j} and b_{1j} are given by

$$\begin{aligned} a_{11} &= A_{11}\cos^2\alpha + A_{66}\sin^2\alpha - P\omega^2 \\ a_{12} &= a_{21} = (A_{12} + A_{66})\sin\alpha\cos\alpha \\ a_{22} &= A_{66}\cos^2\alpha + A_{22}\sin^2\alpha - P\omega^2 \end{aligned} \quad (2-31)$$

and

$$\begin{aligned} b_{11} &= D_{11}k^2\cos^2\alpha + 2D_{16}k^2\sin\alpha\cos\alpha + D_{66}k^2\sin^2\alpha \\ &\quad + A_{44}^* - Ik^2\omega^2 \end{aligned}$$

$$b_{12} = b_{21} = D_{16}k^2\cos^2\alpha + (D_{12} + D_{66})k^2\sin\alpha\cos\alpha + D_{16}k^2\sin^2\alpha$$

$$b_{18} = b_{81} = IA^{*}_{44}k\cos\alpha \quad (2-32)$$

$$b_{22} = D_{66}k^2\cos^2\alpha + 2D_{16}k^2\sin\alpha\cos\alpha + D_{22}k^2\sin^2\alpha + A^{*}_{44} - Ik^2c^2$$

$$b_{28} = b_{82} = IA^{*}_{44}k\sin\alpha$$

$$b_{88} = -A^{*}_{44}k^2 + Pk^2c^2$$

Expanding Equation (2-29) we obtain a quadratic equation in c^2 as

$$c^4 - d_1c^2 + d_2 = 0 \quad (2-33)$$

where

$$d_1 = (A_{11}\cos^2\alpha + A_{22}\sin^2\alpha + A_{66})/P \quad (2-34)$$

$$d_2 = \begin{vmatrix} A_{11}\cos^2\alpha + A_{66}\sin^2\alpha & (A_{12} + A_{66})\sin\alpha\cos\alpha \\ (A_{12} + A_{66})\sin\alpha\cos\alpha & A_{66}\cos^2\alpha + A_{22}\sin^2\alpha \end{vmatrix}$$

It is noted that the phase velocity c does not depend on the wave number k , thus these waves are nondispersive. In studying of transverse impact problem where in-plane deformation is negligible, this nondispersive property has no significant effect. Should in-plane deformation become important, higher order approximation of displacement

components u and v must be assumed and the dispersive property of these in-plane waves could be included.

From Equation (2-34) it is evident that there exist two phase velocities corresponding to two modes of wave. Although these two waves involve both in-plane extensional deformation as well as in-plane shear, from the eigenvectors we are able to tell which one is dominant. Thus we label the two waves as in-plane extensional wave and in-plane shear wave accordingly.

The determinantal equation given by Equation (2-30) yields three positive roots in c^2 indicating that three flexural waves exist. These phase velocities are functions of the wave number k , thus they are dispersive. Among these three modes of wave, only the lowest one corresponding to the transverse shear wave has a finite velocity as $k \rightarrow 0$ or as the wave length becomes infinite. The dispersion curves for the waves of the lowest mode propagating in the directions of 0° , 45° and 90° respectively are plotted in Figure 2.4 with the non-dimensional phase velocity vs. the non-dimensional wavelength λ/h . It can be seen that they all approach the value of $\sqrt{G_{1s}/\rho}$ as the wavelength becomes shorter. The phase velocities for the two higher modes, however, approach different values in different propagation directions when $\lambda \rightarrow 0$. For laminated composite which are anisotropic in general, the phase velocity varies from one direction to another. As a result the wave surface will

ORIGINAL PAGE IS
OF POOR QUALITY

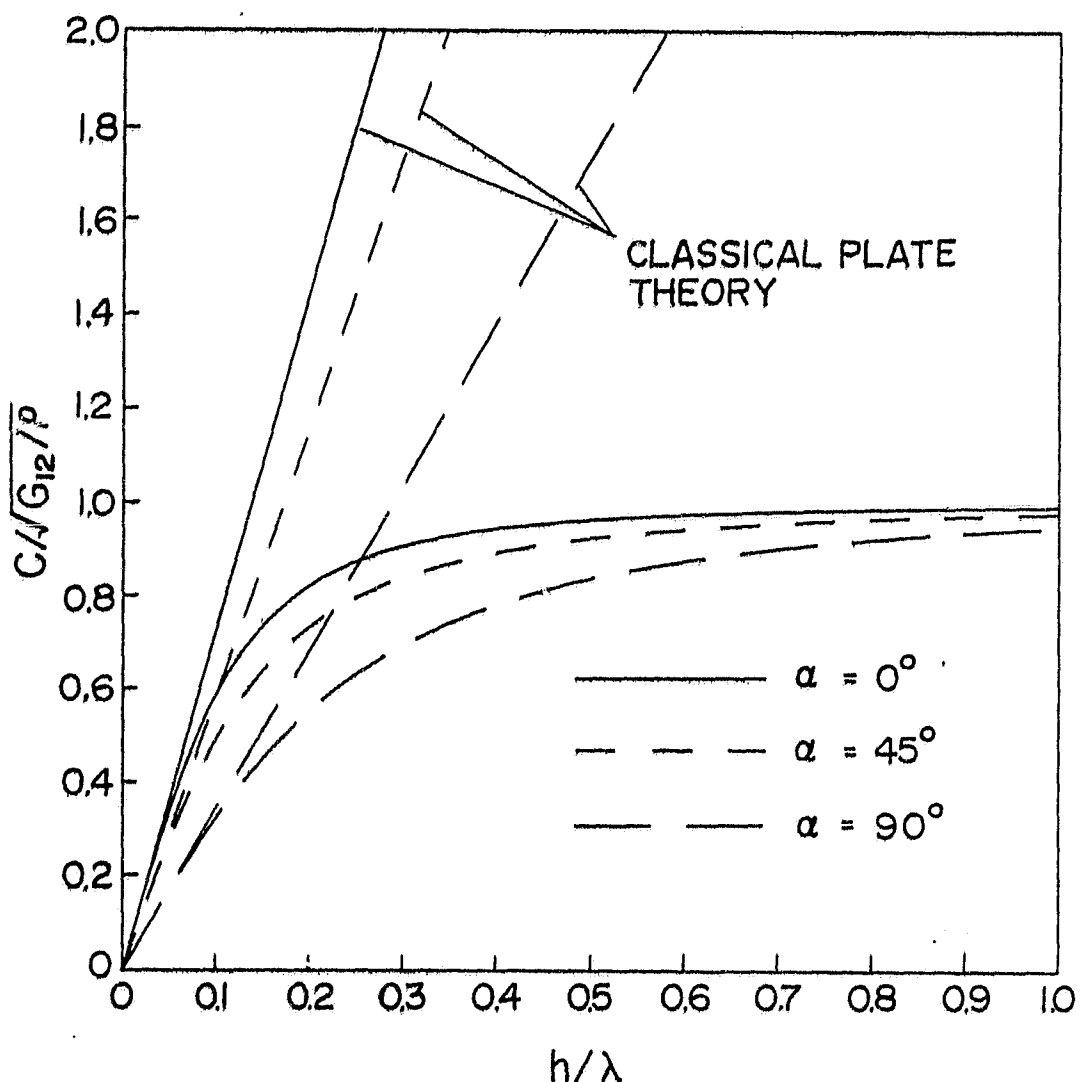


Figure 2.4 Dispersion curves for plane harmonic waves propagating in the 0° - 45° - and 90° - directions

become a rather complicated shape as it propagates. This will be discussed in the next section.

Substitution of $\omega = kc$ in Equation (2-32) yields a set of frequency equations for flexural waves. Figure 2.5 shows the frequency curves of these waves for $\alpha = 0^\circ$, 45° and 90° , respectively, with the non-dimensional frequency vs. the non-dimensional wavelength. The cutoff frequencies for the two higher modes have a value of $\sqrt{12G_{13}/\rho/h}$. Comparing with the exact cutoff frequency $(\pi/h)\sqrt{G_{13}/\rho}$, it can be seen that if the shear correction factor $\pi^2/12$ is introduced, this theory will predict the correct cutoff frequency.

2.3 Propagation of Wave Front

Impact of foreign objects on a laminated plate with a very short duration could generate weak shock waves which will propagate into the rest of the structure with finite velocities, and the positions of the wave fronts define the regions being disturbed at any instant after impact. Damages to the laminated plate may possibly occur as the first wave front hits the weakest part. It is hence important to investigate the propagation of these shocks in the plate. There have been works dealing with the propagation of wave front in anisotropic elastic media [20-22]. Moon [23] presented an analysis of wave surfaces in a laminate by treating it as an equivalent homogeneous

ORIGINAL PAGE IS
OF POOR QUALITY

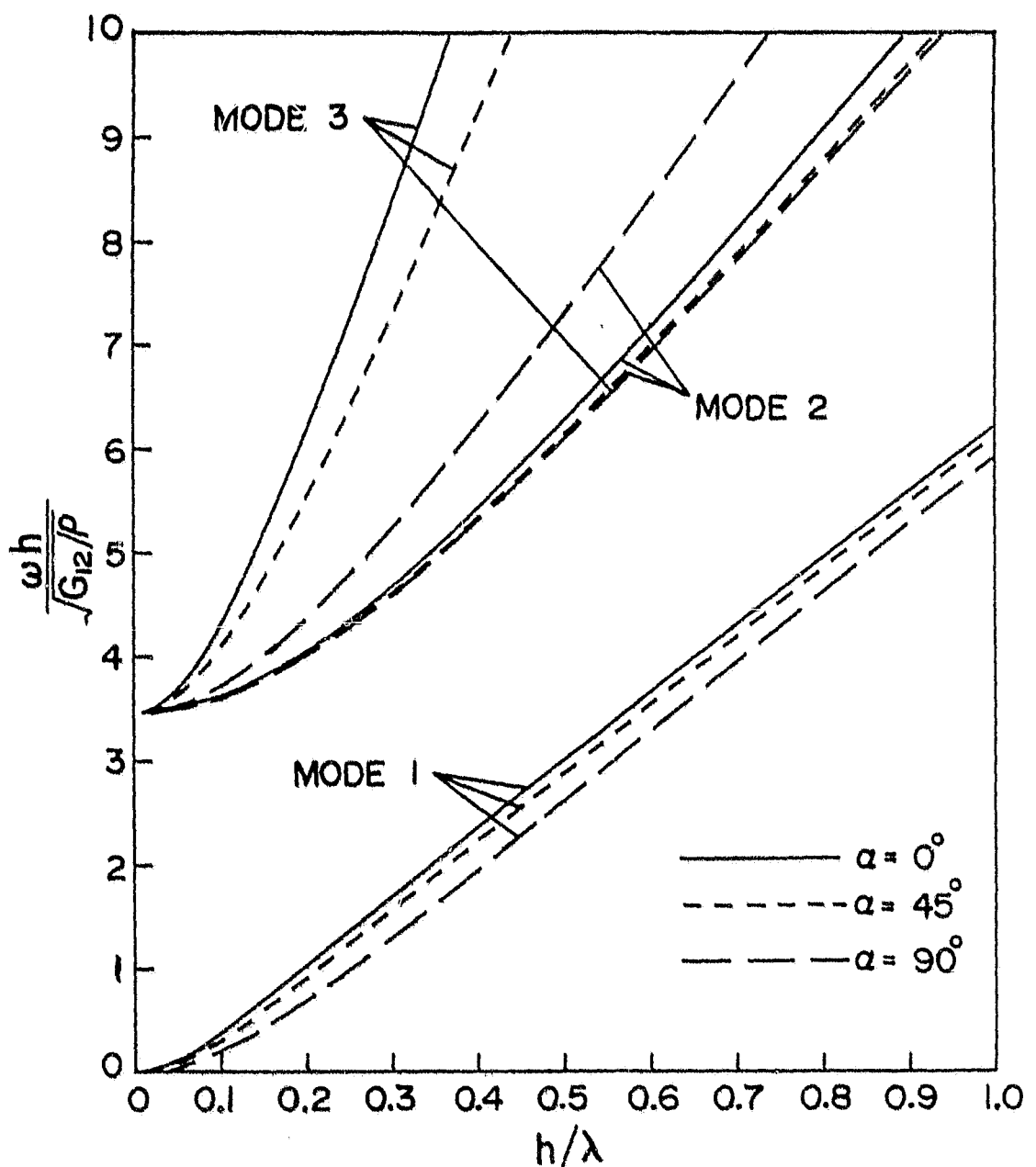


Figure 2.5 Frequency curves for flexural waves propagating in the 0° - 45° - and 90° - directions

orthotropic plate. The acceleration waves and their wave fronts were investigated. The propagation of shock waves in more general laminates which exhibit the bending-extensional coupling were studied by Sun [2]. The ray theory was employed to construct the wave front surface. The growth and decay of the shock strength were also discussed. In this section, the analytical procedures developed by Sun [2] were applied on a $[0^\circ/45^\circ/0^\circ/-45^\circ/0^\circ]_{2s}$ graphite/epoxy laminated plate.

2.3.1. Kinematic Conditions of Compatibility on the Wave Front

A wave front, which will be denoted by Ω , is defined as a surface travelling over the plate as time varies continuously, and across which there may exist a discontinuity in the stress, particle velocity and their derivatives.

Consider a discontinuous surface Ω passing some observation point in a medium at a certain time t . Let f^- be the value of a field function $f(x_i, t)$ (e.g. stress, particle velocity, etc.) behind the surface Ω , and f^+ be the value of f in front of it, then the discontinuity of function f can be expressed as

$$[f] = f^+ - f^- \quad (2-35)$$

In which the right hand side is to be evaluated at the time and location on Ω passing the observation point, and the jump across the wave front is denoted by square bracket.

Surface Ω may be expressed mathematically by an equation of the form

$$\Psi(x_1, t) = 0 \quad (2-36)$$

or, by making t explicit, as

$$\Psi(x_1, t) = F(x_1) - t = 0 \quad (2-37)$$

which represents a family of surfaces in x_1 -space with t as a parameter. By evaluating f^+ and f^- at $t = F(x_1)$, the jump of f across the wave front becomes

$$[f(x_1)] = f^+(x_1, F(x_1)) - f^-(x_1, F(x_1)) \quad (2-38)$$

The rate of change of $[f]$ for an observer moving with Ω is given by

$$\begin{aligned} d[f]/dt &= (\partial f^+/\partial x_1 - \partial f^-/\partial x_1) dx_1/dt + (\partial f^+/\partial t - \partial f^-/\partial t) \\ &= c_1 [\partial f/\partial x_1] + [\partial f/\partial t] \end{aligned} \quad (2-39)$$

where $t = F(x_1)$ is substituted, and $c_1 = dx_1/dt$ are velocity components of wave front relative to the material.

If the laminate theory introduced in previous section is used, then the plate displacement components are u^0 , v^0 , w , ϕ_x and ϕ_y , while the spatial variables are $x_1 = x$ and $x_2 = y$. It is assumed that the integrity of the material is not

affected by the propagation of the stress wave front, then these displacement components will remain continuous. Consequently, we have

$$[u^0] = [v^0] = [w] = [\phi_x] = [\phi_y] = 0 \quad (2-40)$$

across the wave front. Applying the general condition of Equation (2-39) on u^0 , together with Equation (2-40), we obtain

$$[\partial u^0 / \partial x_j] c_j + [\dot{u}^0] = 0 \quad j = 1, 2 \quad (2-41)$$

Let c_n and n_j be the normal velocity and the unit normal on the wave front, respectively, it follows that

$$n_j c_j = c_n \quad (2-42)$$

and Equation (2-41) becomes

$$[\partial u^0 / \partial x_j] = -[\dot{u}^0] n_j / c_n \quad j = 1, 2 \quad (2-43)$$

Similar relations can be derived for the other displacement components v^0 , w , ϕ_x and ϕ_y . Together they specify the kinematic conditions of compatibility on the wave front.

2.3.2 Dynamical Conditions on the Wave Front

Consider a finite volume V of a material medium and denoted by S the boundary or surface of V . For a continuous and differentiable function $f(x_i, t)$ in V , it can be shown

ORIGINAL PAGE IS
OF POOR QUALITY

[23] that

$$\frac{d}{dt} \int_V f(x_1, t) dV = \int_V f_{,t} dV + \int_S G f dS \quad (2-44)$$

under deformation of the medium, where G is the normal velocity of the surface S . In the case where the deformation of the volume V is determined solely by the motion of material particles, we have

$$G = \dot{u}_1 n_1 = \dot{u}_n \quad (2-45)$$

where u_1 is the displacement components, n_1 is the outward normal on S , and \dot{u}_n is the normal velocity of material particle on S . If there exists a discontinuity surface (or wave front) travelling with velocity c_1 in the medium, by choosing this surface as the boundary of V , we have

$$G = c_1 n_1 = c_n \quad (2-46)$$

where c_n is the normal velocity of wave front.

Suppose that a volume V whose motion is determined by the deformation of the material medium, is divided by a travelling surface Ω into two volumes V^- and V^+ as shown in Figure 2.6. The surface S is also divided into two portions S^- and S^+ which form parts of the boundaries of V^- and V^+ , respectively. The remaining part of the boundary is formed by Ω_0 which is a segment of Ω . In Figure 2.6, n_1 denotes the unit normal of Ω in the direction of travelling, and n_1^* denotes the unit outward normal of S .

ORIGINAL PAGE IS
OF POOR QUALITY

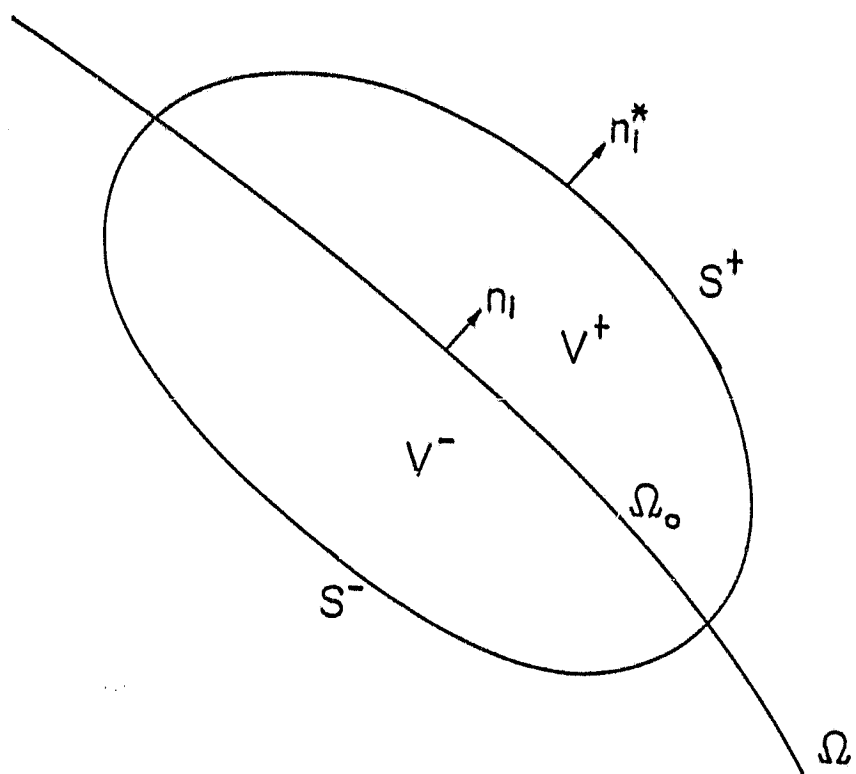


Figure 2.6 A deformed volume V divided by a travelling surface Ω

Taking $f = \rho \dot{u}$, in Equation (2-44) and using equation (2-45) and (2-46), we obtain

$$\frac{d}{dt} \int_V \rho \dot{u}_i dV = \int_V (\rho \dot{u}_i)_t dV + \int_{\partial V^-} \dot{u}_n \rho \dot{u}_i ds + \int_{\partial V^+} c_n \rho \dot{u}_i d\Omega \quad (2-47)$$

$$\frac{d}{dt} \int_V \rho \dot{u}_i dV = \int_V (\rho \dot{u}_i)_t dV + \int_{\partial V^+} \dot{u}_n \rho \dot{u}_i ds - \int_{\partial V^-} c_n \rho \dot{u}_i d\Omega \quad (2-48)$$

where \dot{u}_i and \dot{u}_i^+ are the velocity components of material particle in V^- and V^+ , respectively. Combining the above two equations gives

$$\begin{aligned} \frac{d}{dt} \int_V \rho \dot{u}_i dV &= \int_V (\rho \dot{u}_i)_t dV + \int_{\partial V^-} \dot{u}_n \rho \dot{u}_i ds + \int_{\partial V^+} \dot{u}_n \rho \dot{u}_i ds \\ &\quad + \int_{\partial V^-} c_n \rho (\dot{u}_i - \dot{u}_i^+) d\Omega \end{aligned} \quad (2-49)$$

From theory of elasticity we have

$$\frac{d}{dt} \int_V \rho \dot{u}_i dV = \int_{\partial V} \sigma_{ij} n_j ds \quad (2-50)$$

If we let the volume V approach zero at a fixed time in such a way that it will pass into Ω_0 , then the volume integral in Equation (2-49) will evidently approach zero; however

$$\int_{\partial V^+} \dot{u}_n \rho \dot{u}_i ds \rightarrow - \int_{\partial \Omega_0} \dot{u}_n \rho \dot{u}_i d\Omega \quad (2-51)$$

ORIGINAL PAGE IS
OF POOR QUALITY

$$\int_{\Omega_0^-} \dot{u}_n \rho \dot{u}_i ds = \int_{\Omega_0^+} \dot{u}_n \rho \dot{u}_i d\Omega \quad (2-52)$$

$$\int_{\Omega_0^-} \sigma_{ij} n_j ds = \int_{\Omega_0^+} (\sigma_{ij}^+ - \sigma_{ij}^-) n_j d\Omega \quad (2-53)$$

where σ_{ij}^+ and σ_{ij}^- are the stress components on the sides of Ω_0 , respectively.

Substituting Equations (2-50) through (2-53) into Equation (2-49) gives

$$\int_{\Omega_0^+} (\sigma_{ij}^+ - \sigma_{ij}^-) n_j d\Omega = \int_{\Omega_0^-} \rho \dot{u}_i (c_n - \dot{u}_n^-) d\Omega - \int_{\Omega_0^+} \rho \dot{u}_i^+ (c_n - \dot{u}_n^+) d\Omega \quad (2-54)$$

Using $[\sigma_{ij}]$ and $[\dot{u}_i]$ to represent the jumps of stress and particle velocity across the wave front, and utilizing the fact that $c_n \gg \dot{u}_n$, we obtain

$$\int_{\Omega_0^+} [\sigma_{ij}] n_j d\Omega = - \int_{\Omega_0^-} \rho c_n [\dot{u}_i] d\Omega \quad (2-55)$$

Since this condition is independent of the extent of the surface integration Ω_0 , it follows that

$$[\sigma_{ij}] n_j = - \rho c_n [\dot{u}_i] \quad (2-56)$$

In the case of laminated plate, $i = x, y, z$ and $j = x, y$.

Substitution of Equation (2-6) into Equation (2-56) yields

$$\begin{aligned} [\sigma_{1J}]n_J &= -\rho c_n \{ [\dot{u}^0] + z[\dot{\phi}_x] \} && \text{ORIGINAL PAGE IS} \\ & & & \text{OF POOR QUALITY} \\ [\sigma_{2J}]n_J &= -\rho c_n \{ [\dot{v}^0] + z[\dot{\phi}_y] \} && (2-57) \\ [\sigma_{3J}]n_J &= -\rho c_n [\dot{w}] \end{aligned}$$

Integrating Equation (2-57) over the thickness of plate gives

$$\begin{aligned} [N_x]n_x + [N_{xy}]n_y &= -Pc_n [\dot{u}^0] - Rc_n [\dot{\phi}_x] \\ [N_{xy}]n_x + [N_y]n_y &= -Pc_n [\dot{v}^0] - Rc_n [\dot{\phi}_y] \\ [Q_x]n_x + [Q_y]n_y &= -Pc_n [\dot{w}] \end{aligned} \quad (2-58)$$

Multiplying the first two equations of Equation (2-57) by z and then integrating over the thickness, we obtain two more equations

$$\begin{aligned} [M_x]n_x + [M_{xy}]n_y &= -Rc_n [\dot{u}^0] - Ic_n [\dot{\phi}_x] \\ [M_{xy}]n_x + [M_y]n_y &= -Rc_n [\dot{v}^0] - Ic_n [\dot{\phi}_y] \end{aligned} \quad (2-59)$$

where P , R and I have been defined in Equation (2-24)

The five equations given by Equations (2-58) and (2-59) are the dynamical conditions on the wave front for the laminated plate.

2.3.3 Propagation Velocity of the Wave Front

Across the wave front, the laminate constitutive relations given by Equation (2-20) can be written as

$$\begin{bmatrix} [N] \\ [M] \\ [Q] \end{bmatrix} = \begin{bmatrix} A & B & 0 \\ B & D & 0 \\ 0 & 0 & A^* \end{bmatrix} \begin{bmatrix} [\epsilon] \\ [\kappa] \\ [\gamma] \end{bmatrix}$$

ORIGINAL PAGE IS
OF POOR QUALITY (2-60)

where

$$\begin{aligned} \{[N]\}^T &= \{[N_x], [N_y], [N_{xy}]\} \\ \{[M]\}^T &= \{[M_x], [M_y], [M_{xy}]\} \\ \{[Q]\}^T &= \{[Q_x], [Q_y]\} \end{aligned} \quad (2-61)$$

are the jumps of the stress resultants, and

$$\begin{aligned} \{[\epsilon]\}^T &= \{[\partial u^0 / \partial x], [\partial v^0 / \partial y], [\partial u^0 / \partial y] + [\partial v^0 / \partial x]\} \\ \{[\kappa]\}^T &= \{[\partial \phi_x / \partial x], [\partial \phi_y / \partial y], [\partial \phi_x / \partial y] + [\partial \phi_y / \partial x]\} \\ \{[\gamma]\}^T &= \{[\partial w / \partial y], [\partial w / \partial x]\} \end{aligned} \quad (2-62)$$

are the jumps of the strain components. In Equation (2-62), the conditions $[\phi_x] = [\phi_y] = 0$ are substituted.

Substituting of Equation (2-43) and the similar relations for other kinematic variables in Equation (2-60), we can express the jumps of the stress resultants in terms of the jumps of the time derivatives of the displacement components u^0 , v^0 , w , ϕ_x and ϕ_y . These relations are then substituted in Equations (2-58) and (2-59), which results in five homogeneous equations. For $[0^\circ/45^\circ/0^\circ/-45^\circ/0^\circ]_{2s}$ graphite/epoxy laminated plate which is symmetrical and balanced (i.e. $B_{1j} = 0$, $A_{16} = A_{26} = 0$, $R = 0$ and $D_{16} = D_{26}$), these five equations are uncoupled into three groups as

$$[a_{ij}] \begin{Bmatrix} [\dot{u}^0] \\ [\dot{v}^0] \end{Bmatrix} = 0 \quad \text{ORIGINAL MODE NO. OF POOR QUALITY} \quad (2-63)$$

$$[b_{ij}] \begin{Bmatrix} [\phi_x] \\ [\phi_y] \end{Bmatrix} = 0 \quad (2-64)$$

$$(A^{*44} - P c_n^2) [W] = 0 \quad (2-65)$$

In which $[a_{ij}]$ and $[b_{ij}]$ are both two by two symmetric matrices, and their entries are given by

$$\begin{aligned} a_{11} &= n_x^2 A_{11} + n_y^2 A_{66} - P c_n^2 \\ a_{12} &= a_{21} = n_x n_y (A_{12} + A_{66}) \\ a_{22} &= n_x^2 A_{66} + n_y^2 A_{22} - P c_n^2 \end{aligned} \quad (2-66)$$

$$\begin{aligned} b_{11} &= n_x^2 D_{11} + 2n_x n_y D_{16} + n_y^2 D_{66} - I c_n^2 \\ b_{12} &= b_{21} = D_{16} + n_x n_y (D_{12} + D_{66}) \\ b_{22} &= n_x^2 D_{66} + 2n_x n_y D_{16} + n_y^2 D_{22} - I c_n^2 \end{aligned} \quad (2-67)$$

It can be seen that Equation (2-63) describes the in-plane extensional and the in-plane shear wave fronts, Equation (2-64) describes the bending moment and the twisting moment wave fronts and Equation (2-65) describes the transverse shear wave front.

From Equation (2-65), we obtain the normal velocity with which the transverse shear wave front propagates as

$$c_n^2 = A^{*44}/P \quad (2-68)$$

It is noted that this velocity is independent of the direction of propagation, and is called directionally

Isotropic wave front.

Equations (2-63) and (2-64) yield non-trivial solutions only if the determinant of the coefficients matrices vanish, i.e.

$$|a_{ij}| = 0 \quad (2-69)$$

$$|b_{ij}| = 0 \quad (2-70)$$

Each of the above equations can be expanded into a quadratic equation of c_n^2 . For $[0^\circ/45^\circ/0^\circ/-45^\circ/0^\circ]_{2S}$ graphite/epoxy laminated plate, the normal velocities of wave fronts corresponding to the in-plane modes and flexural modes are plotted in Figure 2.7 and 2.8, respectively. It is noted that the normal velocities of the in-plane extensional and in-plane shear modes are symmetrical about x-axis and y-axis, while there is no such symmetry for the bending moment and twisting moment modes.

2.3.4 Wave Surface and Ray

From Figure 2.7 and 2.8, it can be seen that for laminated composites which are anisotropic in general, the in-plane and flexural wave fronts travel with different normal velocities in different directions. In other words, the initial shape of a wave surface will be distorted after it propagates. However, Equations (2-66) and (2-67) show

ORIGINAL PAGE IS
OF POOR QUALITY

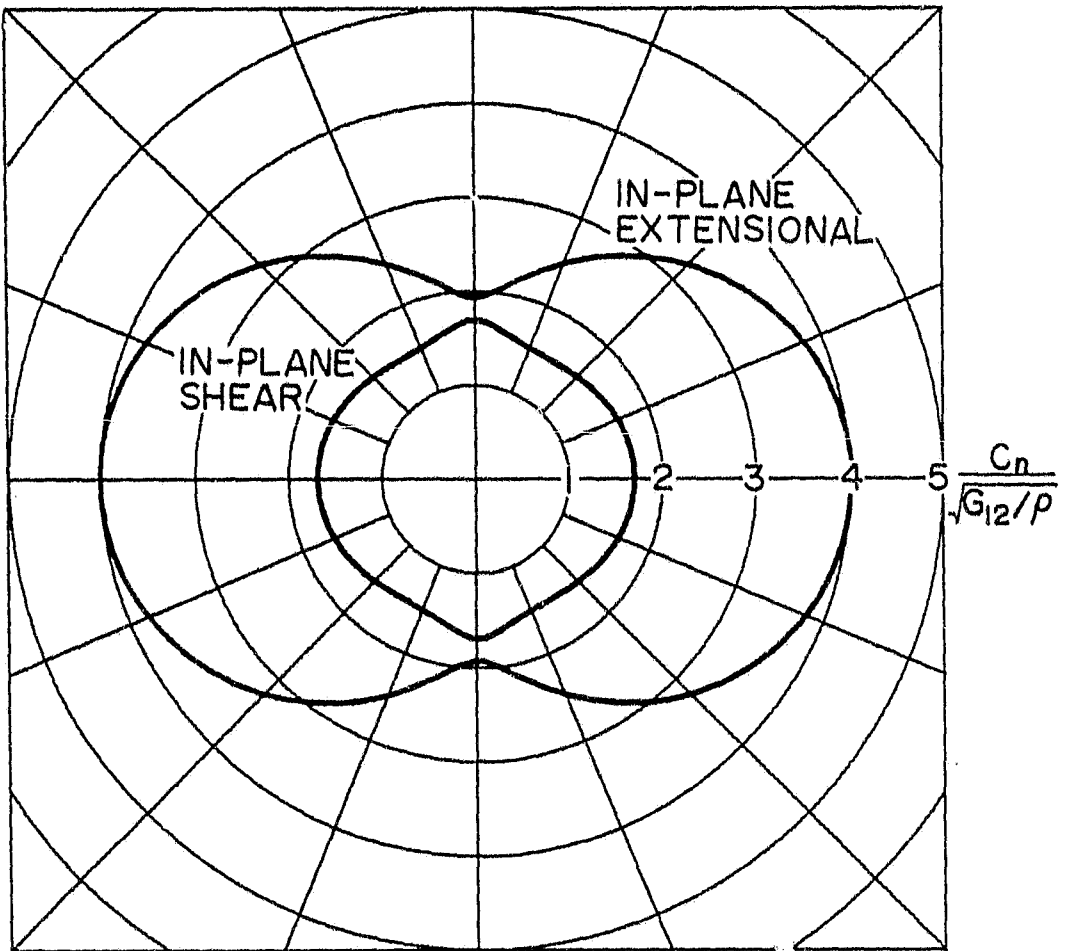


Figure 2.7 Normal velocities of in-plane wave fronts

ORIGINAL PAGE IS
OF POOR QUALITY

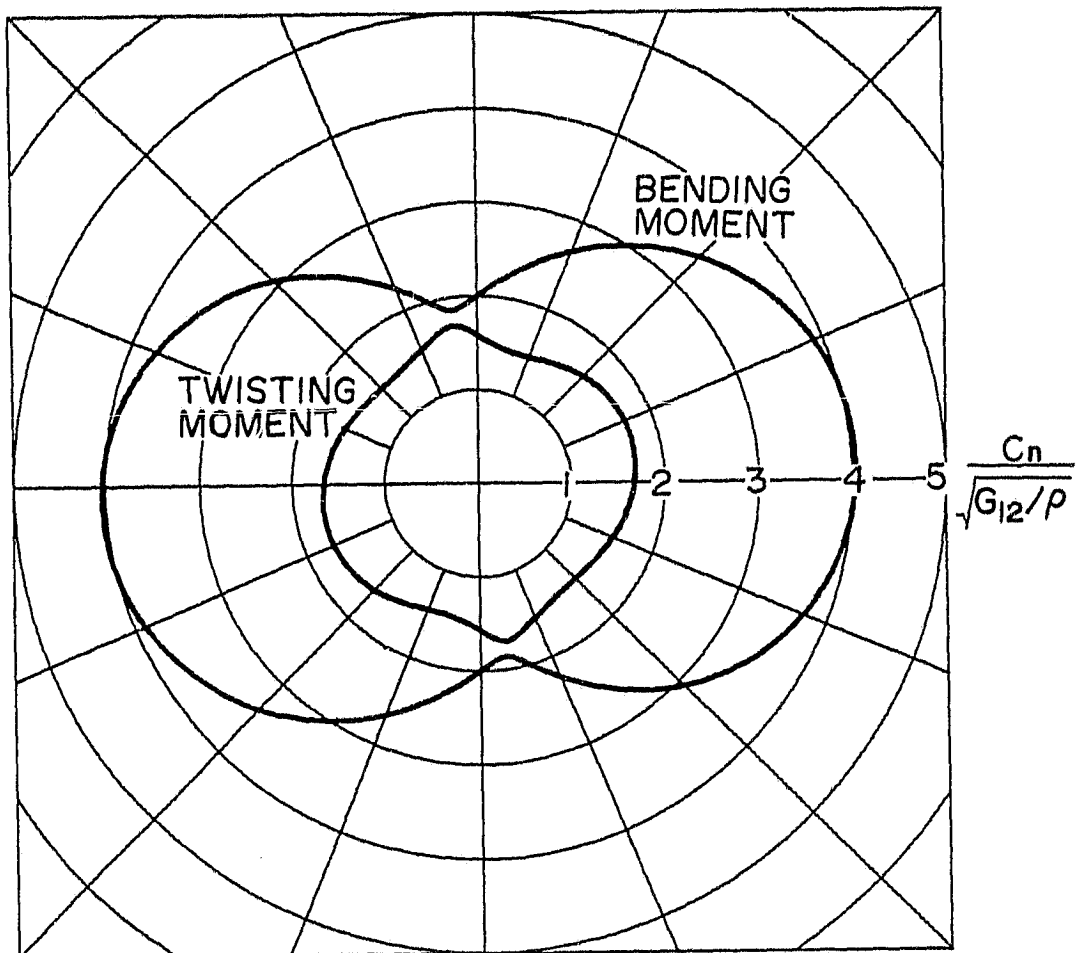


Figure 2.8 Normal velocities of flexural wave fronts

that for any fixed normal direction n_i , c_n is a constant. Connecting the points having the same unit normals to the travelling wave front surface, we obtain a family of lines which are called rays. Thus, along a ray, the normal velocity of wave front remains unchanged. By using the ray theory which has been well established in the field of geometrical optics, we are able to construct the wave front surface.

Recall Equation (2.37)

$$F(x_i) - t = 0 \quad i = 1, 2 \quad (2-37)$$

which represents a family of wave fronts propagating over the plate with t as a parameter. It follows that

$$dF/dt = (\partial F / \partial x_i)(dx_i / dt) = (\partial F / \partial x_i)c_i = 1 \quad (2-71)$$

By putting

$$p_i = \partial F / \partial x_i = \nabla F \quad (2-72)$$

Equation (2-71) becomes

$$p_i c_i = 1 \quad (2-73)$$

Since p_i is normal to the surface F , it can be written as

$$p_i = |p_i| n_i \quad (2-74)$$

where $|p_i|$ denotes the length of p_i . Combining (2-73) and (2-74), we obtain

$$|p_1|n_1c_1 = |p_1|c_n = 1 \quad (2-75)$$

from which we obtain

$$p_1 = n_1/c_n \quad (2-76)$$

In Equation (2-76), p_1 is called the slowness vector which has the direction normal to the wave front with the magnitude being equal to the inverse of normal velocity c_n .

Substituting Equation (2-76) in Equation (2-69) and (2-70), we obtain two equations in terms of p_1 ,

$$\begin{vmatrix} p_x^2 A_{11} + p_y^2 A_{66} - P & p_x p_y (A_{12} + A_{66}) \\ p_x p_y (A_{12} + A_{66}) & p_x^2 A_{66} + p_y^2 A_{22} - P \end{vmatrix} = 0$$

$$\begin{vmatrix} p_x^2 D_{11} + 2p_x p_y D_{16} + p_y^2 D_{66} - I & D_{16} + p_x p_y (D_{12} + D_{66}) \\ D_{16} + p_x p_y (D_{12} + D_{66}) & p_x^2 D_{66} + 2p_x p_y D_{16} + p_y^2 D_{22} - I \end{vmatrix} = 0$$

which can be written in a general form as

$$g(p_1) = 0 \quad l = 1, 2 \quad (2-77)$$

In view of Equation (2-72), we recognize that Equation (2-77) may be regarded as a set of first-order partial differential equation for F . A standard method of solving first-order partial differential equation is by means of characteristics [24], which reduces the equation to a system of first-order ordinary differential equations. In our case, Equation (2-77) then is equivalent to the following

$$\frac{dx}{ds} = \frac{\partial g}{\partial p_x} \quad \frac{dy}{ds} = \frac{\partial g}{\partial p_y} \quad (2-78)$$

$$\frac{dp_x}{ds} = -\frac{\partial g}{\partial x} \quad \frac{dp_y}{ds} = -\frac{\partial g}{\partial y} \quad (2-79)$$

where s is a parameter. These equations, together with Equation (2-77) describe the ray geometry and the normal direction of the wave front propagating along the ray.

From Equation (2-78), we have

$$\frac{dy}{dx} = (\frac{\partial g}{\partial p_y}) / (\frac{\partial g}{\partial p_x}) \quad (2-80)$$

Since the normal direction of wave front along a ray is constant, it can be seen from Equation (2-76) that p_1 is also constant along a ray. For laminated composite which is assumed to have homogeneous material properties, Equation (2-77) shows that $g(p_1)$ does not depend on x_1 , consequently, $\frac{\partial g}{\partial p_x}$ and $\frac{\partial g}{\partial p_y}$ are all constants along a ray. Thus, the solution of Equation (2-80) is then given by

$$y = \xi(x - x_0) + y_0 \quad (2-81)$$

where x_0 and y_0 are the initial values of x and y at $t = 0$, and $\xi = (\frac{\partial g}{\partial p_y}) / (\frac{\partial g}{\partial p_x})$. This equation shows that the rays in a homogeneous solid are straight lines.

From Equations (2-73) and (2-77), we have

$$c_1 dp_1 = 0 \quad (2-82)$$

$$dg = (\frac{\partial g}{\partial p_1}) dp_1 = 0 \quad (2-83)$$

Eliminating dp_i from these equations yields

$$dx_i/dt = c_i = (\partial g/\partial p_i)/(p_j \partial g/\partial p_j) \quad (2-84)$$

where summation over j is understood.

Equation (2-84) can be solved to obtain the position of wave front at time t . Again, since $\partial g/\partial p_i$ and p_i are all constant along a ray, we obtain the solution of Equation (2-84) as

$$x = (\partial g/\partial p_x)t/(p_j \partial g/\partial p_j) + x_0 \quad (2-85)$$

$$y = (\partial g/\partial p_y)t/(p_j \partial g/\partial p_j) + y_0 \quad (2-86)$$

where x_0 and y_0 denote the initial wave position at $t = 0$.

Consider at $t = 0$, a wave front forms a circle given by

$$\begin{aligned} x_0 &= h \cos\alpha \\ y_0 &= h \sin\alpha \end{aligned} \quad (2-87)$$

At this instant, the normal directions to the wave front coincide with the radial directions. Due to the different velocities of propagation in directions, this initial shape would be distorted. By using Equations (2-85) and (2-86), the subsequent positions of the wave front can be determined. Figures 2.9-2.12 show the wave front positions at two consecutive instants after $t = 0$ for the in-plane extensional, in-plane shear, bending moment and twisting moment modes, respectively, for the $[0^\circ/45^\circ/0^\circ/-45^\circ/0^\circ]_{2s}$

graphite/epoxy laminated plate. It is noted that for symmetrical laminates, the in-plane modes are uncoupled from the bending modes. The rays along which the normal directions to the wave front are 0° , 45° and 90° , respectively, are also shown in the figures. It is seen that the wave fronts of the in-plane extensional and the in-plane shear modes possess symmetry with respect to x-axis and y-axis. The wave fronts of the bending and twisting moments, however, lose their original symmetry with respect to x-axis and y-axis. This is an indication that in performing analysis of flexural deformation of this laminate, one can not take a quadrant for analysis, a practice followed by many authors dealing with homogeneous and isotropic plates.

From Figures 2.9-2.12, it is also interesting to note that ray geometries for these two groups of wave fronts are quite different. For the in-plane extensional and in-plane shear wave fronts, the rays coincide with the normal directions when $\alpha = 0^\circ$ and 90° . Along other directions, the direction of the ray deviates from the normal direction of the wave front. It was discussed in [2] that the degree of spreading of rays is proportional to the decay of the stress amplitude at the wave front. Thus, from Figures 2.9 and 2.11, one can conclude that the strength of the in-plane extensional and bending moment wave fronts decay more rapidly in the y-direction than in the x-direction.

ORIGINAL PAGE IS
OF POOR QUALITY

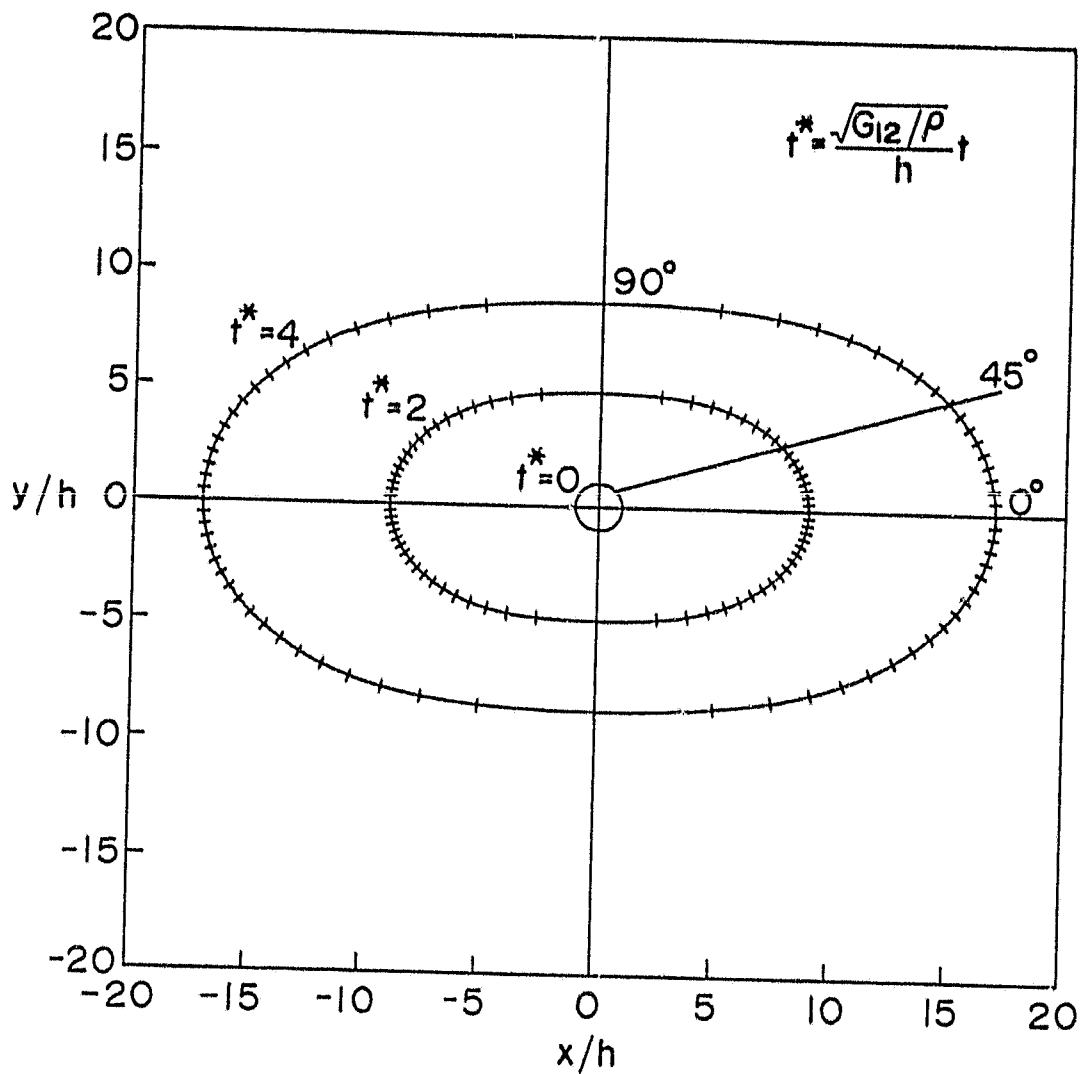


Figure 2.9 Wave front positions at different times and rays for in-plane extensional mode

ORIGINAL PAGE IS
OF POOR QUALITY

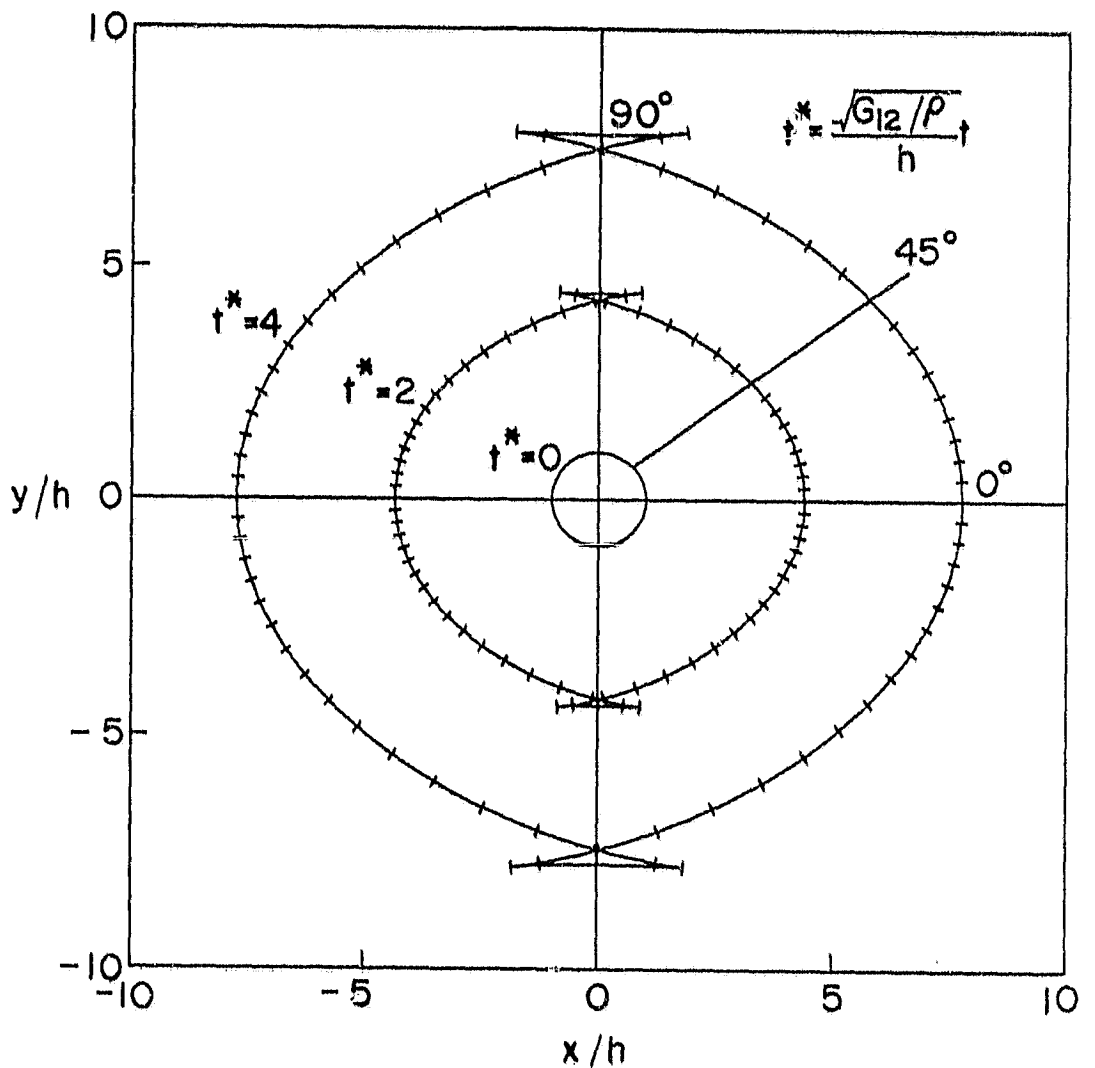


Figure 2.10 Wave front positions at different times and rays for in-plane shear mode

ORIGINAL PAGE IS
OF POOR QUALITY

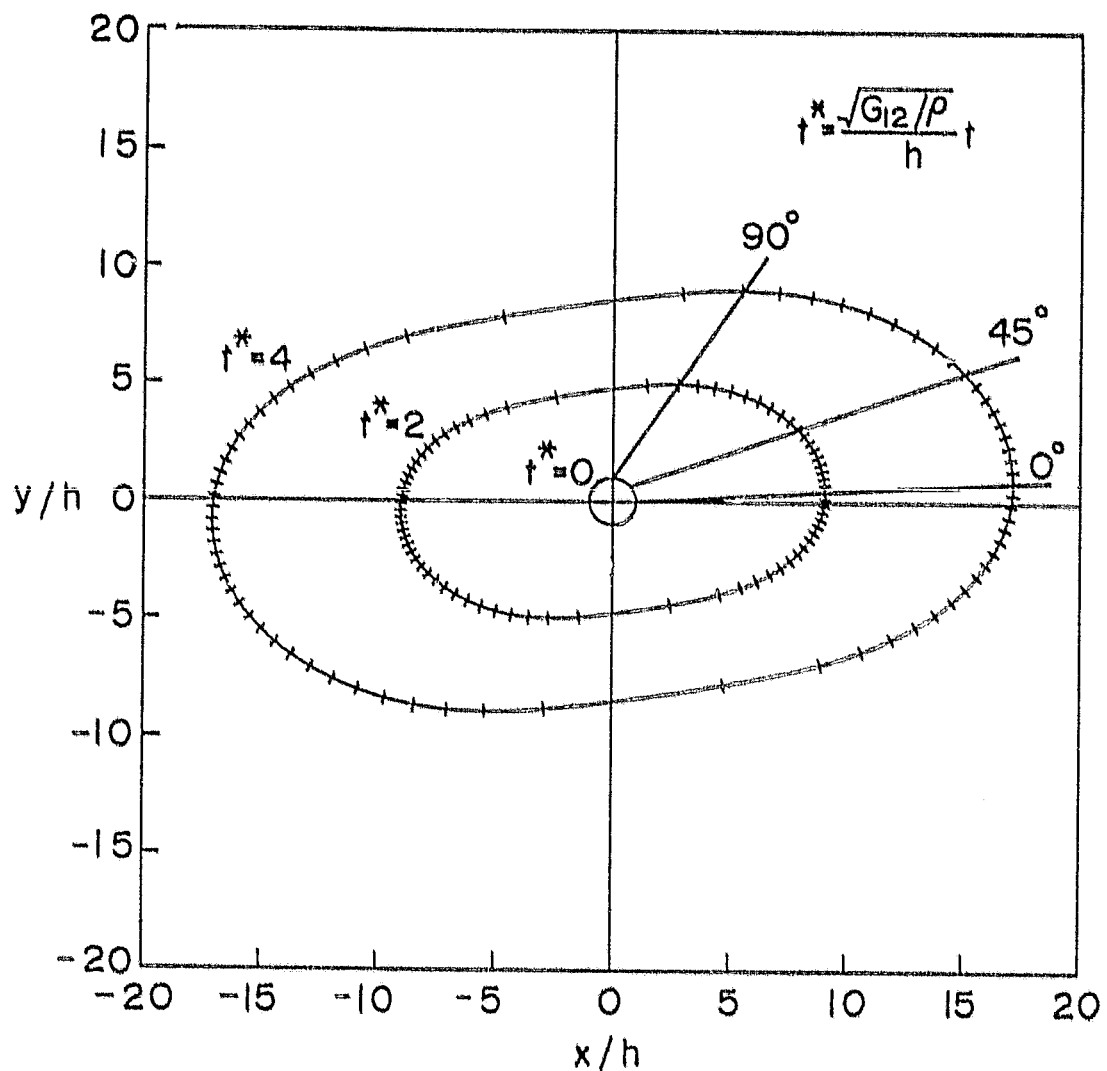


Figure 2.11 Wave front positions at different times and rays for bending mode

ORIGINAL PAGE IS
OF POOR QUALITY

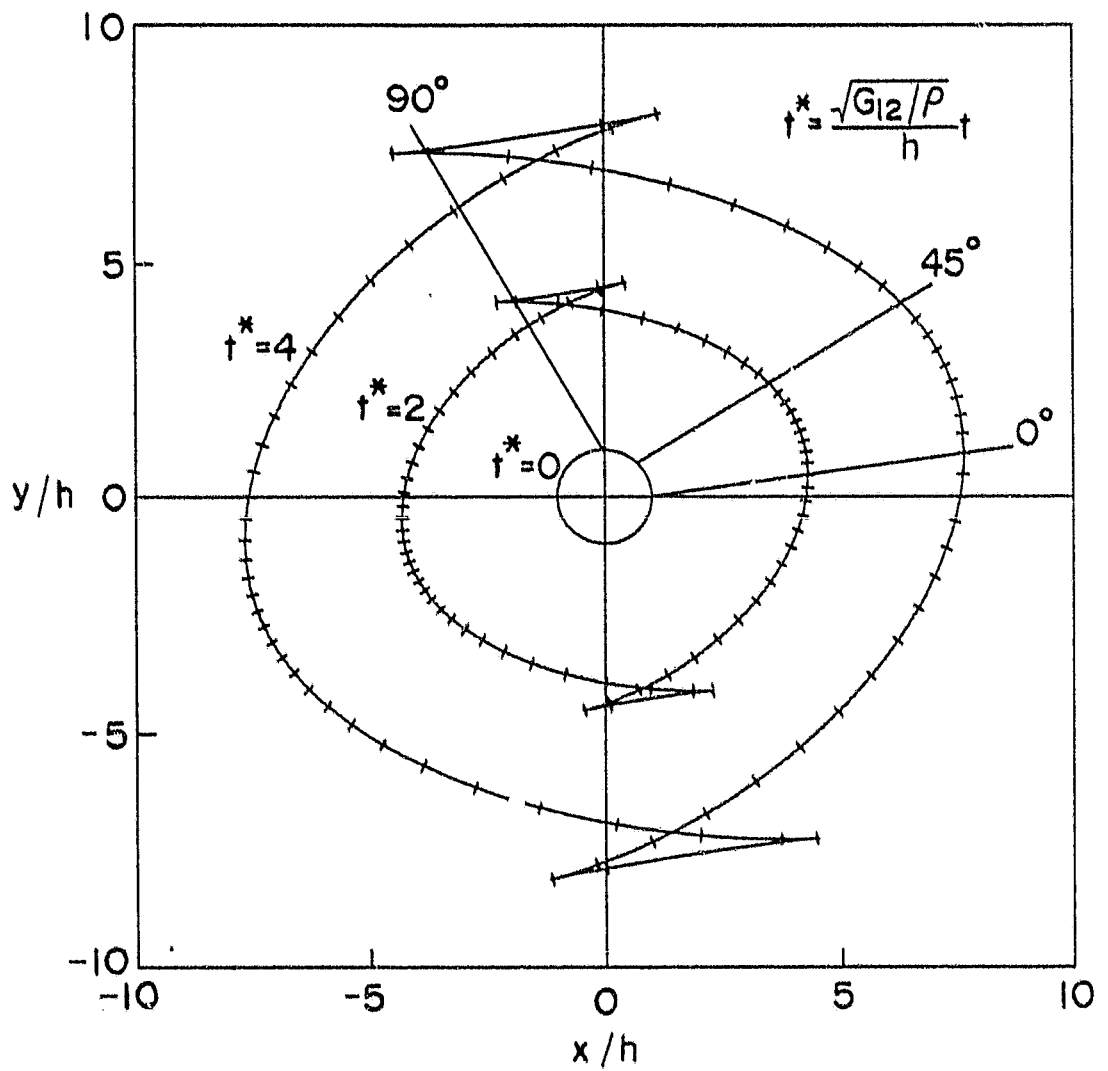


Figure 2.12 Wave front positions at different times and rays for twisting mode

A photoelastic study of anisotropic waves in a fiber reinforced composite has been done by Dally et al. [9]. The waves was produced by a explosive charge in a small hole on the plate. The result showed clearly an elliptic-like stress wave front pattern. This indicates that stress waves in anisotropic materials propagate with different velocities in different directions.

CHAPTER 3

STATICAL INDENTATION LAWS

A brief introduction of the historical development on impact problem involving homogeneous isotropic materials was given by Goldsmith [12]. Hertz [11] was the first to obtain a satisfactory solution on contact law for two isotropic elastic spherical bodies. When letting the radius of one of the spheres go to infinity, this law then describes the contact behavior between a sphere and an elastic half-space. The Hertzian law, in spite of being static and elastic in nature, has been widely applied to impact analyses where permanent deformations were produced. The use of this law beyond the elastic limit has been justified on the basis that it appears to predict accurately most of the impact parameters that can be experimentally verified.

In studying impact responses of laminated composites, the problem becomes extremely complicated. One may easily realize that the Hertzian contact law which was derived based on homogeneous isotropic materials may not be adequate in describing the contact behavior of laminated composites due to their anisotropic and nonhomogeneous properties. Moreover, most of the laminated composites have finite thickness which can not be represented by a half-space. In

many existing analytical works [25], loadings to the laminates were assumed known, and the responses of the laminates were assumed elastic.

Willis [26] obtained explicit formulas for Hertzian contact law for transversely isotropic half-space pressed by a rigid sphere, and extended it to the application of Impact problems. It was shown that

$$F = k\alpha^n \quad (3-1)$$

with $n = 3/2$ is valid for the contact force F and the indentation α , where k is a contact coefficient whose value depends on the material properties of the target and the sphere, and the radius of sphere.

A modified contact law with

$$k = (4/3) \frac{\frac{R_s^{1/2}}{1 - \nu_s^2} + \frac{1}{E_t}}{\frac{1}{E_s}} \quad (3-2)$$

was used [13] in an analytical study on impact of laminated composites. In Equation (3-2), R_s , ν_s and E_s are the radius, Poisson's ratio and Young's modulus of the sphere, respectively, and E_t is the Young's modulus of the laminates in thickness direction. It was also suggested by Sun *et al.* [27] that the value of k can be experimentally determined.

ORIGINAL PAGE IS
OF POOR QUALITY

Recently Yang and Sun [14] have conducted static indentation tests on the $[0^\circ/45^\circ/0^\circ/-45^\circ/0^\circ]_{2s}$ graphite/epoxy laminates using spherical steel indenters of 0.25 in. and 0.5 in. diameters. The results were fitted into Equation (3-1) and were found that the 3/2 power is valid. In addition, it was also observed that even for small amounts of load there were significant permanent indentations. This implies that the unloading curve has to be different from the loading curves. In order to account for the permanent deformation, the equation

$$F = F_m \left(\frac{\alpha - \alpha_0}{\alpha_m - \alpha_0} \right)^q \quad (3-3)$$

proposed by Crook [28] was used to model the unloading path where F_m is the contact force at which unloading begins, α_m is the indentation corresponding to F_m , and α_0 denotes the permanent indentation in an unloading cycle. Equation (3-3) can be rewritten as

$$F = s(\alpha - \alpha_0)^q \quad (3-4)$$

in which

$$s = F_m / (\alpha_m - \alpha_0)^q \quad (3-5)$$

is called unloading rigidity. In order to simplify the modeling of the unloading law, it was assumed [14] that the value of s for all the unloading curves remains the same.

Consequently, a constant α_{cr} given by

$$\alpha_{cr} = k/s \quad (3-6)$$

was introduced. It was also shown that $q=5/2$ fitted the unloading path very well, and the permanent indentation α_0 was then related to α_m by

$$\begin{aligned} \alpha_0/\alpha_m &= 1 - (\alpha_{cr}/\alpha_m)^{2/5} && \text{as } \alpha_m > \alpha_{cr} \\ \alpha_0 &= 0 && \text{as } \alpha_m \leq \alpha_{cr} \end{aligned} \quad (3-7)$$

The value of α_{cr} was found to be independent of the size of the indenter and hence can be regarded as a material constant.

It was also mentioned in [14] and [29] that there were some practical difficulties in performing the tests. Since the indentation was measured step by step using a dial gage and readings on the gage were taken about 10 to 20 seconds after the load was increased by one step, the creep effect may cause an appreciable error to the results. Another important problem was that it was almost impossible to measure the permanent indentation accurately using the dial gage. In order to overcome these problems, a Linear Variable Differential Transformer (LVDT) was used in this study to measure the indentation.

The LVDT is an electromechanical transducer that produces an electrical output proportional to the displacement.

Connecting this output and the one from the strain indicator which is used to measure the applied loading to a X-Y plotter, one can obtain a continuous loading-unloading curve. By changing the loading rate which can be applied as fast as 50 lb./sec., it is possible to examine the significance of creep effect on the contact law. The starting point and final point of a loading-unloading cycle, which represent respectively the instants of contact and separation of the indenter and the specimen, can be easily determined from the curve. Thus, the measurements of permanent indentations are much more accurate than those using the dial gage.

3.1 Specimens and Experimental Procedure

Two groups of test specimens were prepared from a $[0^\circ/45^\circ/0^\circ/-45^\circ/0^\circ]_{2s}$ graphite/epoxy laminate. They were cut in the way such that the longitudinal axis of the beam specimen of the first group was parallel to the 0° fiber direction while the second one was perpendicular to it. The latter then becomes $[90^\circ/45^\circ/90^\circ/-45^\circ/90^\circ]_{2s}$ laminated beams. The thickness of the beam was 0.106 in. and the width was approximately 1.25 in.. In all tests, the specimens were clamped at both ends. It was shown in [14] that the span of the specimen in the range of 2 in. to 6 in. has little effect on the contact law. Hence, only one span, i.e. 2 in., was used in the test.

The experimental set-up is shown schematically in Figure 3.1. LVDT was mounted on a 'C' bracket fixed to the loading piston so that only the relative movement between the indenter and the specimen was recorded. The load was applied pneumatically by a plunger and it was measured using a load cell and a strain indicator. Outputs from LVDT and strain indicator were fed into an X-Y plotter so that a continuous force-indentation curve can be obtained. Two spherical steel indenters of diameters 0.5 in. and 0.75 in. were used.

3.2 Experimental Results

3.2.1 Loading Curves

The experimental curves were first digitized into some discrete data points and then fitted into Equation (3-1) using least-squares method. Figures 3.2 and 3.3 show the test data and the fitted curves for 0.5 in. diameter indenter. It can be seen from these figures that the 3/2 power index gives very good results. However, the contact coefficient k of $[0^\circ/45^\circ/0^\circ/-45^\circ/0^\circ]_{2s}$ specimen is less than the one of $[90^\circ/45^\circ/90^\circ/-45^\circ/90^\circ]_{2s}$ specimen by about 7 %. During the test, larger deflections were observed for the second group of specimen due to their lower flexural rigidity. This means that the contact area is also larger and the indentation under same amount of loading should be

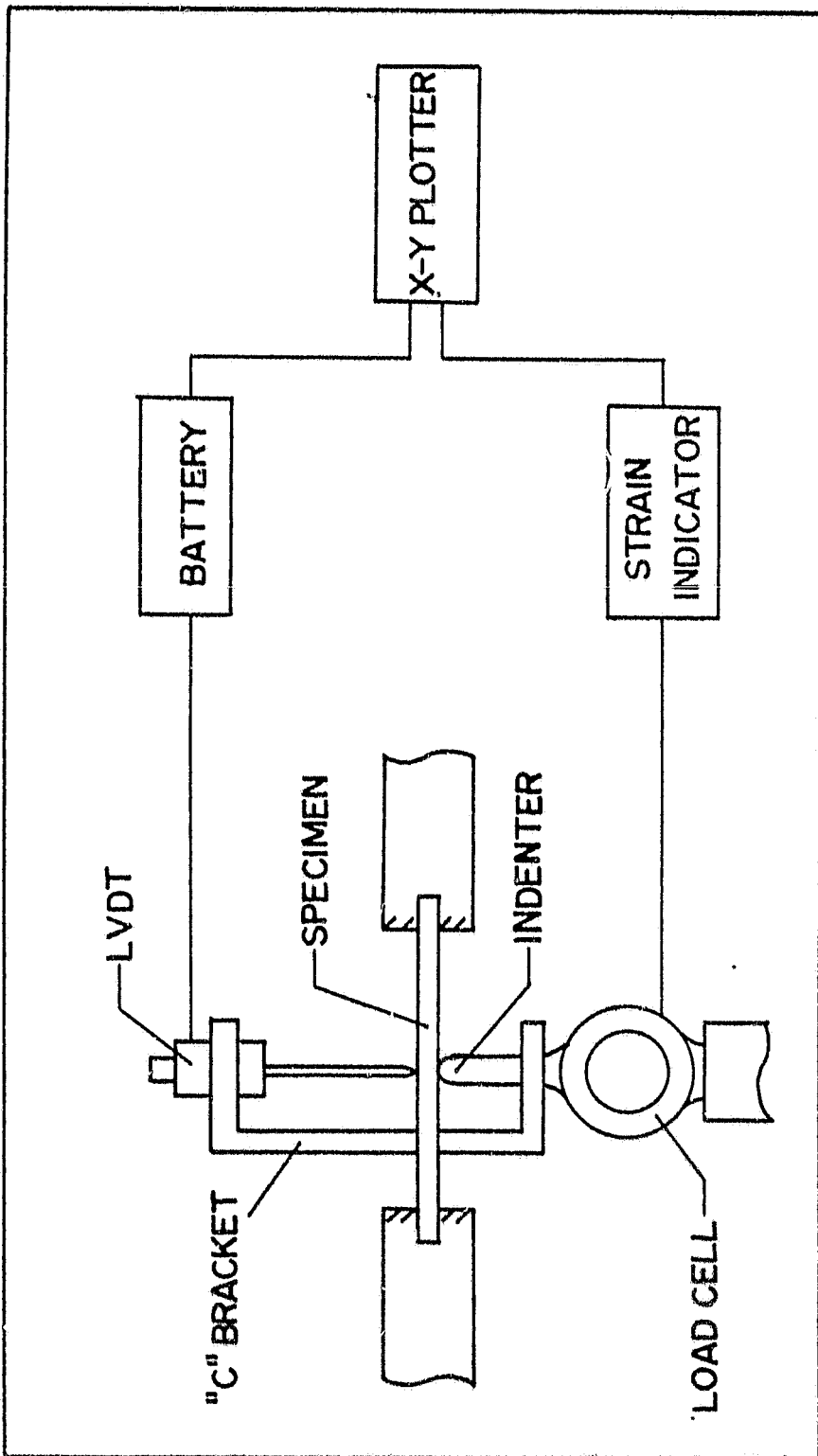


Figure 3.1 Schematic diagram for the indentation test set-up

ORIGINAL PAGE IS
OF POOR QUALITY

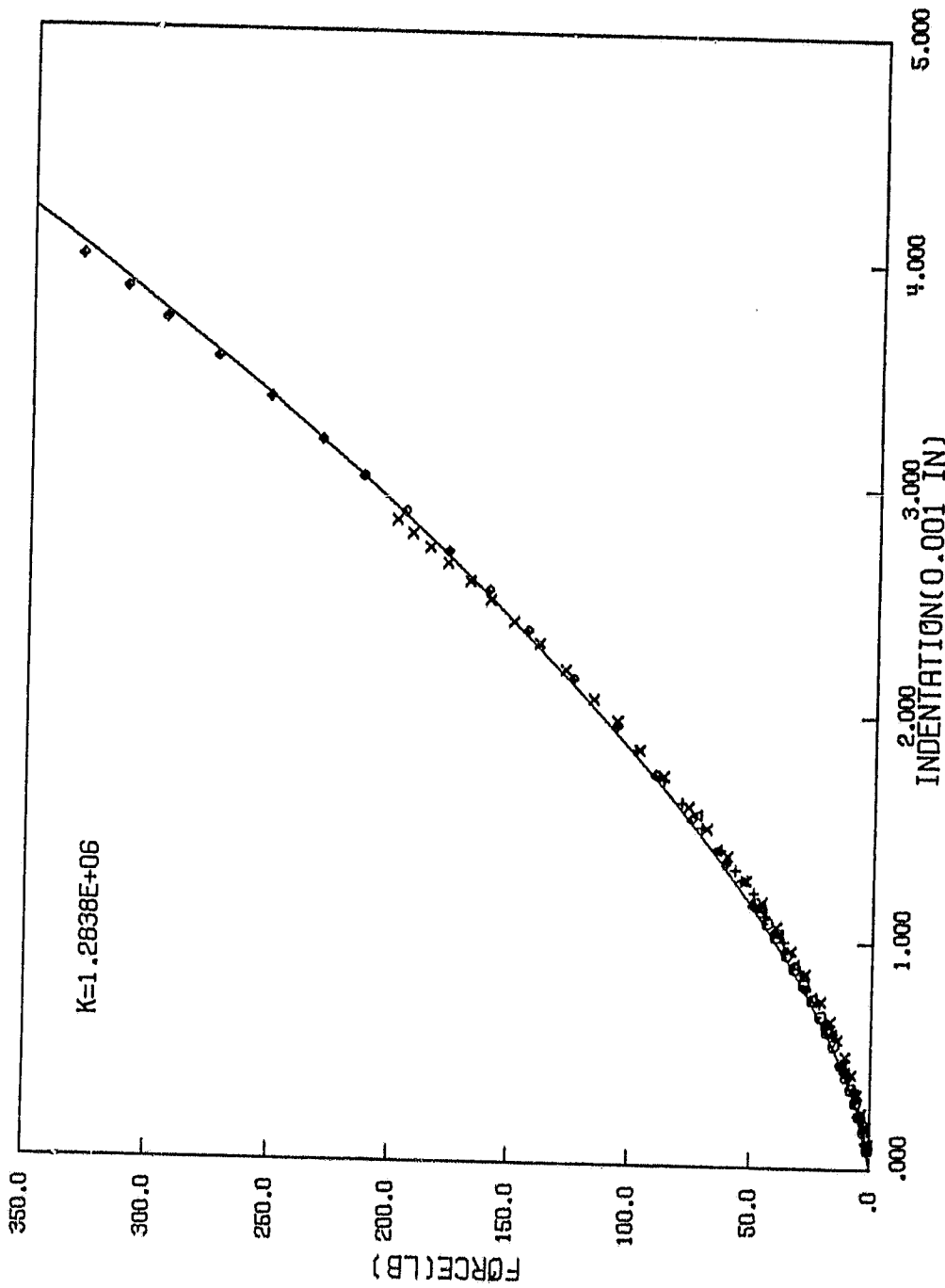


Figure 3.2 Loading curve of $[0^\circ/45^\circ/0^\circ/-45^\circ/0^\circ]^{2s}$ specimens with 0.5 inch indenter ($n=3/2$)

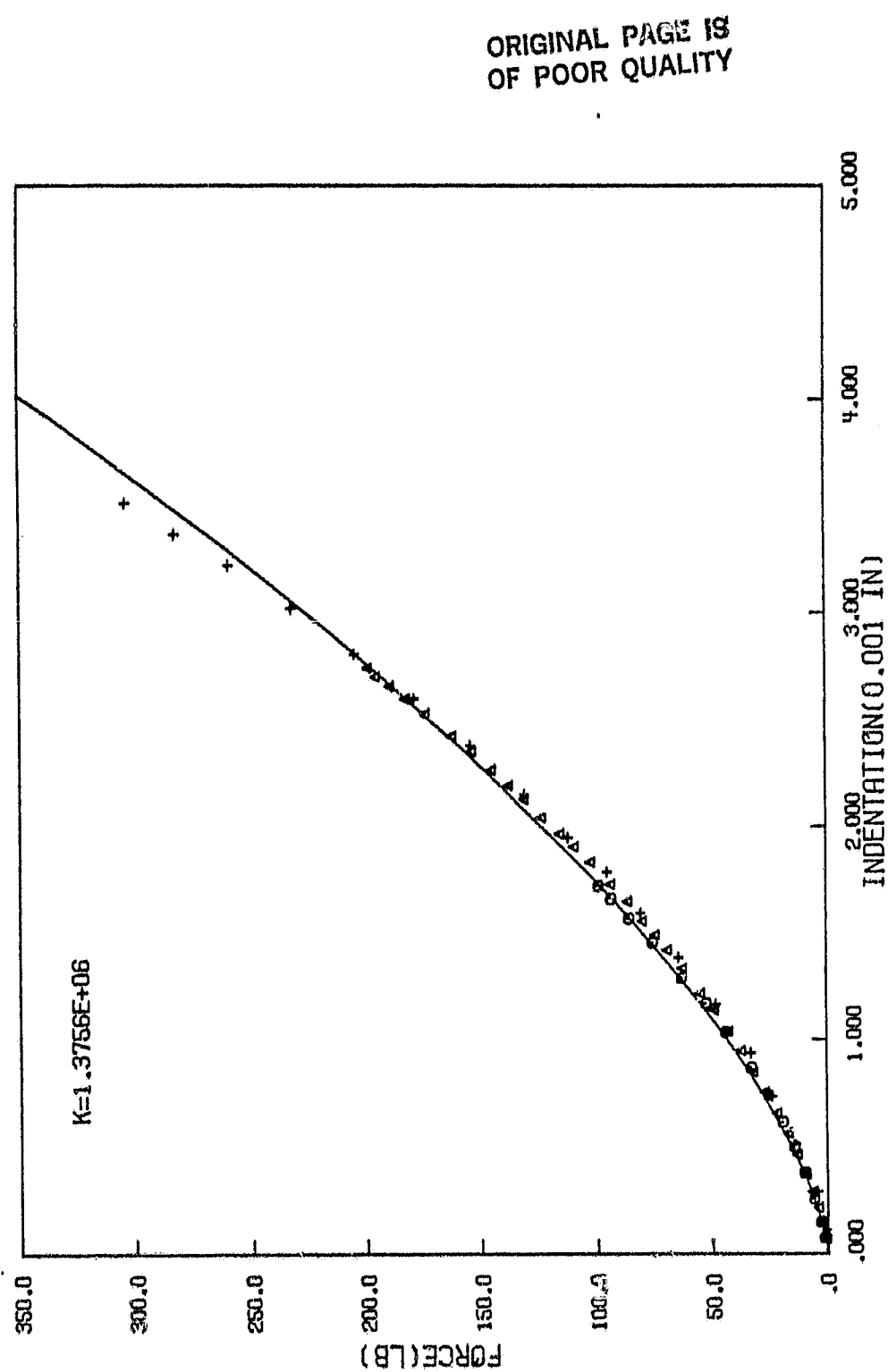


Figure 3.3 Loading curve of [90°/45°/90°/90°/-45°/90°]_{2s} specimens with 0.5 inch indenter ($n=3/2$)

smaller comparing with the first group of specimens. Consequently, the higher value of k for the $[90^\circ/45^\circ/90^\circ/-45^\circ/90^\circ]_{2s}$ specimens is reasonable.

The results for 0.75 in. diameter indenter are presented in Figures 3.4 and 3.5. Again, good agreement between the experimental data and fitted curves indicates that the 3/2 power index for loading law is valid. The values of k for both indenters are summarized in Table 3.1. It should be noted that the average value of k obtained from the two groups of specimens was used later in a finite element analysis of impact responses.

3.2.2 Unloading Curves

By choosing a suitable value for q , it can be seen from Equation (3-5) that once the relation between α_0 and α_m is established, the unloading rigidity s is then determined. Test results show that the permanent indentations α_0 and the corresponding maximum indentations α_m exhibit a rather linear relationship. The equation given by

$$\alpha_0 = s_p (\alpha_m - \alpha_p) \quad (3-8)$$

is obtained from the test data for both 0.5 in. and 0.75 in. indenters using least-squares fitting method, and are plotted in Figure 3.6. In Equation (3-8), α_p can be considered as a critical value of indentation. Once the amount of indentation exceeds α_p , permanent deformation will occur.

ORIGINAL PAGE IS
OF POOR QUALITY

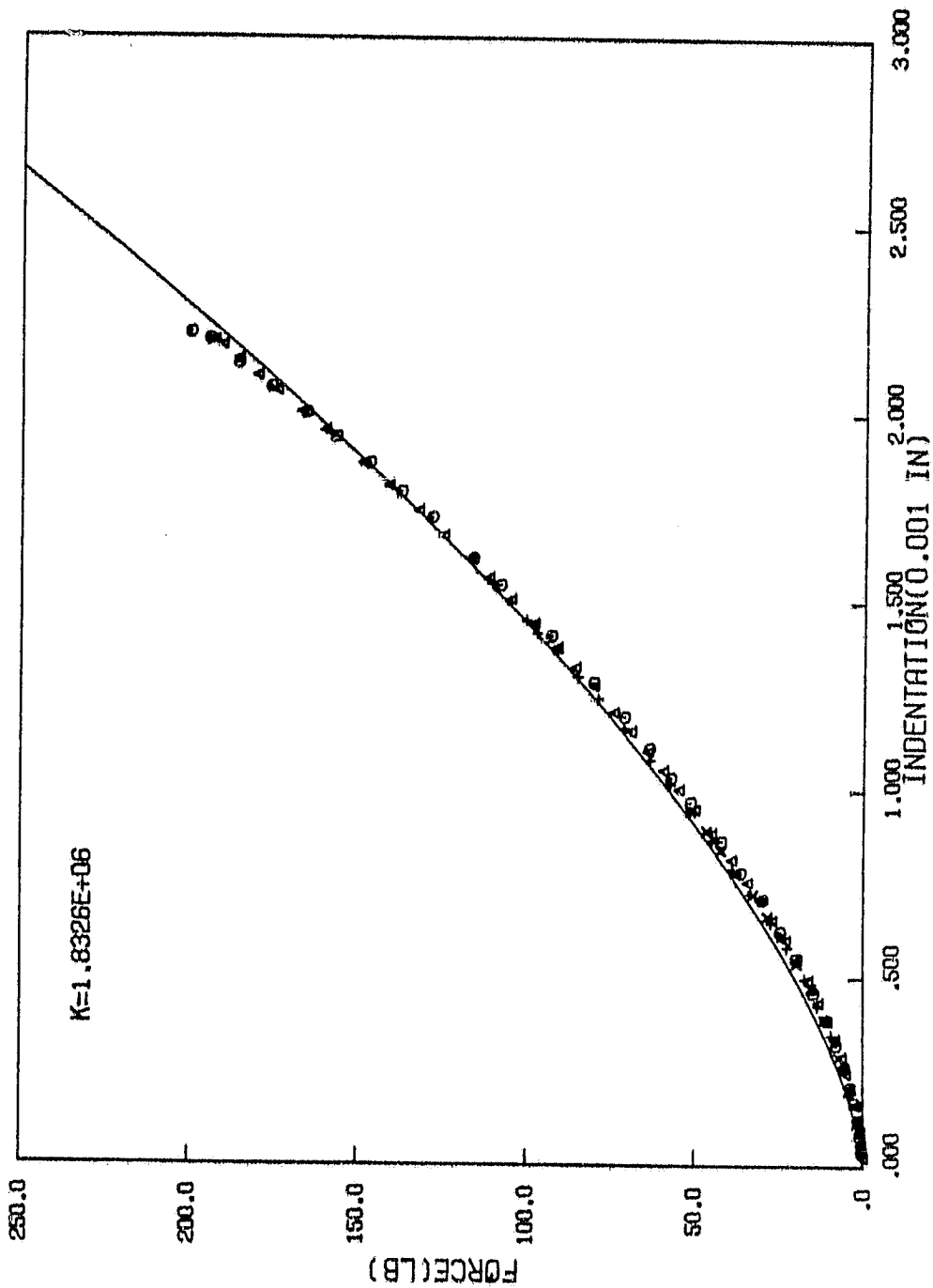


Figure 3.4 Loading curve of $[0^\circ/45^\circ/0^\circ/-45^\circ/0^\circ]_{25}$ specimens with 0.75 inch indenter ($n=3/2$)

ORIGINAL PAGE IS
OF POOR QUALITY

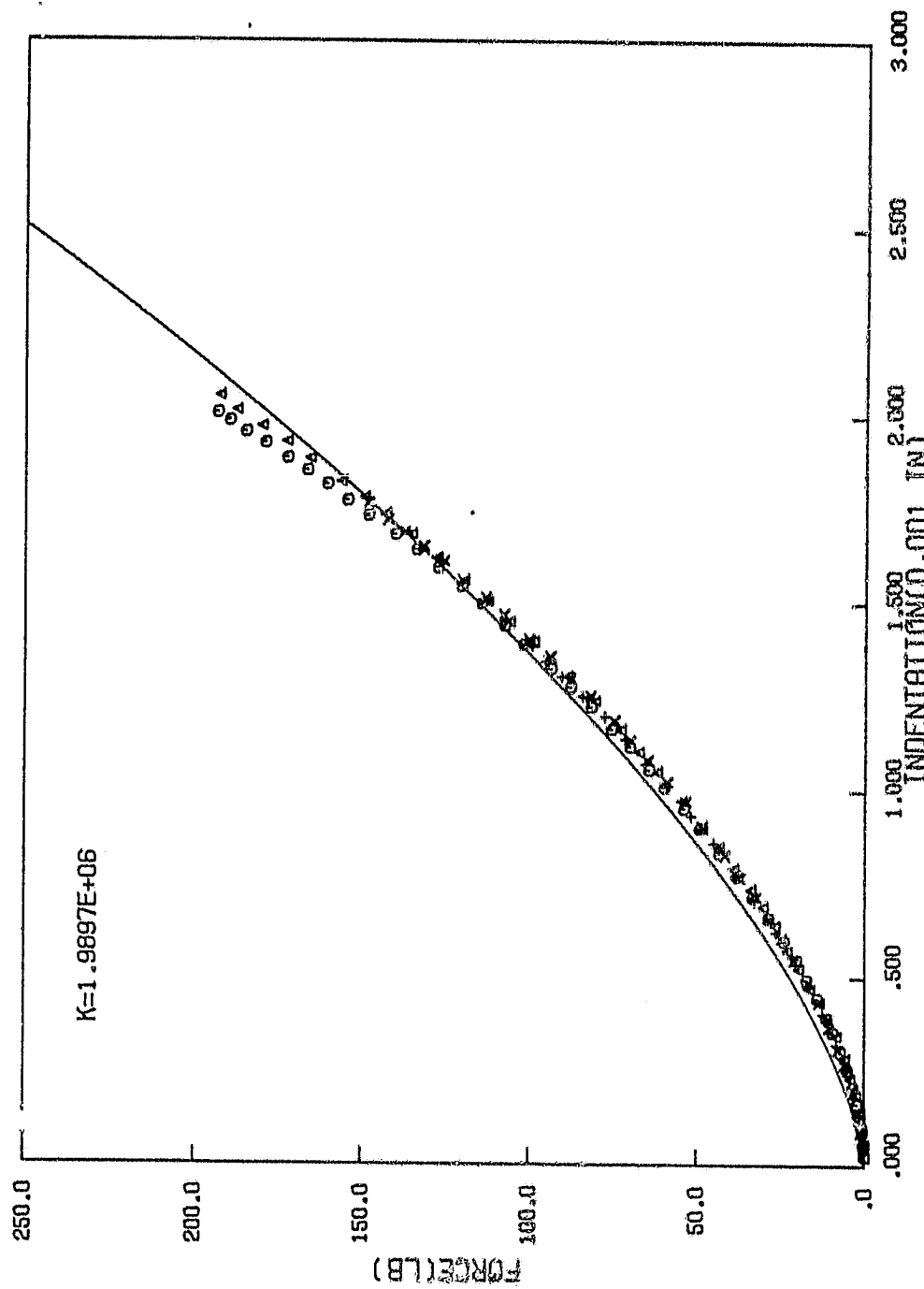


Figure 3.5 Loading curve of $[90^\circ/45^\circ/90^\circ/-45^\circ/90^\circ]_{2S}$ specimens with 0.75 inch Indenter ($n=3/2$)

ORIGINAL PAGE IS
OF POOR QUALITY

Table 3.1
Contact coefficient k of loading law $F = k\alpha^{1.5}$

Size of Indenter (in)	0.5		0.75	
	Group 1 ⁺	Group 2 [‡]	Group 1 ⁺	Group 2 [‡]
$k(\text{lb/in}^{1.5})$	1.284×10^6	1.376×10^6	1.833×10^6	1.990×10^6
Average k	1.330×10^6			1.912×10^6
Ref. [14]	9.694×10^5			

⁺ $[0^\circ/45^\circ/0^\circ/-45^\circ/0^\circ]_{2s}$ specimens

[‡] $[90^\circ/45^\circ/90^\circ/-45^\circ/90^\circ]_{2s}$ specimens

ORIGINAL PAGE IS
OF POOR QUALITY

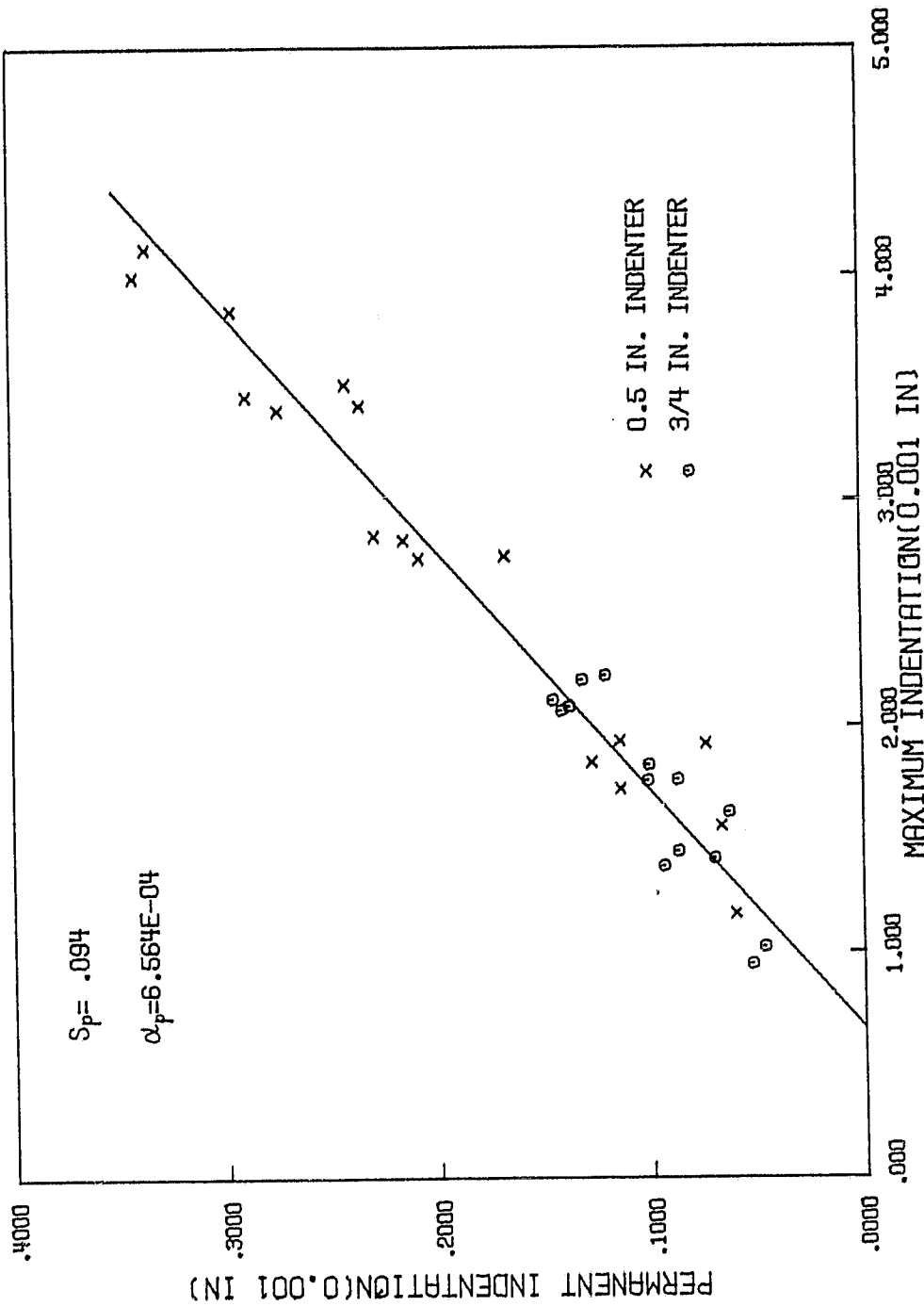


Figure 3.6 Relation between permanent indentation and maximum indentation

Substitution of Equation (3-8) and (3-1) into Equation (3-5) yields

$$s = \frac{k\alpha_m^{3/2}}{[(1 - s_p)\alpha_m + s_p\alpha_p]^q} \quad \text{if } \alpha_m \geq \alpha_p \quad (3-9)$$

$$s = \frac{k\alpha_m^{3/2}}{\alpha_m^q} \quad \text{if } \alpha_m < \alpha_p \quad (3-10)$$

These two equations along with Equation (3-4) are then used to fit the experimental unloading curves in finding the value of q .

Yang [14] has shown that $q = 2.5$ fits the test results for both 0.25 in. and 0.5 in. indenters quite well. In this study, however, the values of 2.2 and 1.8 were found to give the best fitting for 0.5 in. and 0.75 in. indenters, respectively using the aforementioned method (Figures 3.7-3.10). For convenience, $q = 2.5$ was used for 0.5 in. indenter while $q = 2.0$ was chosen for 3/4 in. indenter. The results of the curve-fitting are presented in Figures 3.11-3.14. Further discussions on the unloading law will be given in Section 3.3.

ORIGINAL PAGE IS
OF POOR QUALITY

ORIGINAL PAGE IS
OF POOR QUALITY

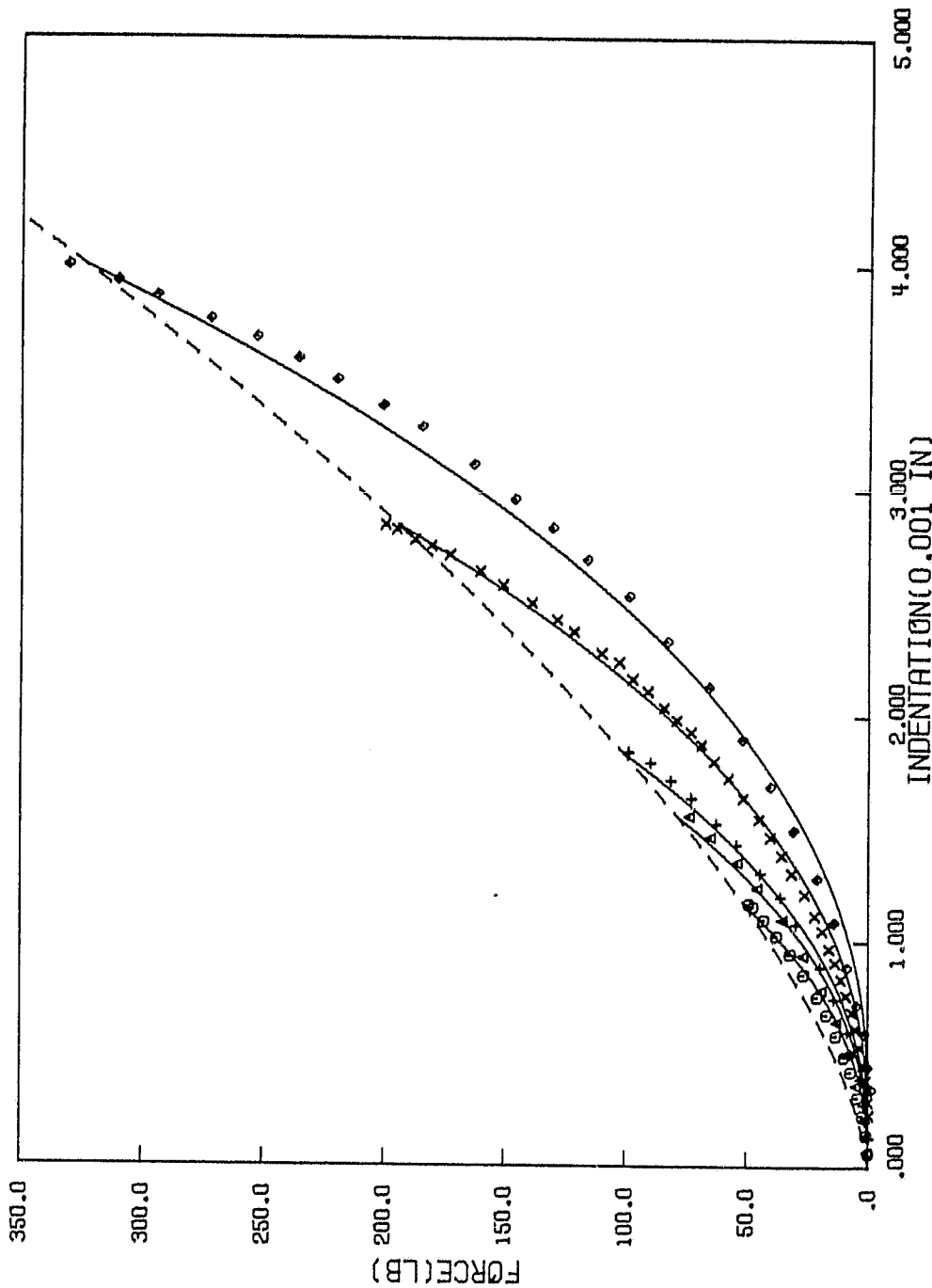


Figure 3.7 Unloading curves of $[0^\circ/45^\circ/0^\circ/-45^\circ/0^\circ]_2 s$ specimens with 0.5 inch indenter ($q=2.2$)

ORIGINAL PAGE IS
OF POOR QUALITY

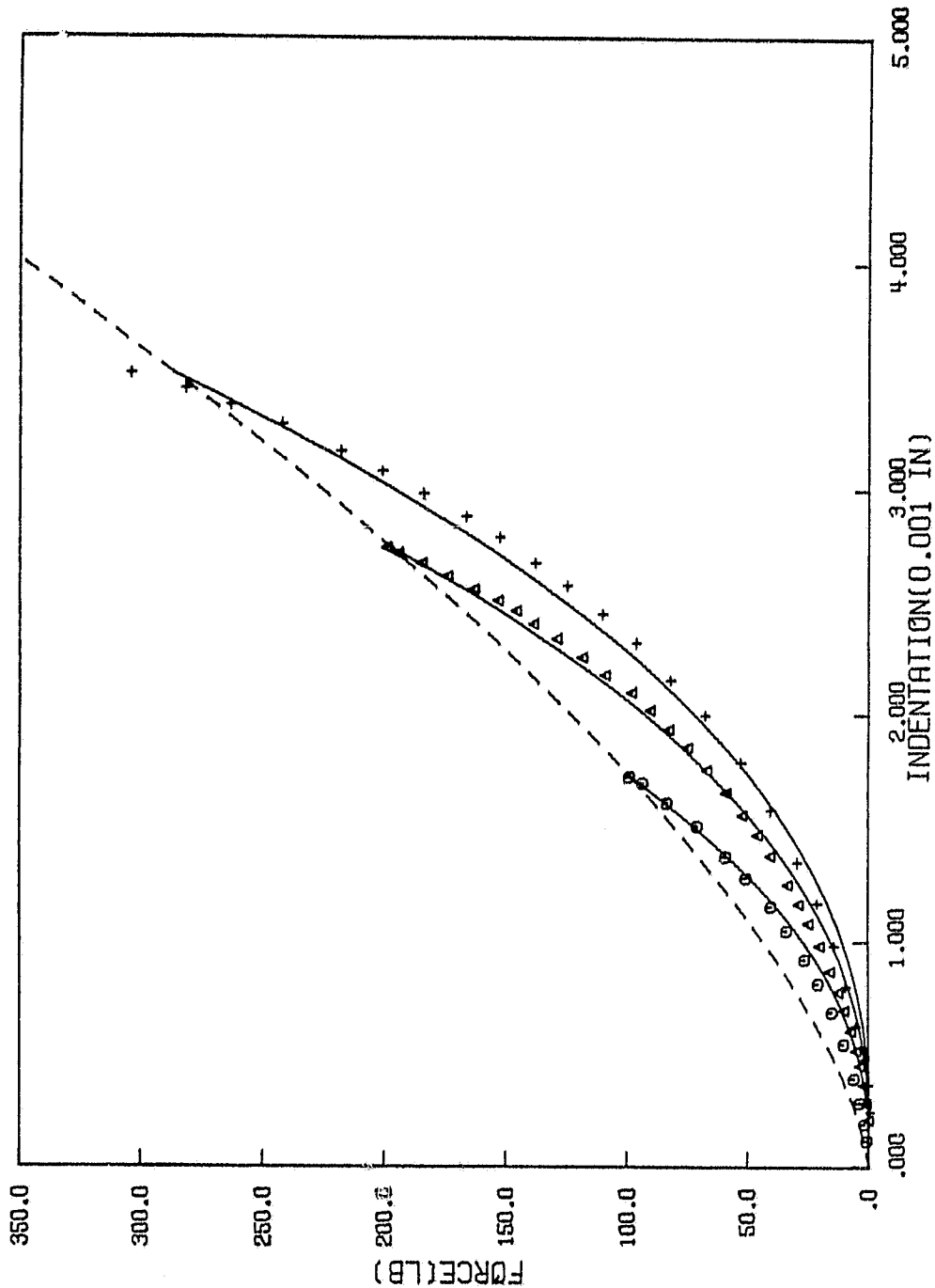


Figure 3.8 Unloading curves of $[90^\circ/45^\circ/90^\circ/-45^\circ/90^\circ]_{2s}$ specimens with 0.5 inch indenter ($q=2.2$)

ORIGINAL PAGE IS
OF POOR QUALITY

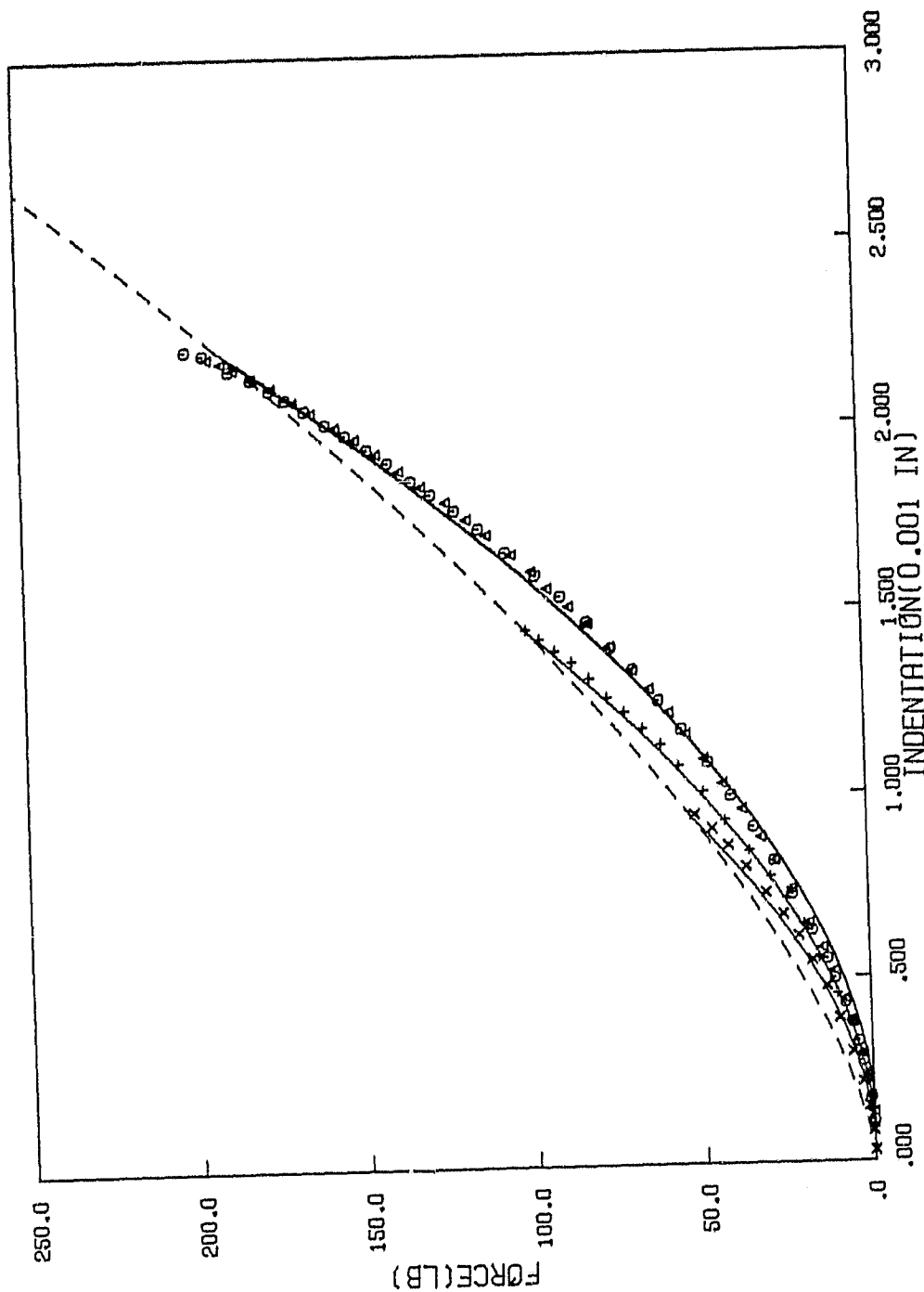


Figure 3.9 Unloading curves of $[0^\circ/45^\circ/0^\circ/-45^\circ/0^\circ]_2s$ specimens with 0.75 inch indenter ($q=1.8$)

ORIGINAL PAGE IS
OF POOR QUALITY

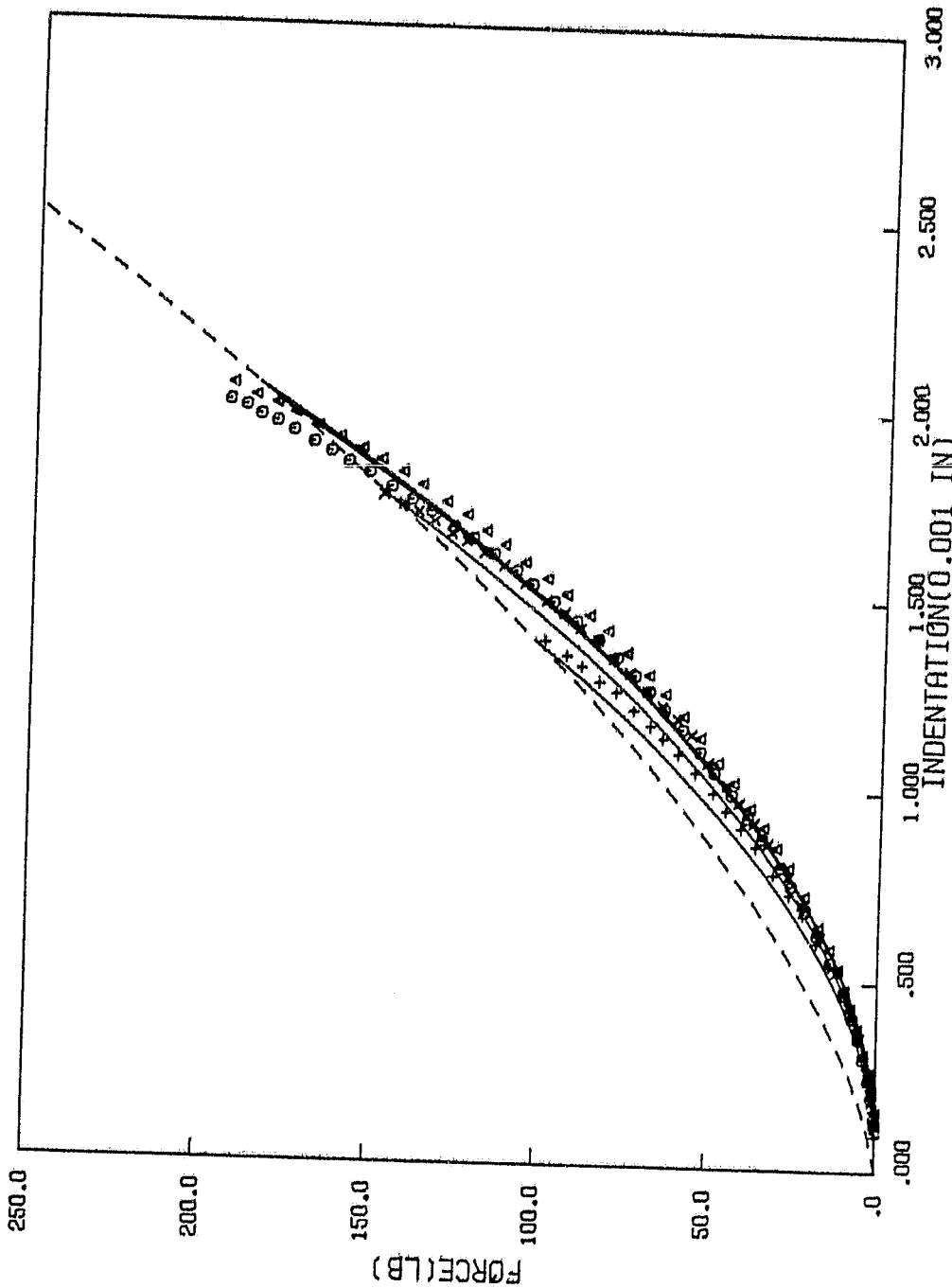


Figure 3.10 Unloading curves of $[90^\circ/45^\circ/90^\circ/-45^\circ/90^\circ]_{2s}$ specimens with 0.75 inch indenter ($q=1.8$)

ORIGINAL PAGE IS
OF POOR QUALITY

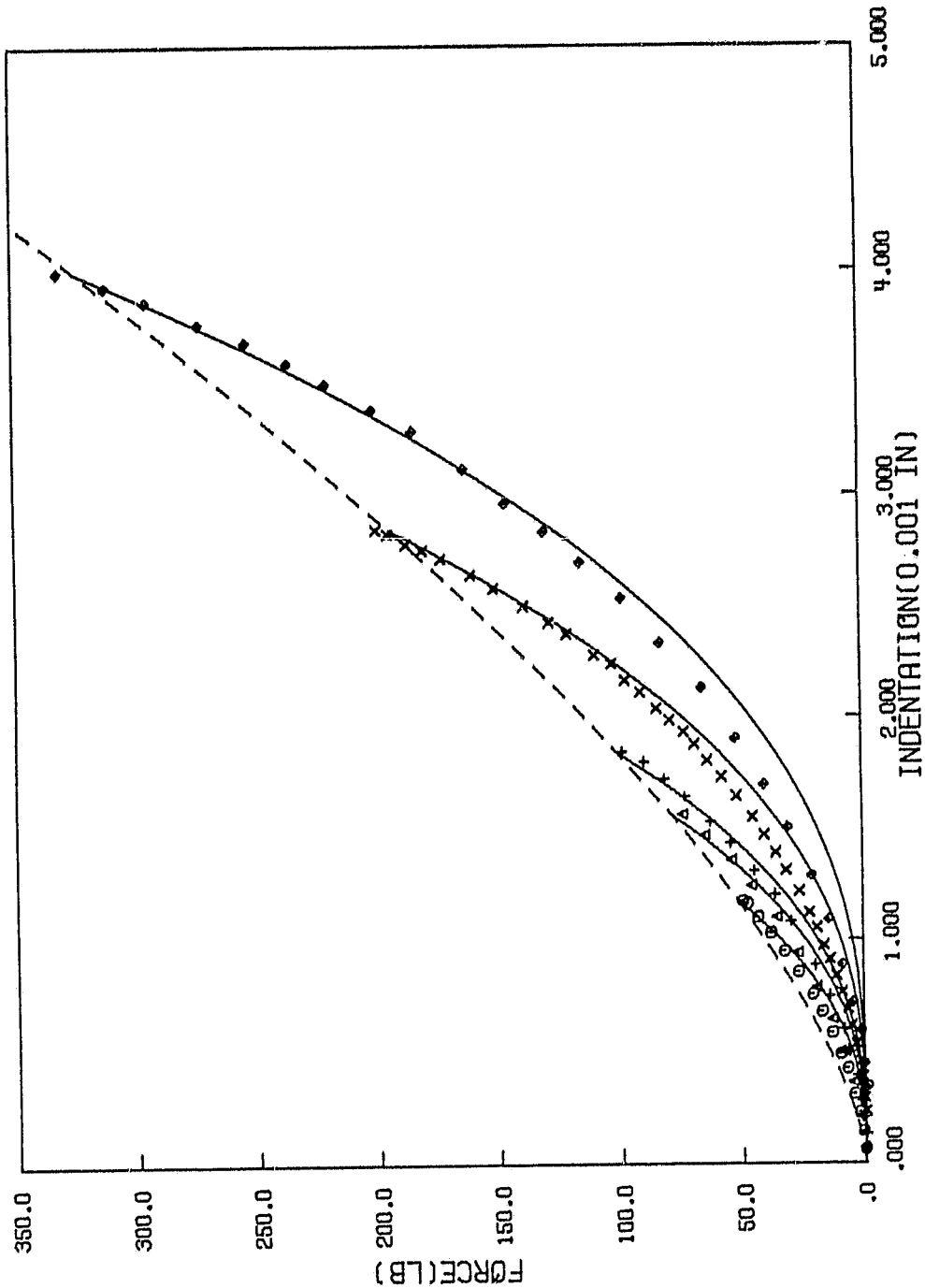


Figure 3.11 Unloading curves of $[0^\circ/45^\circ/0^\circ/-45^\circ/0^\circ]_s^2$ specimens with 0.5 inch indenter ($q=2.5$)

ORIGINAL PAGE IS
OF POOR QUALITY

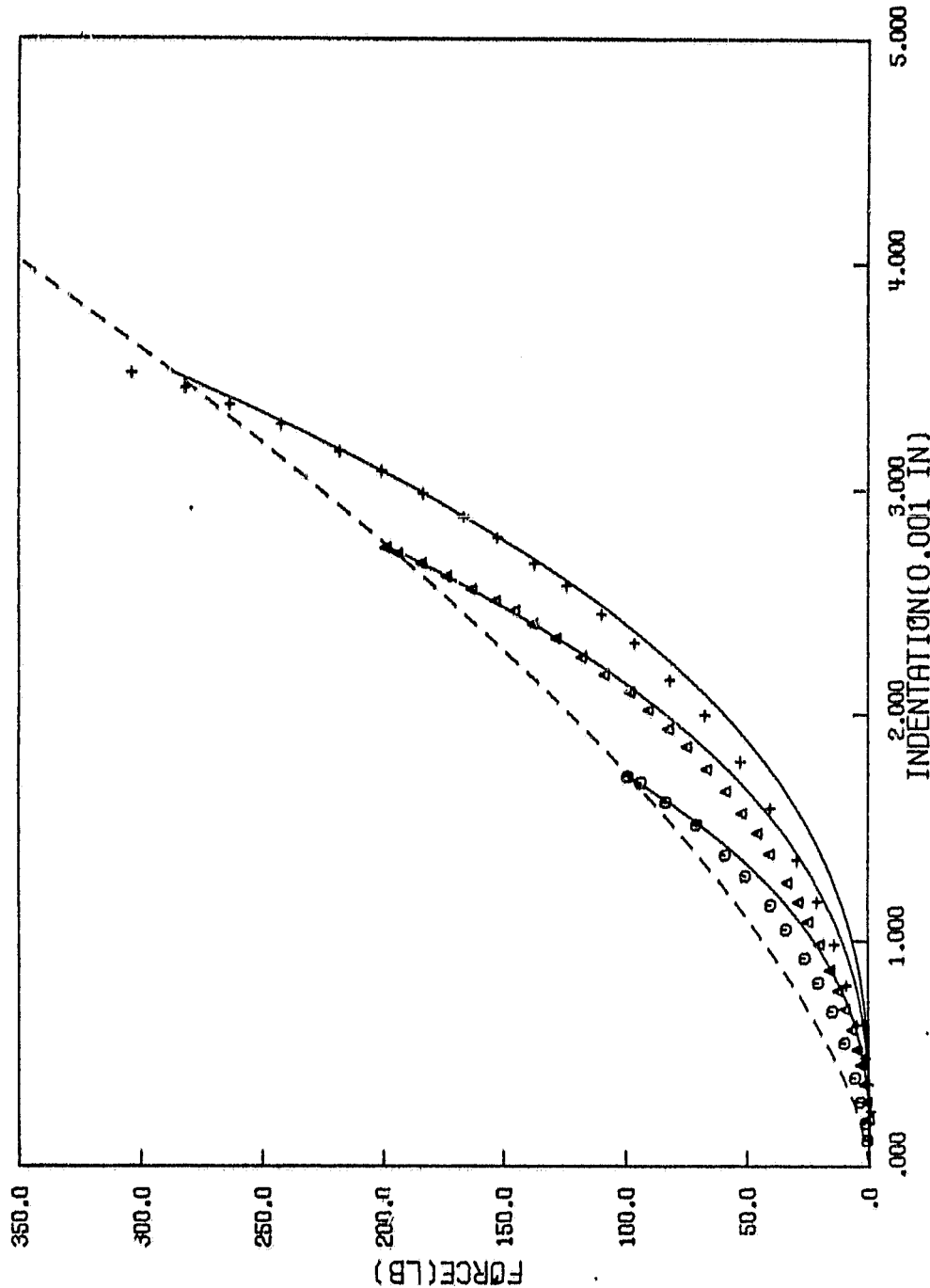


Figure 3.12 Unloading curves of $[90^\circ/45^\circ/90^\circ/-45^\circ/90^\circ]_s$ specimens with 0.5 inch indenter ($q=2.5$)

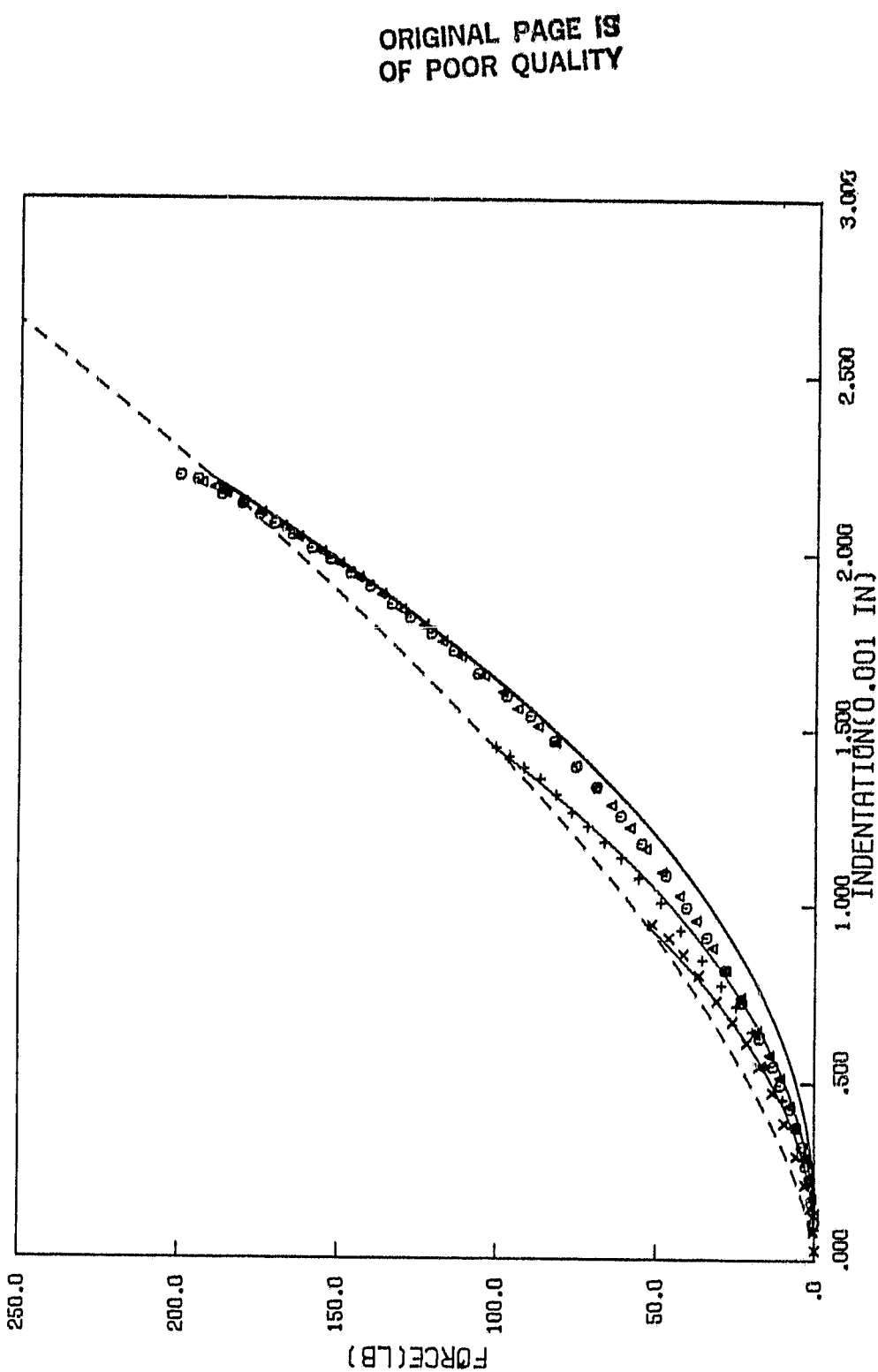


Figure 3.13 Unloading curves of $[0^\circ/45^\circ/0^\circ/-45^\circ/0^\circ]_{0.75}$ specimens with 0.75 inch indenter ($q=2.0$)

ORIGINAL PAGE IS
OF POOR QUALITY

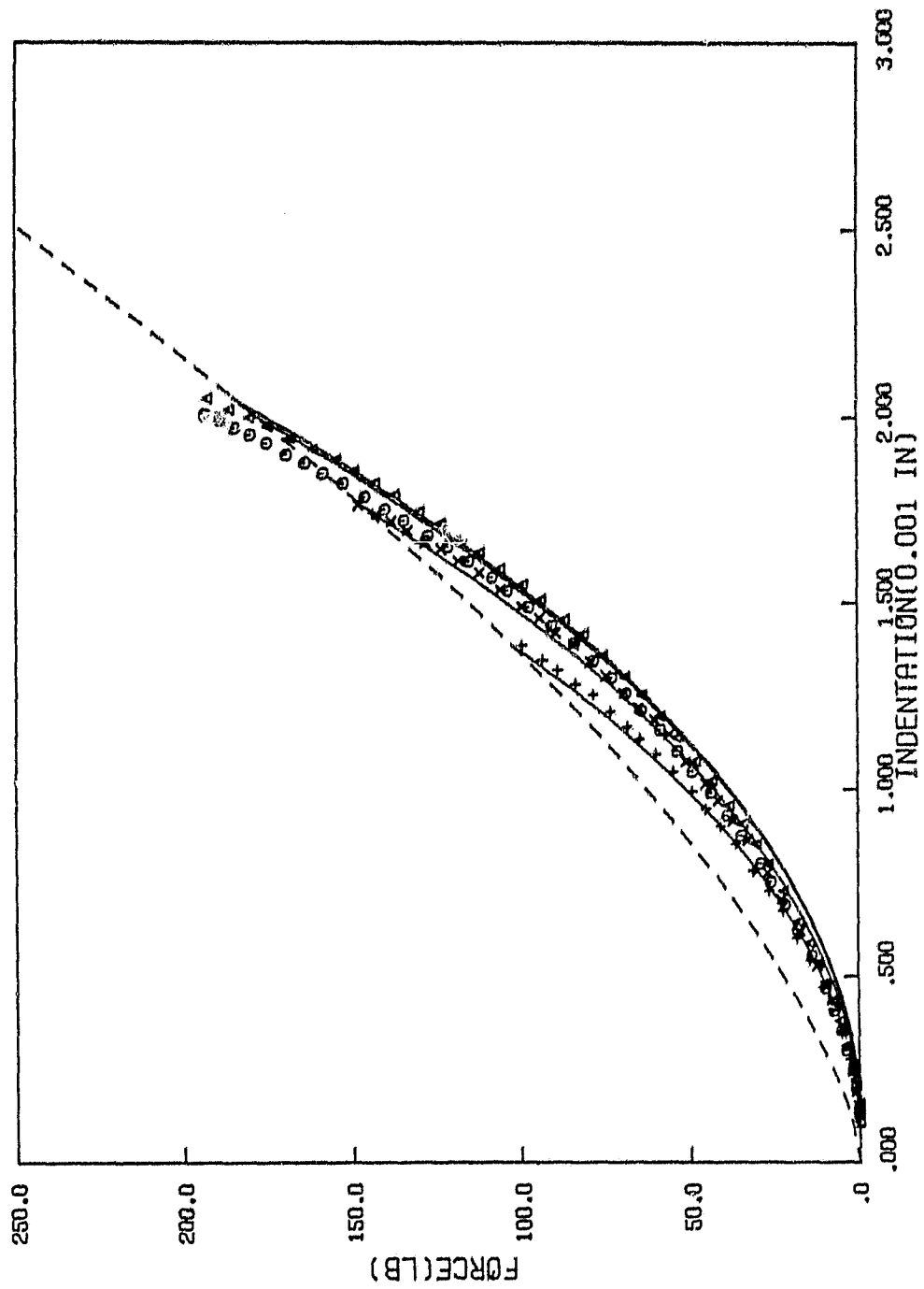


Figure 3.14 Unloading curves of [90°/45°/90°/-45°/90°]2s specimens with 0.75 inch indenter ($q=2.0$)

3.2.3 Reloading Curves

ORIGINAL PAGE IS
OF POOR QUALITY

The equation

$$F = k_1 (\alpha - \alpha_0)^p \quad (3-11)$$

suggested by Yang [14] was used to model the reloading curve, where k_1 is called reloading rigidity and $p = 3/2$ was found to fit the experimental data quite well. It was also observed that the reloading curve always returns to where the unloading began, and hence the reloading rigidity can be determined by

$$k_1 = F_m / (\alpha_m - \alpha_0)^{3/2} \quad (3-12)$$

In other words, the reloading test is not necessary provided the unloading condition is specified. Some reloading curves obtained following Equations (3-11) and (3-12), and the experimental data are presented in Figures 3.15-3.18.

3.3 Discussion

As mentioned before, due to creep the loading rate may affect the contact law (i.e. the value of k). A series of tests with different loading rates was performed to examine this point. The maximum loading rate the test equipment can apply without exceeding its capacity is about 50 lb/sec.. It was found that in the range of 5 lb/sec. to 50 lb/sec., the values of k showed very little scatter, and the effect

ORIGINAL PAGE IS
OF POOR QUALITY

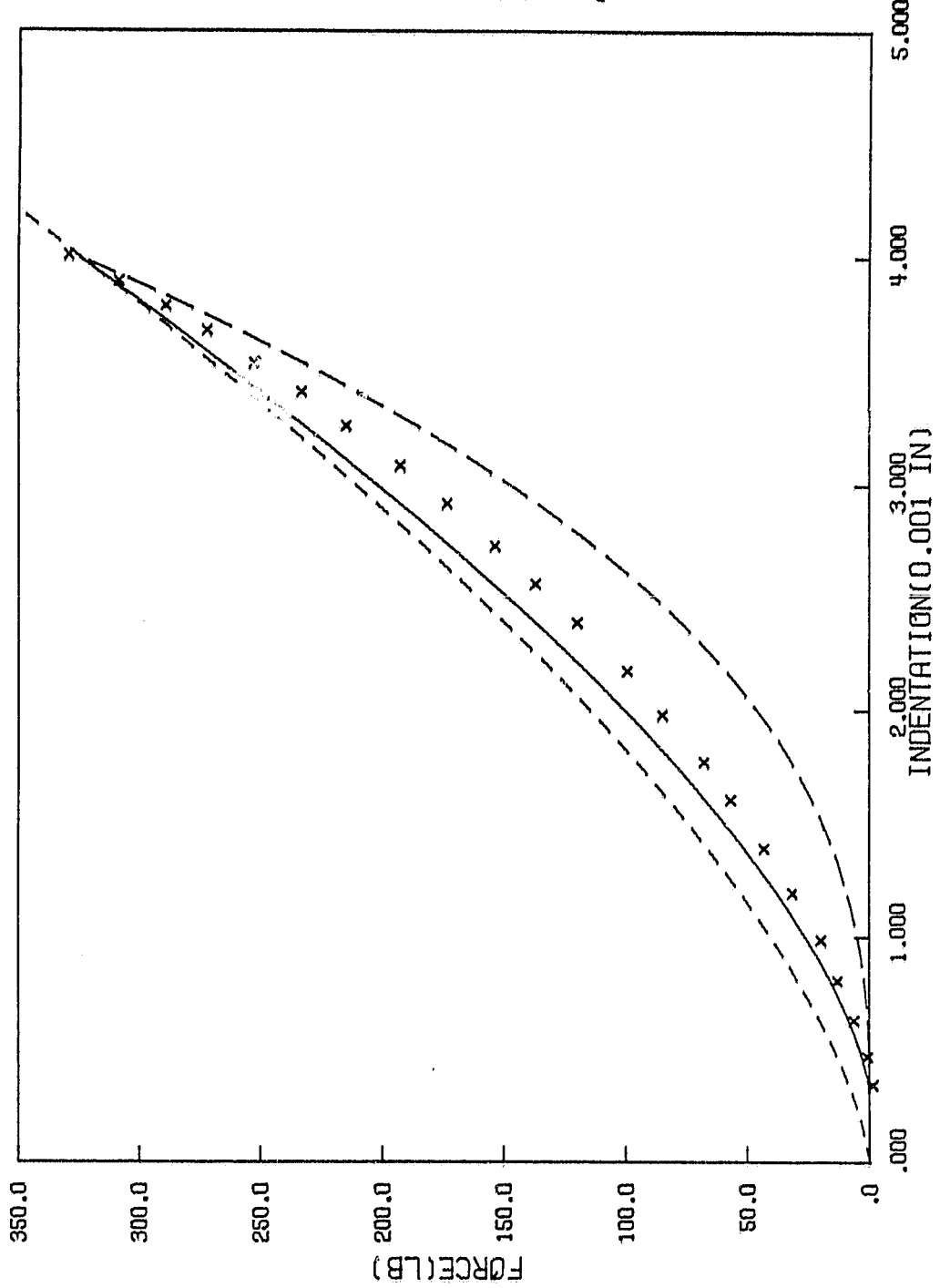


Figure 3.15 Reloading curve of $[0^\circ/45^\circ/0^\circ/-45^\circ/0^\circ]_{2s}$ specimens with 0.5 inch indenter ($P=1.5$)

ORIGINAL PAGE IS
OF POOR QUALITY

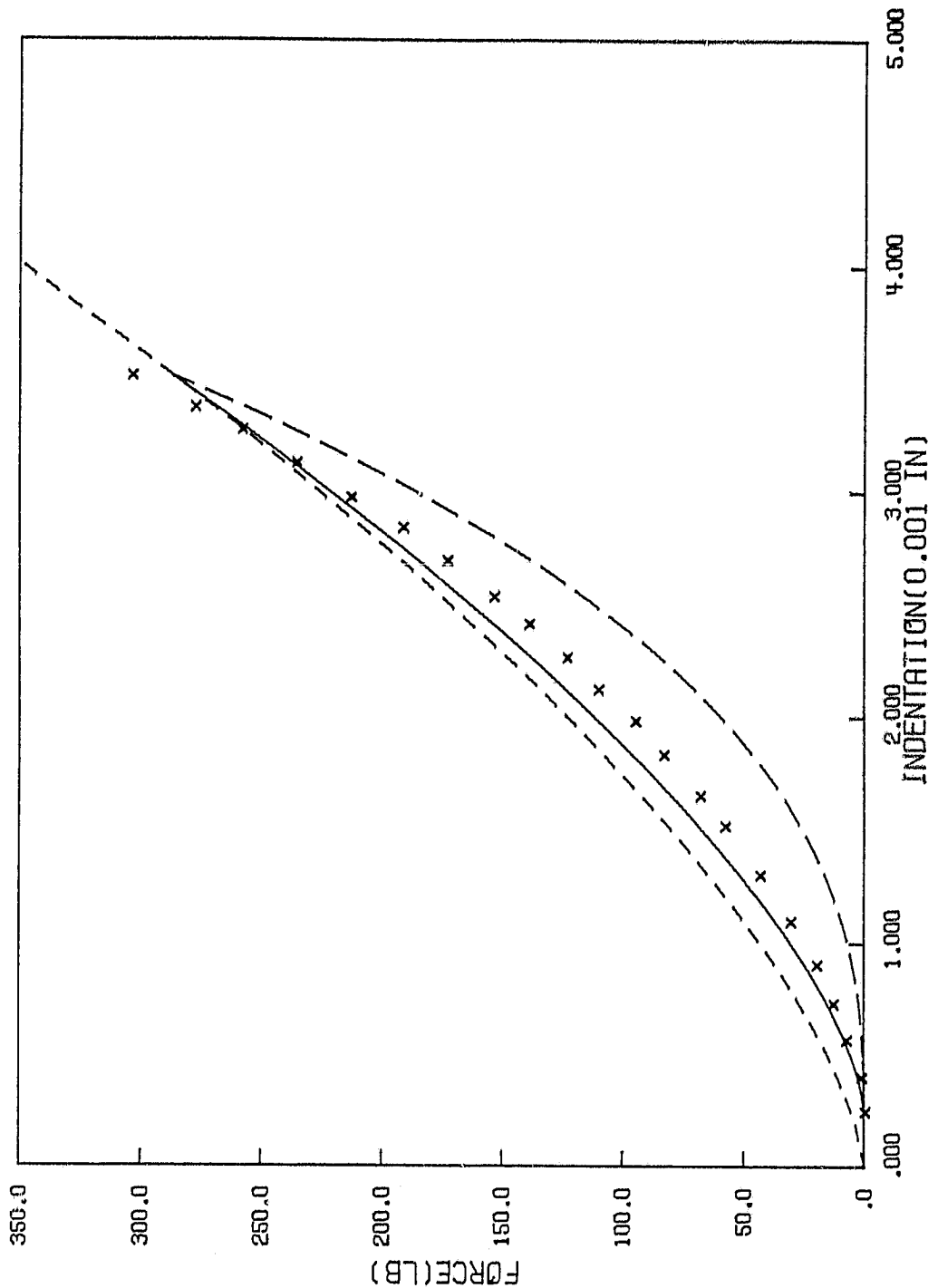


Figure 3.16 Reloading curve of [90°/45°/90°/-45°/90°]2s specimens with 0.5 inch indenter ($p=1.5$)

ORIGINAL PAGE IS
OF POOR QUALITY

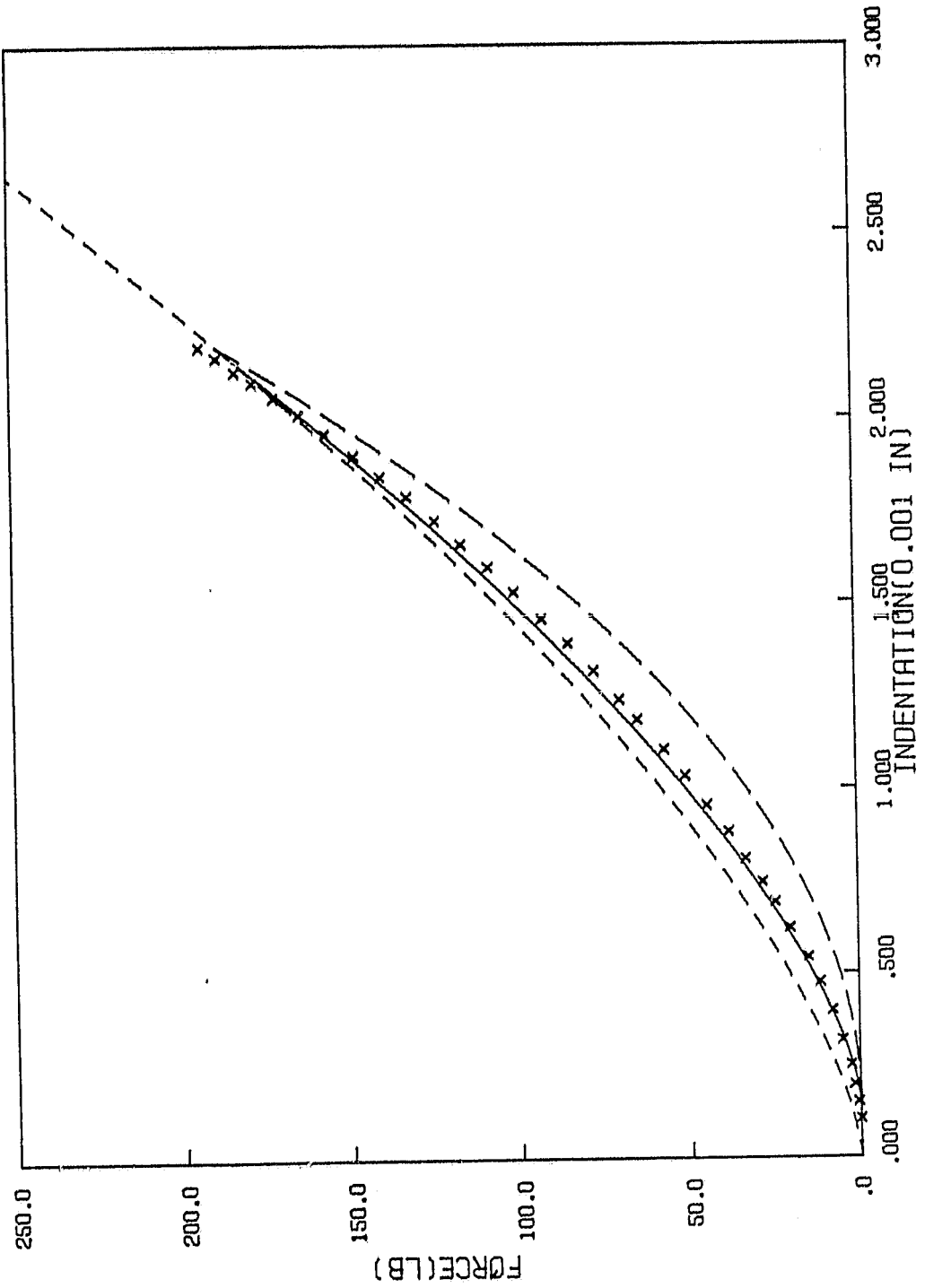


Figure 3.17 Reloading curve of $[0^\circ/45^\circ/0^\circ/-45^\circ/0^\circ]^{2S}$ specimens with 0.75 inch indenter ($p=1.5$)

ORIGINAL PAGE IS
OF POOR QUALITY

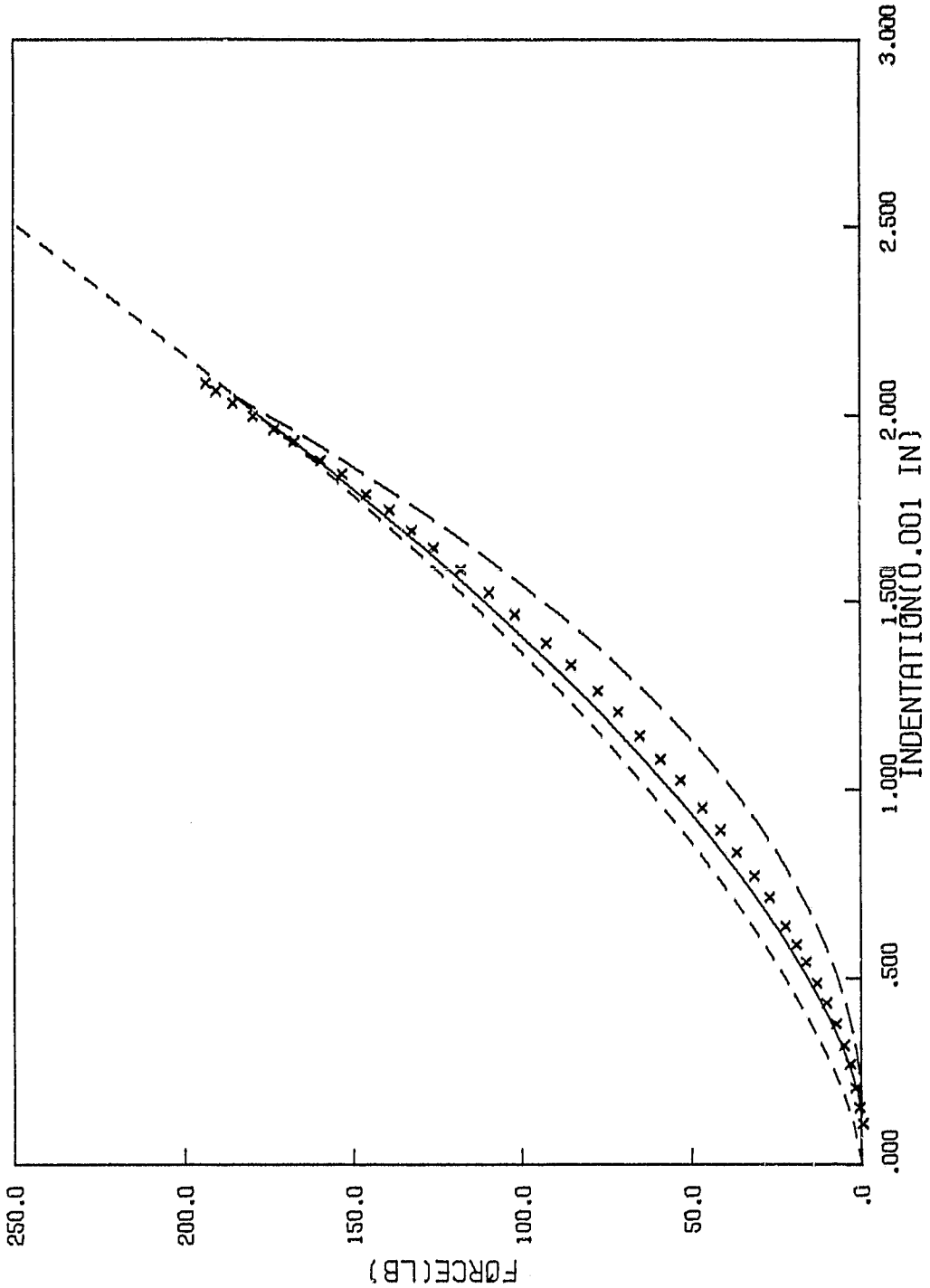


Figure 3.18 Reloading curve of [90°/45°/90°/-45°/90°]2s specimens with 0.75 inch indenter ($p=1.5$)

due to local material nonhomogeneity in the composite may be even greater than the one due to the loading rate. However, an appreciable decrease of the value k was observed when the loading rate was lower than 1 lb/sec.. In some extreme cases where loadings were applied as slow as 10 lb/min., the average value of k for 0.5 in. indenter was very close to the one obtained previously by Yang [14] using dial gage to measure the indentation. In this study, the loading rates for all tests were approximately equal to 10 lb/sec..

Unlike the exponent n of the loading law for which the value of $3/2$ seems to yield good agreement with all experimental data, the exponent q of the unloading law (Equation 3-3 or 3-4) reveals much wider deviation for different sizes of indenter. Value of $q = 3/2$ corresponding to an elastic recovery according to the Hertzian theory was previously used by Crook [28] in a study of impacts between metal bodies. The experimental results from [14] and present study show that the value of q varies from 1.5 to 2.5. Local plastic deformation, anisotropic properties of composite material and unloading rate are all possible causes for this deviation. Obviously, an analytical study to determine the value of q as function of aforementioned factors is impracticable. Since the purpose of this study is to establish a contact law that can be used in the analysis of impact, the validity of this law must be verified from impact experiment. This will be investigated

In the next chapter.

ORIGINAL PAGE IS
OF POOR QUALITY

From Equation (3-3) or (3-4), it can be seen that α_0 plays an essential role in the unloading law and hence the value of it must be estimated accurately. Both of Equation (3-7) used by Yang [14] and Equation (3-8) used in this study for calculating α_0 were obtained experimentally, in which α_{cr} and α_p are considered to be material constants and were determined using α_0 and α_m from test data. However, it was pointed out in [14] that the values of α_0 might not be the true permanent indentations. They were the values which could make the power law given by Equation (3-4) fit the total data under the unloading path. In fact, the load corresponding to the value of $\alpha_{cr} = 3.16 \times 10^{-3}$ in. obtained in [14] is about 200 lb. for 0.5 in. indenter, which is apparently too high. The value of $\alpha_p = 6.564 \times 10^{-4}$ in. obtained in this study, which corresponds to about 20 lb of loading, seems more reasonable as a critical value in indentation. For comparison, the relations between unloading rigidity s and maximum indentation α_m using Equation (3-7) with $\alpha_{cr} = 3.16 \times 10^{-3}$ in. and Equation (3-8) with $\alpha_p = 6.564 \times 10^{-4}$ in., respectively, are plotted in Figure 3.19. It is interesting to see that these two equations give almost the same values of s up to $\alpha_m = 4 \times 10^{-3}$ in. which is approximately the maximum indentation before failure could occur to the specimen. The advantage of using Equation (3-7) for the formulation of the unloading law is

ORIGINAL PAGE IS
OF POOR QUALITY

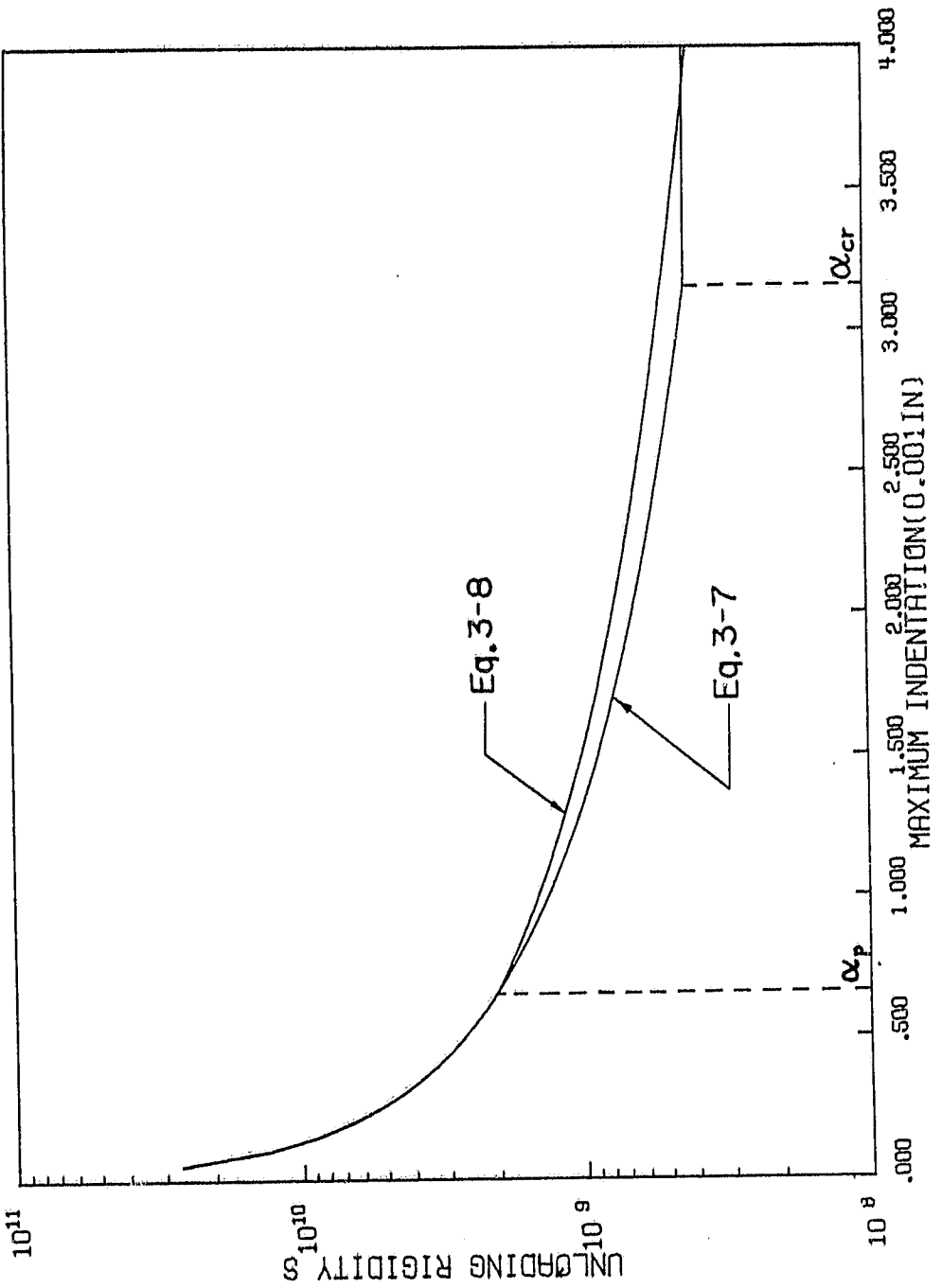


Figure 3.19 Unloading rigidity s as function of maximum indentation

that the value of s is constant for any α_m once the indentation passes α_{cr} , and only one unloading test is necessary to determine α_{cr} provided the load is high enough to produce permanent indentations. The use of Equation (3-9) needs performing many tests to obtain a proper relation between α_0 and α_m according to Equation (3-8). However, it should be noted that Equation (3-7) is valid only if $q = 5/2$ is used in the unloading equation (3-4), while Equation (3-8) has no such restriction.

ORIGINAL PAGE IS
OF POOR QUALITY

ORIGINAL PAGE IS
OF POOR QUALITY

CHAPTER 4

IMPACT EXPERIMENTS

High velocity impacts usually result in very small contact time and the material under impact loadings may behave differently from static contact due to the strain rate effect. The statically determined contact laws presented in the previous chapter thus must be verified experimentally before it can be applied to the impact analysis. Wang [15] has conducted many impact experiments on laminated composite beams and plates using spherical steel balls as impactors. The strain response histories at various points on the specimens were recorded and compared with the finite element analysis with which the contact laws obtained by Yang [14] was incorporated. The results showed that the test data agreed with the predictions using the statical indentation laws quite well. In this chapter, an attempt was made to measure the contact force directly so that the applicability of statical contact laws in impact analysis can be further evaluated.

ORIGINAL PAGE IS
OF POOR QUALITY

4.1 Experimental Procedure

A 6 in. by 4 in. laminated plate cut from a $[0^\circ/45^\circ/0^\circ/-45^\circ/0^\circ]_2s$ graphite/epoxy panel was used as the impact target. The 0° -direction was arranged to parallel the long side of the plate. Seven strain gages (Micro Measurement Company TYPE EA-13-062 AQ 350) were placed at different locations as shown in Figure 4.1 to record the dynamic strain histories. One of the gages was placed on the surface directly opposite to the impact point to trigger the oscilloscope. This plate was hung with two strings at two corners to achieve the free boundary condition.

The projectile was made of an impact-force transducer with a spherical steel cap of 0.75 inch in diameter glued on the impact side and a steel rod of 5/8 inch in diameter glued on the other side as shown in Figure 4.2. It was then attached to a thin rod to form a pendulum which could produce impact velocities up to 150 in/sec. The total mass of the projectile is $0.000181 \text{ lb-sec}^2/\text{in}$.

The schematic diagram for this impact experimental set-up is shown in Figure 4.3. Signals from gages and transducer were amplified by a 3A9 Textronix amplifier and displayed on the screen of an oscilloscope.

ORIGINAL PAGE IS
OF POOR QUALITY

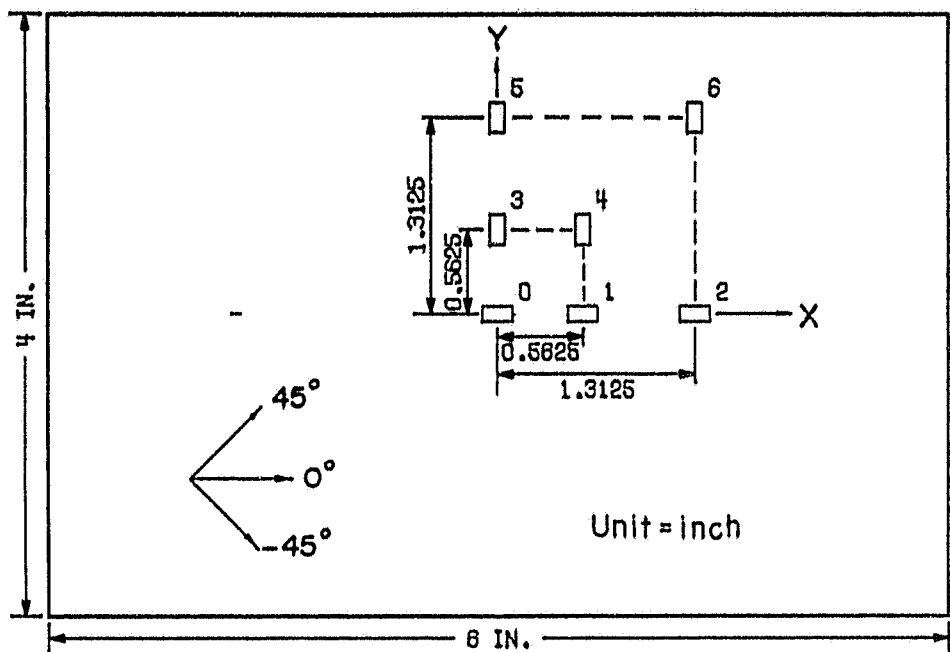
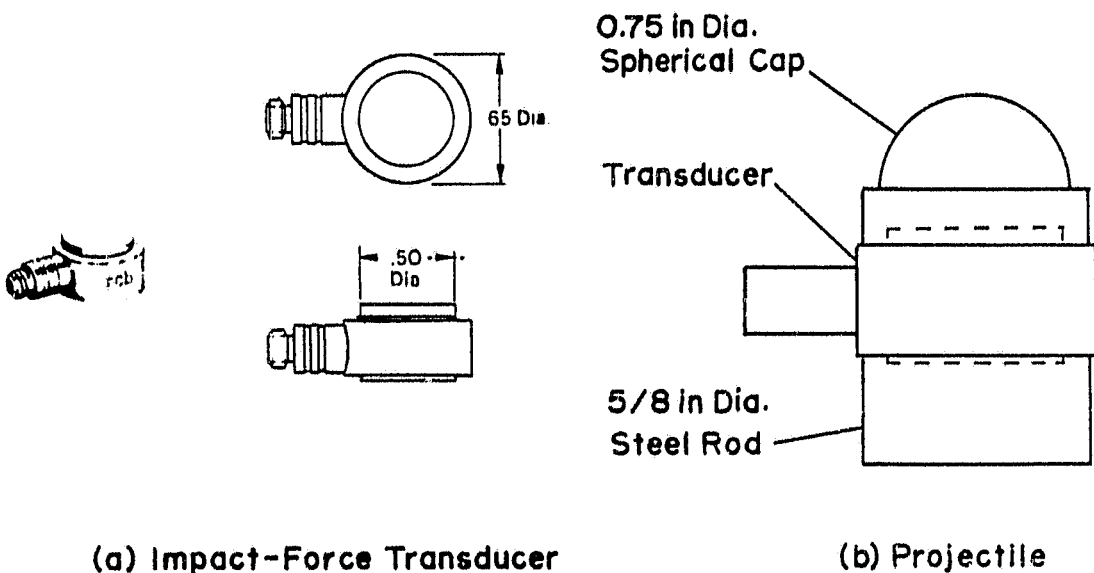


Figure 4.1 Laminate dimension and strain gage locations



(a) Impact-Force Transducer

(b) Projectile

Figure 4.2 Graphical illustration of impact projectile

ORIGINAL PAGE IS
OF POOR QUALITY.

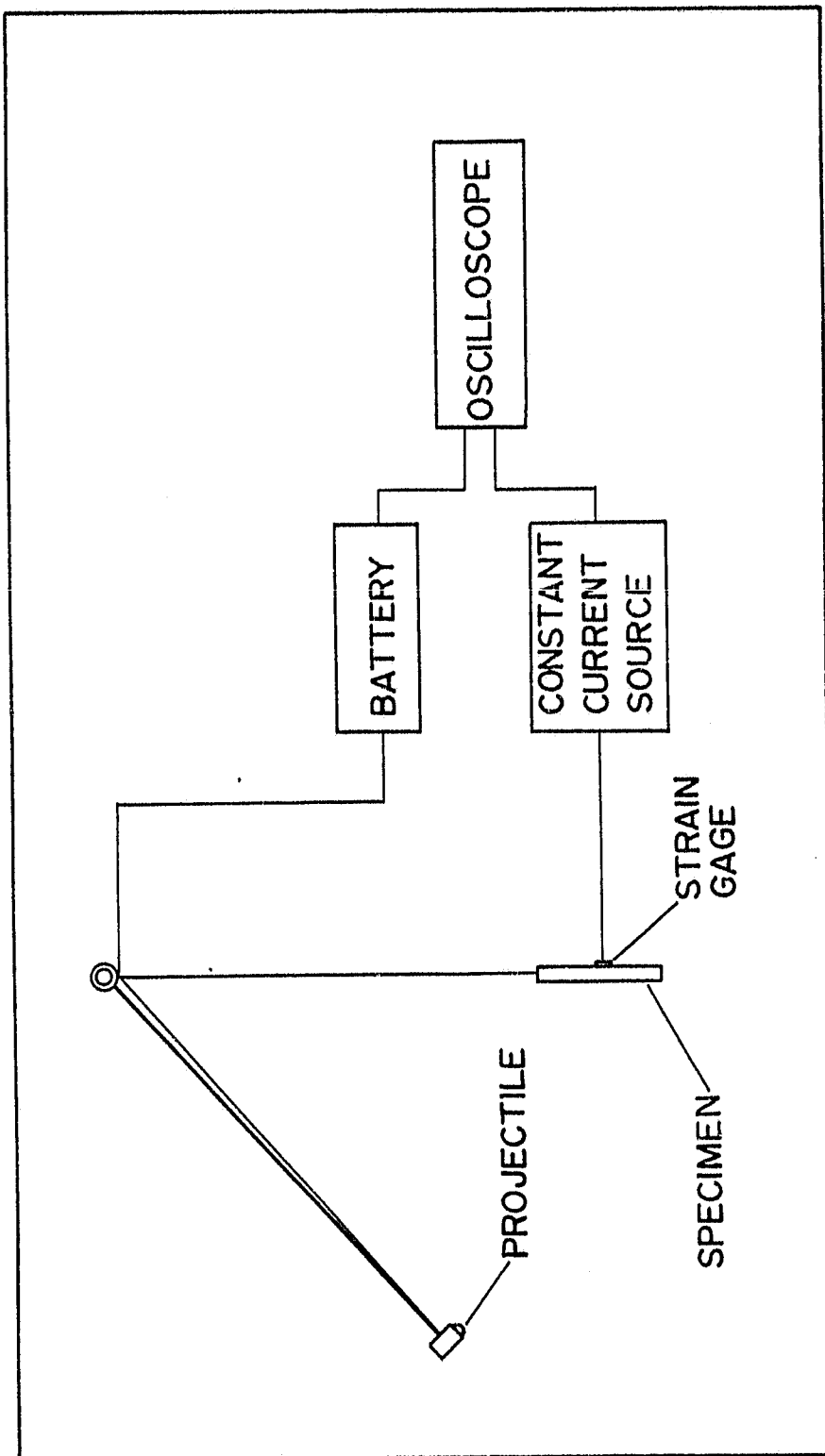


Figure 4.3 Schematic diagram for the impact experimental set-up

4.2 Calibration of Impact-Force Transducer

ORIGINAL PAGE IS
OF POOR QUALITY

The Impact-force transducer used was Model 200A05 marketed by PCB Piezotronics Inc. Some of it's specifications are shown in Table 4.1 [30]. The structure of this transducer contains two thin quartz disks operating in a thickness compression mode and sandwiched between hardened steel cylindrical members. A built-in amplifier can reduce the high impedance of the voltage from the quartz element and provides an output voltage which can be read out on oscilloscope, recorder, etc.. The impact force is then computed using the equation,

$$F = V_F/c_F \quad (4-1)$$

where V_F is the output voltage and c_F is the sensitivity of the transducer. Since the value of c_F in Table 4.1 was obtained under quasi-static condition [30], it must be verified under impact condition first so that later the results from impact experiment can be correctly interpreted.

A circular cylindrical steel rod of 2 inch in diameter and 1.19 inch long hung on strings was used as the impact target to calibrate the transducer. The acceleration of the rod was measured by using a Model 302A accelerometer which was mounted on the end of the rod opposite to the impacted end as shown in Figure 4.4. The total weight of the target is 1.105 lb.

**ORIGINAL EDITION
OF POOR QUALITY**

Table 4.1
Specifications for Model 200A05 Impact-Force Transducer

Range, Compression (5V output)	lb.	5,000
Maximum Compression	lb.	10,000
Resolution (200 μ V p-p noise)	lb.	0.2
Stiffness	lb/ μ in	100
Sensitivity	mV/lb	1.0
Resonant Frequency (no load)	Hz	70,000
Rise Time	μ sec	10
Discharge Time Constant (T.C.)	sec	2,000
Low-Frequency (-5%)	Hz	0.0003
Linearity, B.F.S.L.	%	1
Output Impedance	ohms	100
Excitation (thru C.C.diode)	VDC/mA	+18 to 24/2 to 20
Temperature Coefficient	%/ $^{\circ}$ F	0.03
Temperature Range	$^{\circ}$ F	-100 to +250
Shock (no load)	g	10,000

ORIGINAL PAGE IS
OF POOR QUALITY

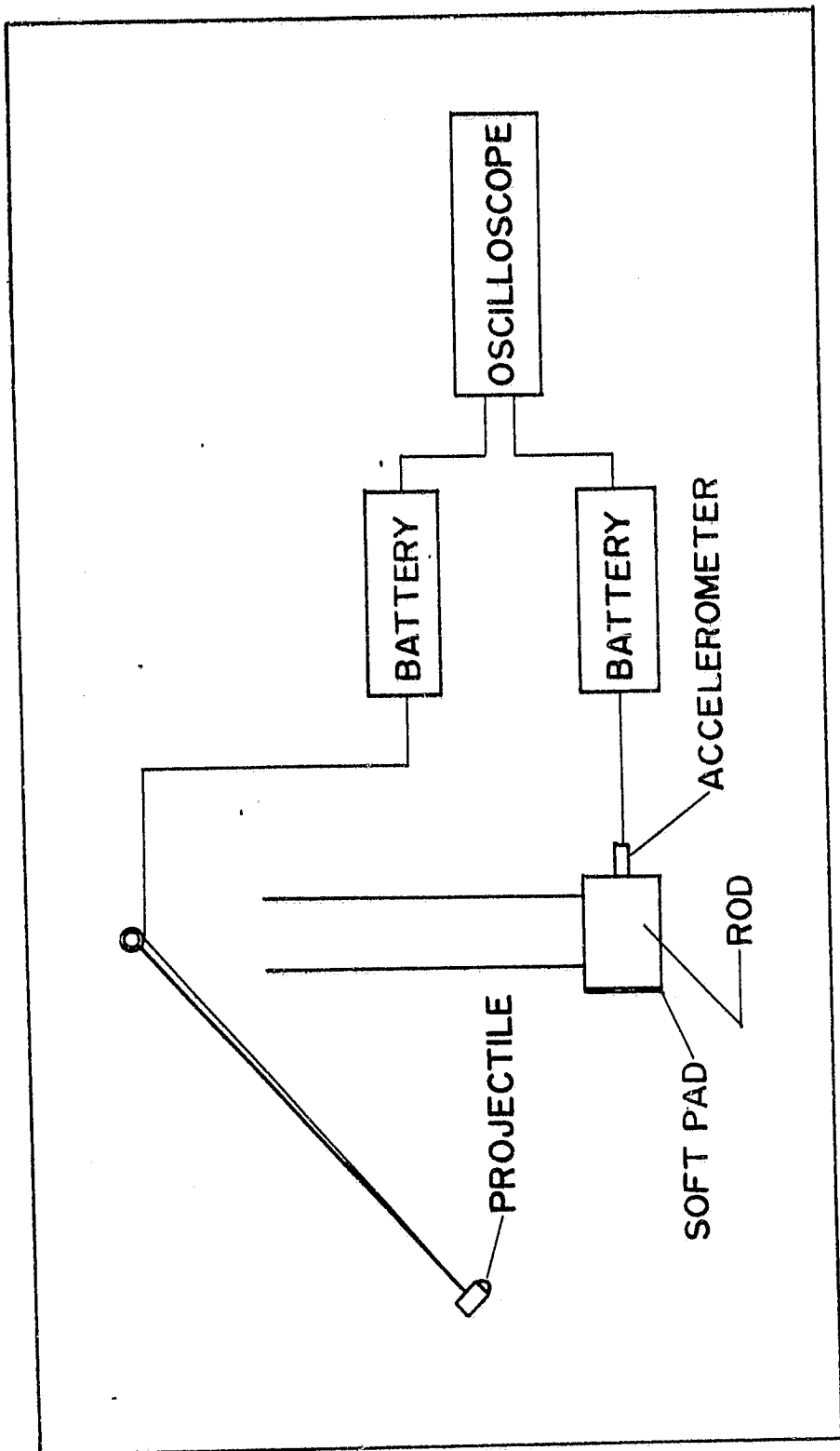


Figure 4.4 Experimental set-up for the calibration of impact-force transducer

C - 2

Using Equation (4-1) and

$$a = V_a/c_a \quad (4-2)$$

$$F = ma \quad (4-3)$$

we obtain

$$c_F = (c_a/m)(V_F/V_a) \quad (4-4)$$

where V_a and c_a are the output voltage and the sensitivity of the accelerometer, respectively, a is acceleration of the target, and m is the mass of the target.

When impacting a metal projectile on a metal target with no pad on the impact surface, a high frequency ringing can be seen at the output of the transducer. In order to obtain smooth output curves, a soft pad was placed on the impact region of the target to eliminate the high frequency ringing. The cause of this ringing phenomenon will be discussed later. Typical output voltages of transducer and accelerometer read from the oscilloscope are shown in Figure 4.5. Values of V_F were plotted vs the corresponding values of V_a taken from these two curves at several discrete points in time and then fitted into a straight line as shown in Figure 4.6. The slope of this line represents the ratio of V_F/V_a which is then substituted in Equation (4-4) to calculate the sensitivity c_F .

ORIGINAL PAGE IS
OF POOR QUALITY

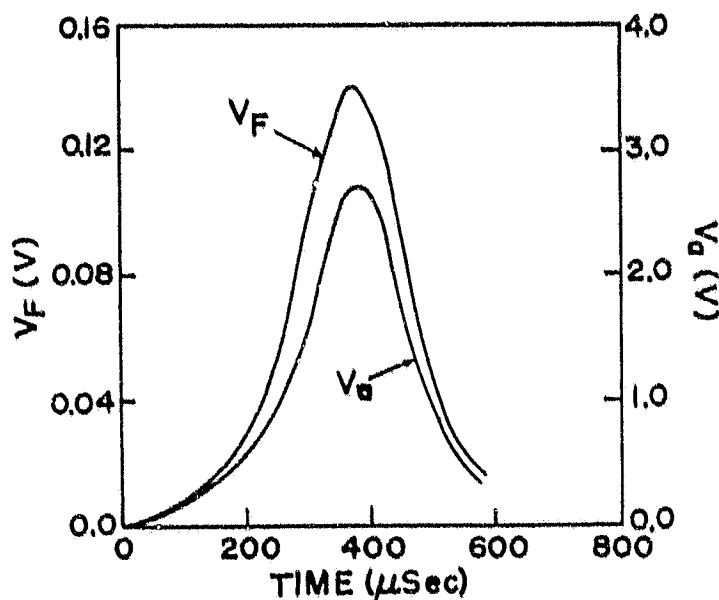


Figure 4.5 Typical output voltages from transducer and accelerometer

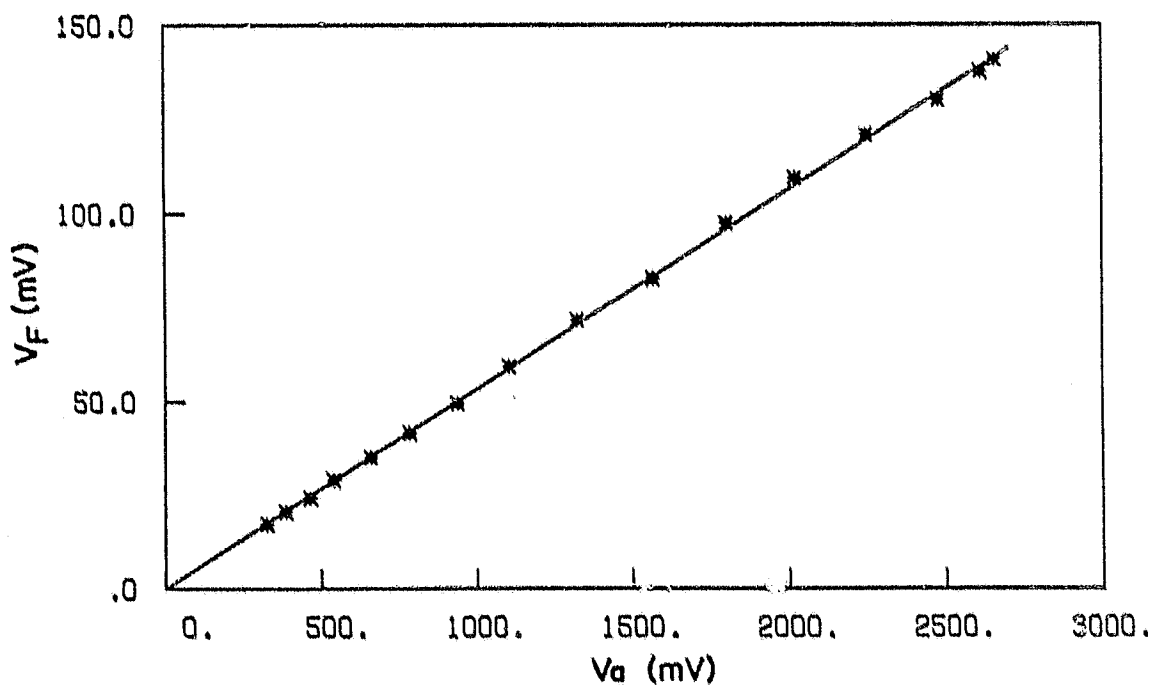


Figure 4.6 Relation between V_F and V_a

Assuming the sensitivity of the accelerometer c_a is correct, and using Equation (4-4) and the test data, the average value of c_F calculated was 0.494 mV/lb.. A comparison with the value of 1.0 mV/lb from Table 4.1 shows that the test result has more than 50% error. However, since the quartz elements are located at the center of the projectile while the impact force is applied at the end, we were not certain that the force history picked up by the quartz elements did represent the real history of the impact force. The following simple analysis was performed to examine this uncertainty.

Consider a 1 in. long steel rod with free-free boundary conditions. For a impulse loading given by

$$F(t) = F_0 \exp[-(t-\tau)^2/4b^2] \quad (4-5)$$

at one end, the force history at the midpoint of the rod, $F_m(t)$, was computed and plotted in Figure 4.7 together with the applied force history. It should be noted that the values of $F_0 = 1000$ lb., $\tau = 200 \times 10^{-6}$ sec. and $b = 40 \times 10^{-6}$ sec. were chosen in Equation (4-5) so that the applied force history is similar to the experimental loading histroy. From Figure 4.7, it can be seen that $F_m(t)$ is only about half of the applied force $F(t)$. The average ratio of $F_m(t)/F(t)$ was obtained to be 0.498, which is very close to the value of c_F obtained previously. The accelerations at the two ends and the midpoint of the rod were also

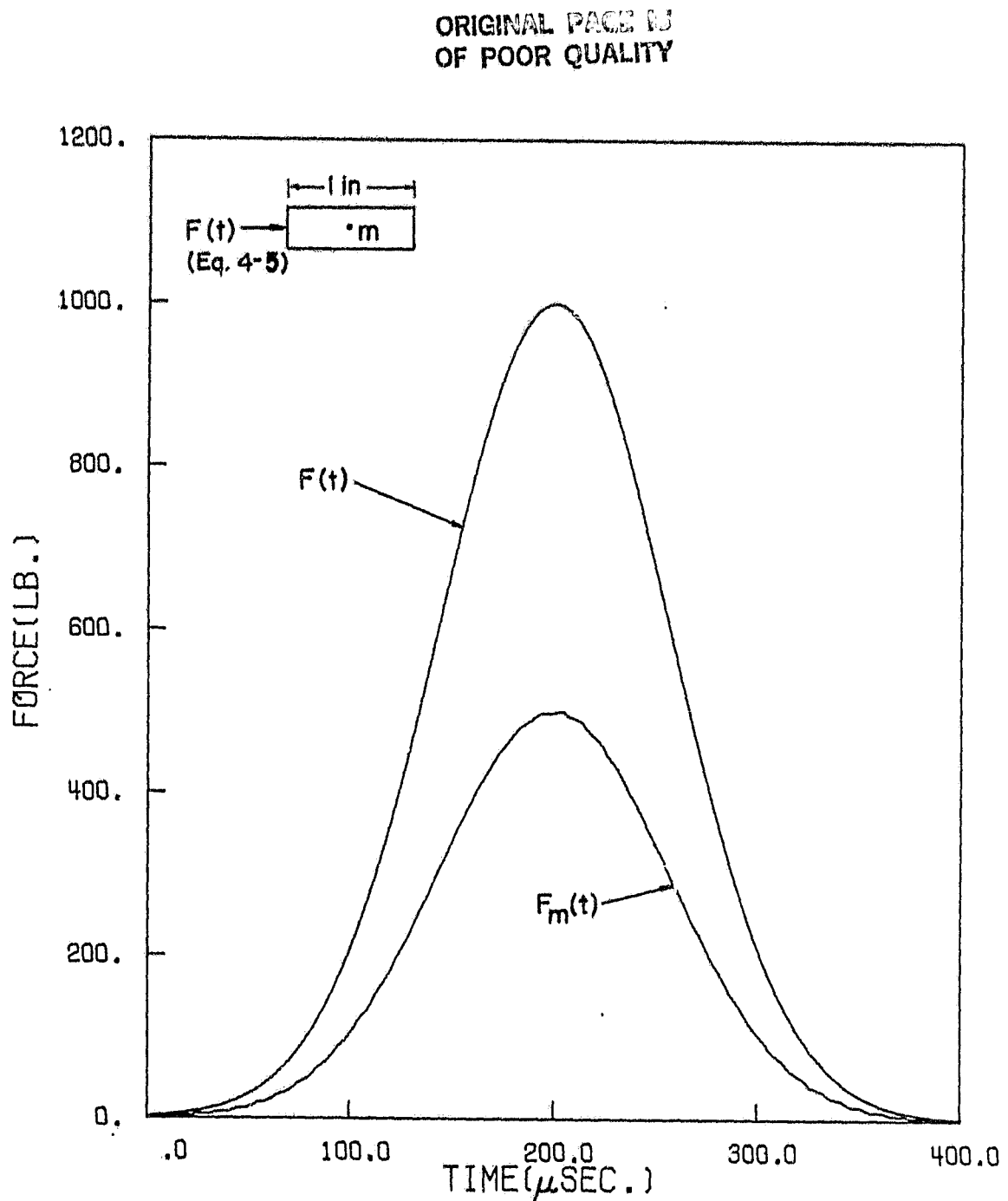


Figure 4.7 Assumed exponential impulsive loading and the response history at the midpoint of the rod

calculated and plotted in Figure 4.8. It shows that the magnitudes of acceleration at any position of the rod have virtually no difference. This indicates that the accelerometer did measure the real acceleration of the target while the impact-force transducer only picked up the force history at the point of its own position. In other words, the wave motion in the projectile can not be neglected, hence it must be treated as an elastic body.

Repeating the previous analysis by changing the impulse loading of Equation (4-5) to

$$F(t) = F_0 \sin(\pi t/b) \quad (4-6)$$

and letting $F_0 = 1000$ lb. and $b = 400 \times 10^{-6}$ sec., we obtain the force history at the midpoint of the rod as shown in Figure 4.9. Comparing Figure 4.9 with Figure 4.8, it is clear that the initial slope of the impulse forcing function would affect the amplitude of ringing. The steeper the initial slope is, the higher the amplitude of ringing will be. When impacting the steel projectile on graphite/epoxy surface, this ringing phenomenon was also observed.

ORIGINAL PAGE IS
OF POOR QUALITY

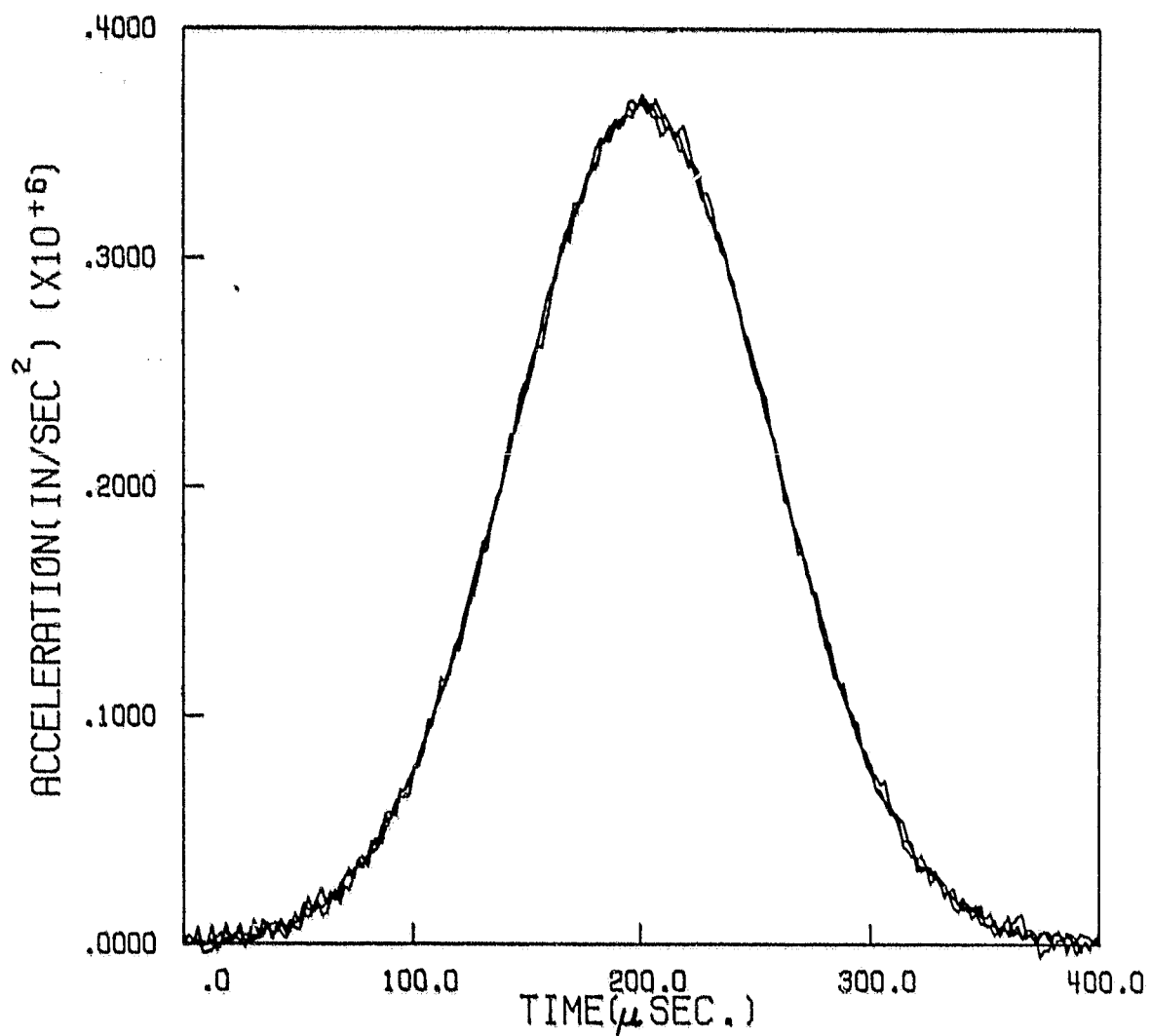


Figure 4.8 Accelerations of rod for assumed exponential impulsive loading

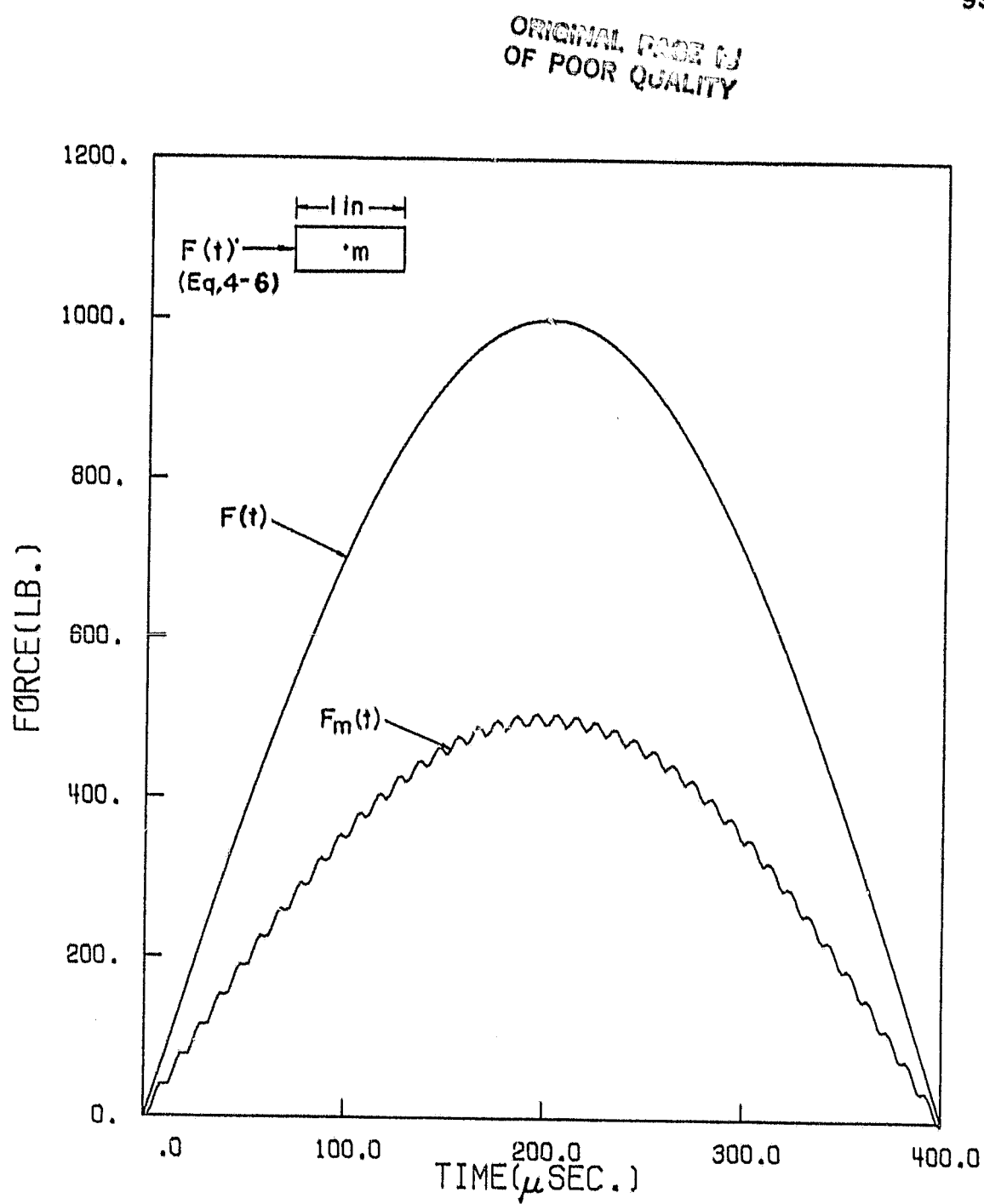


Figure 4.9 Assumed sine-function impulsive loading and the response history at the midpoint of the rod

4.3 Finite Element Analysis

ORIGINAL PAGE IS
OF POOR QUALITY

4.3.1 Plate Finite Element

A 9-node Isoparametric plate finite element (see Figure 4.10) developed by Yang [31] based upon the laminate theory of Whitney and Pagano [18] was used to model the dynamic motion of the laminated plate. At each node there are five degrees of freedom. Among them, u^0 , v^0 and w are displacement components of mid-plane in the x -, y - and z -direction, respectively, and ϕ_x and ϕ_y are rotations of the cross-sections perpendicular to the x - and y -axis, respectively. For symmetric laminates, the flexural deformation is uncoupled from the in-plane extensional and shear deformations, and hence, the degrees of freedom corresponding to u^0 and v^0 can be neglected in the transverse impact problem.

The Isoparametric plate finite element is developed using the following shape functions:

For corner nodes:

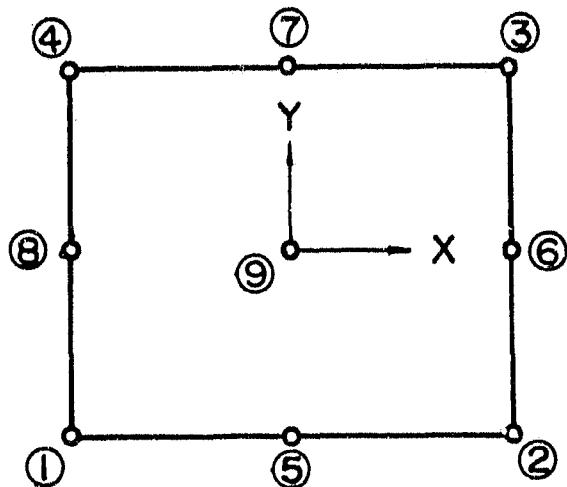
$$S_1 = (1/4)(1+\xi_0)(1+\eta_0)(\xi_0+\eta_0-1) + (1/4)(1-\xi^2)(1-\eta^2) \quad (4-7)$$

For nodes at $\xi = 0$ and $\eta = \pm 1$:

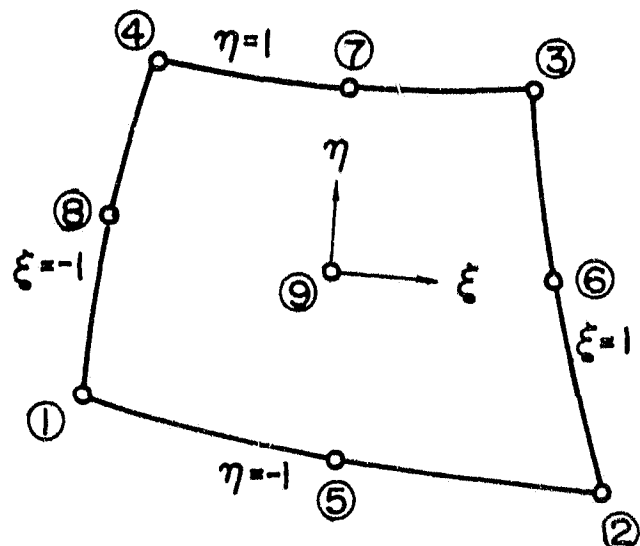
$$S_1 = (1/2)(1-\xi^2)(\eta_0+\eta^2) \quad (4-8)$$

For nodes at $\xi = \pm 1$ and $\eta = 0$:

ORIGINAL PLATE IS
OF POOR QUALITY



(a) PARENT ELEMENT



(b) DISTORTED ELEMENT

Figure 4.10 9-node isoparametric plate element

$$S_1 = (1/2)(\xi_0 + \xi^2)(1 - \eta^2) \quad \text{ORIGINAL PAGE IS OF POOR QUALITY} \quad (4-9)$$

For the center node:

$$S_1 = (1/2)(1 - \xi^2)(1 - \eta^2) \quad (4-10)$$

In the above shape functions, ξ and η are normalized local coordinates, and

$$\xi_0 = \xi\xi_1, \quad \eta_0 = \eta\eta_1 \quad (4-11)$$

where ξ_1 and η_1 are the natural coordinates of node 1 (Figure 4.10).

Using the shape functions, the plate displacements w , ϕ_x and ϕ_y are approximated by

$$\begin{bmatrix} w \\ \phi_x \\ \phi_y \end{bmatrix} = \sum_{i=1}^9 [S_i] \{q_p\}_i \quad (4-12)$$

where $\{q_p\}_i$ is the nodal displacement vector at node i and

$$[S]_i = S_i [I]^{3x3} \quad (4-13)$$

The stiffness and mass matrices are obtained by numerical integration using Gauss quadrature. Following standard finite element procedures, the system stiffness matrix $[K_p]$ and mass matrix $[M_p]$ are assembled from the element matrices. The equations of motion are expressed in matrix

form as

ORIGINAL PAGE IS
OF POOR QUALITY

$$[M_p]\{\ddot{q}_p\} + [K_p]\{q_p\} = \{P_p\} \quad (4-14)$$

where

$$\{P_p\}^T = \{0, \dots, F, \dots, 0\} \quad (4-15)$$

is the force vector in which F is the contact force associated with the degree of freedom corresponding to the w-displacement at the impact point. The subscript p in Equations (4-12) through (4-15) denotes those are quantities corresponding to laminated plate.

4.3.2 Modeling of Projectile

In Section 4.2 we showed that in order to interpret the experimental transducer response, it is necessary to treat the projectile as an elastic body. A higher order rod finite element developed by Yang and Sun [32] was used to model the projectile. This element has two degrees of freedom at each node, namely the axial displacement u and its first derivative $\partial u / \partial x$. It has been shown that this higher order element is far more superior than the elements with less degrees of freedom in the analysis of dynamic problems. The displacement function is taken as

$$u = a_1 + a_2x + a_3x^2 + a_4x^3 \quad (4-16)$$

where a_i are constant coefficients. Solving these coefficients in terms of the nodal degrees of freedom and substituting into Equation (4-16), we obtain

$$u = \{N\}^T \{q_r\}_e \quad (4-17)$$

where

$$\{q_r\}_e^T = \{(u)_1, (\partial u / \partial x)_1, (u)_2, (\partial u / \partial x)_2\} \quad (4-18)$$

is the vector of element nodal degrees of freedom, and

$$\{N\}^T = \{f_1(x), f_2(x), f_3(x), f_4(x)\} \quad (4-19)$$

in which

$$f_1(x) = (1 - x/L)^2(1 + 2x/L)$$

$$f_2(x) = x(1 - x/L)^2$$

$$f_3(x) = x^2/L^2(3 - 2x/L)$$

$$f_4(x) = x^2/L(x/L - 1)$$

are shape functions. The subscript r in Equation (4-17) denotes quantities corresponding to the rod.

Using variational principle, the equations of motion for one element are obtained as

$$[m_r] \{\ddot{q}_r\}_e + [k_r] \{q_r\}_e = \{p_r\}_e \quad (4-20)$$

where $\{p_r\}_e$ is the vector of the generalized forces associated with the nodal degrees of freedom $\{q_r\}_e$, $[m_r]$ is the element mass matrix whose entries are given by

$$(m_r)_{ij} = \rho A \int_0^L f_i f_j dx \quad i, j = 1, 2, 3, 4 \quad (4-21)$$

and $[k_r]$ is the element stiffness matrix whose entries are given by

$$(k_r)_{ij} = EA \int_0^L f_i' f_j' dx \quad i, j = 1, 2, 3, 4 \quad (4-22)$$

In Equations (4-21) and (4-22), ρ , E and A are mass density, Young's modulus and cross-sectional area of the projectile, respectively, and L is the length of the element. The explicit forms of $[k_r]$ and $[m_r]$ are given by

$$[k_r] = \frac{EA}{30L} \begin{bmatrix} 36 & 3L & -36 & 3L \\ 3L & 4L^2 & -3L & -L^2 \\ -36 & -3L & 36 & -3L \\ 3L & -L^2 & -3L & 4L^2 \end{bmatrix} \quad (4-23)$$

and

$$[m_r] = \frac{\rho AL}{420} \begin{bmatrix} 156 & 22L & 54 & -13L \\ 22L & 4L^2 & 13L & -3L^2 \\ 54 & 13L & 156 & -22L \\ -13L & -3L^2 & -22L & 4L^2 \end{bmatrix} \quad (4-24)$$

Following the usual manner, the system stiffness and mass matrices are assembled from the element stiffness and mass matrices, and the system equations of motion are expressed as

ORIGINAL PAGE IS
OF POOR QUALITY

$$[M_r]\{\ddot{q}_r\} + [K_r]\{q_r\} = \{P_r\} \quad (4-25)$$

where

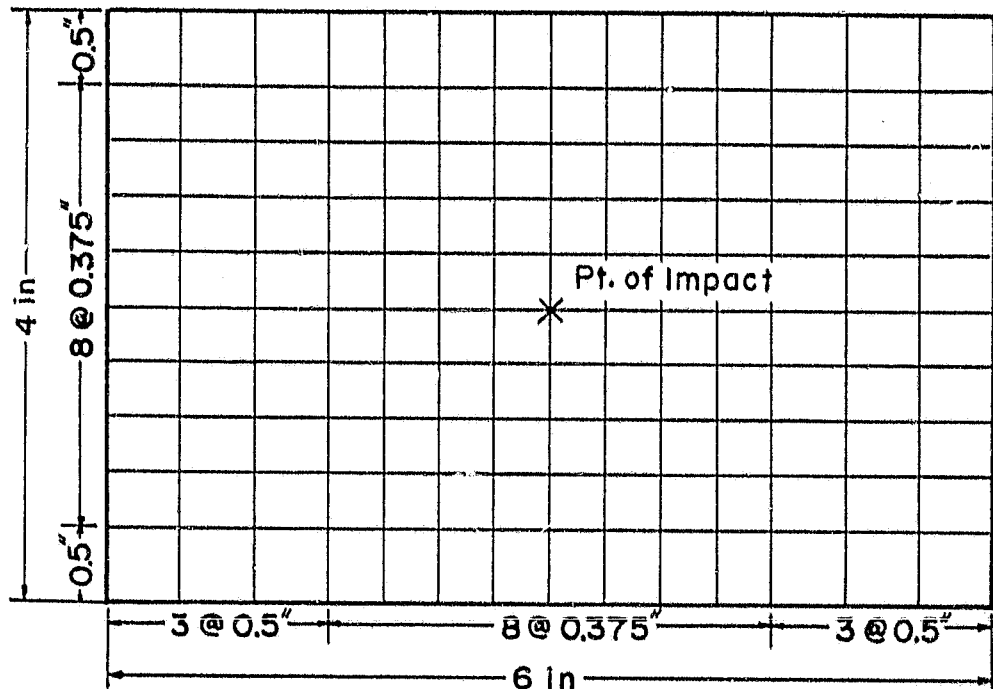
$$\{P_r\}^T = \{F, 0, \dots, 0\} \quad (4-26)$$

in which F is the contact force applied at the impacting end of the projectile.

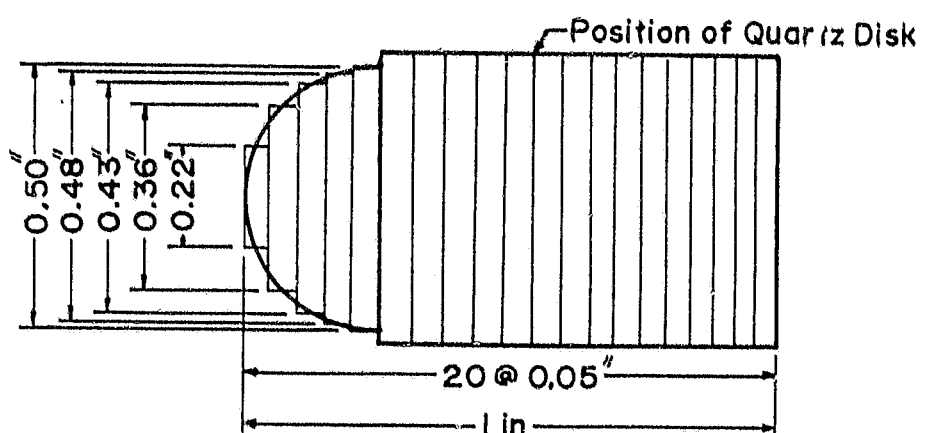
4.4. Results and Discussion

The 6 in. by 4 in. graphite/epoxy laminate was modeled by 140 (14 x 10 mesh) plate elements while the projectile was modeled by 20 rod elements (see Figure 4.11). The two sets of equations (4-14) and (4-25) along with the contact laws given by Equations (3-1), (3-3) and (3-11) were solved simultaneously. The finite difference method with $\Delta t = 0.2$ μ sec. was used to integrate the time variable. A coarser finite element mesh for plate was used and it was found that the present mesh yielded converged solutions. A 3-Dimensional analysis using 112 axisymmetric finite elements to model the projectile was also performed, and the results showed the response at the midpoint of the projectile to have no significant difference comparing with the one obtained by using rod elements.

An impact velocity of 115 in/sec was used in the experiment. Figures 4.12-4.17 show the strain response histories at the six locations picked up by the strain



(a) Plate



(b) Projectile

Figure 4.11 Finite element mesh for laminated plate and projectile

gages. The results obtained using the finite element methods and the contact laws are also shown in these figures. It is evident that the finite element solutions agree with the experimental data very well.

In Figure 4.18, the experimental transducer responses and the computed transducer responses using finite element are plotted against time as curve I and curve II, respectively. The computed contact force history is also plotted as curve III. It can be seen that the magnitudes of curve I and curve II agree fairly well. The frequencies of ringing for these two curves, however, are quite different. For the finite element results, the time interval between two consecutive peaks of ringing is approximately equal to the time that the longitudinal stress wave needed to travel the distance between two ends of the projectile. This indicates that the ringing is simply caused by the transient wave travelling back and forth in the projectile.

From Figure 4.18 we can see that curve I has exact 9 peaks in 180 microseconds, and the time interval between two consecutive peaks is about 20 microseconds. It is noted that this transducer has a rise time of 10 microseconds (see Table 4.1), which is the time it needs to reach the maximum response. Any input signal with period smaller than twice of this value will be smoothed out by the transducer, and the output signal may appear to have lower frequency. In other words, the period of the output signal will be at

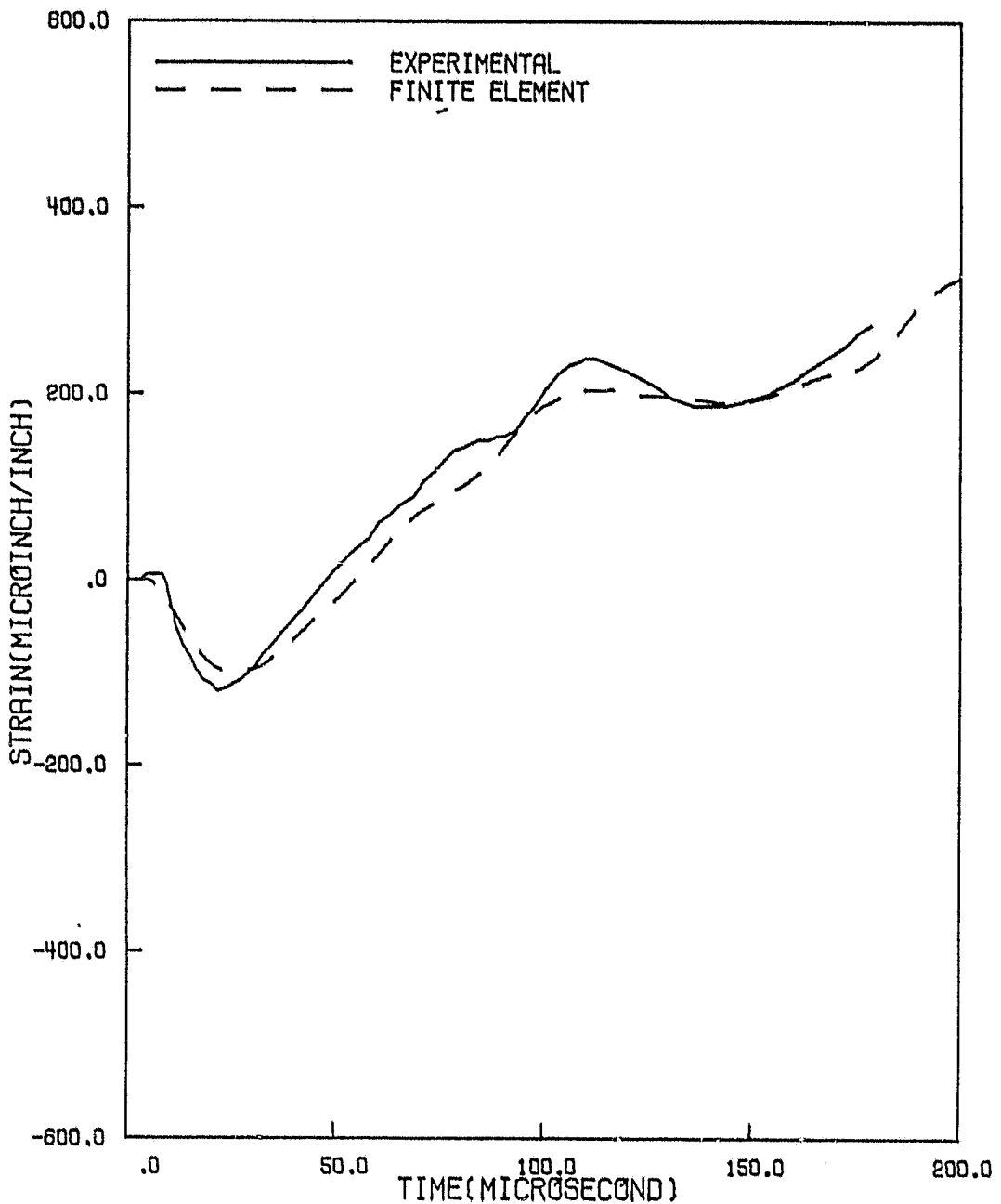


Figure 4.12 Strain response history at gage No.1

ORIGINAL PAGE IS
OF POOR QUALITY

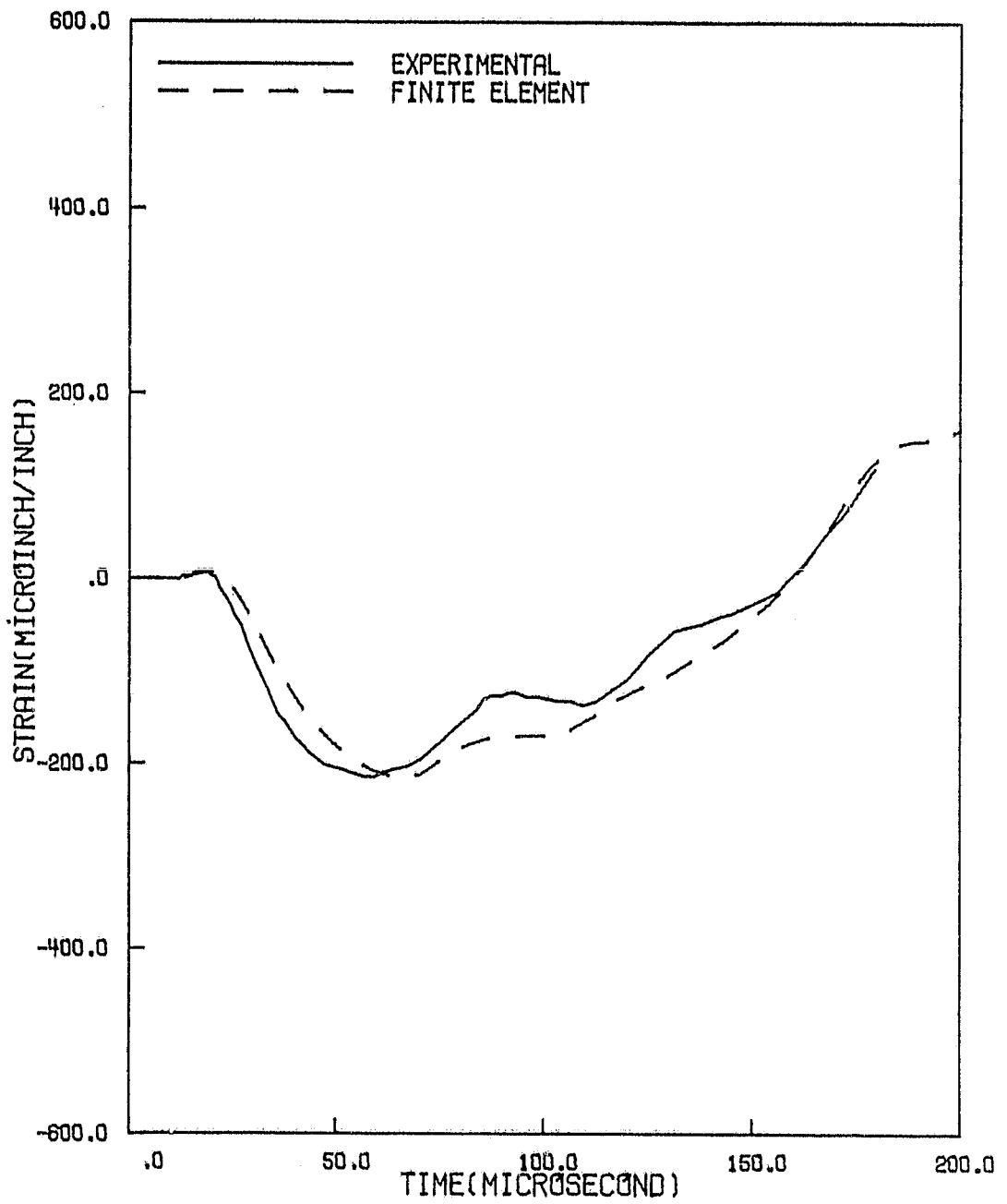


Figure 4.13 Strain response history at gage No.2

ORIGINAL PAGE IS
OF POOR QUALITY

105
~~ORIGINAL PAGE IS
OF POOR QUALITY~~

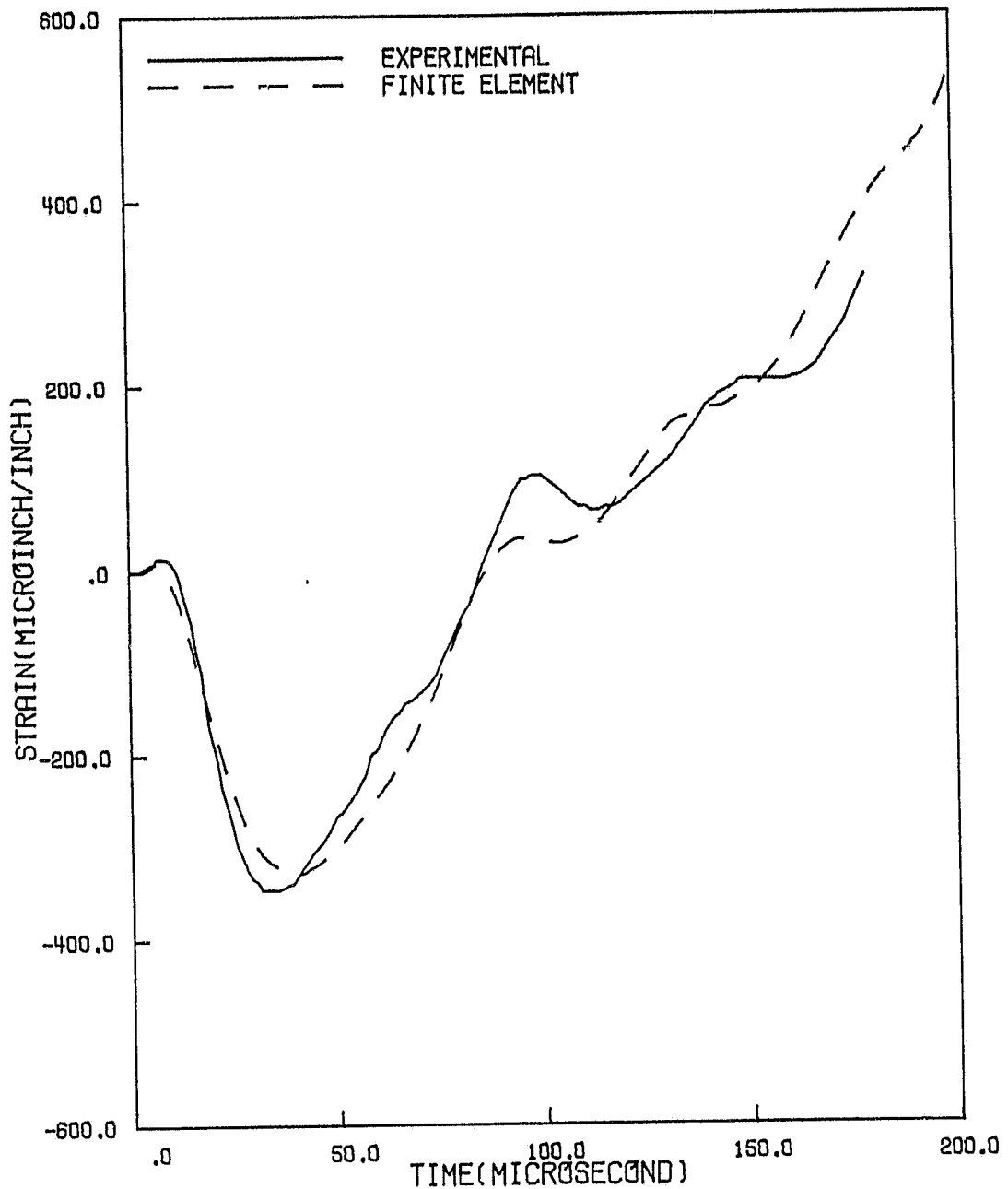


Figure 4.14 Strain response history at gage No.3

ORIGINAL PAGE IS
OF POOR QUALITY

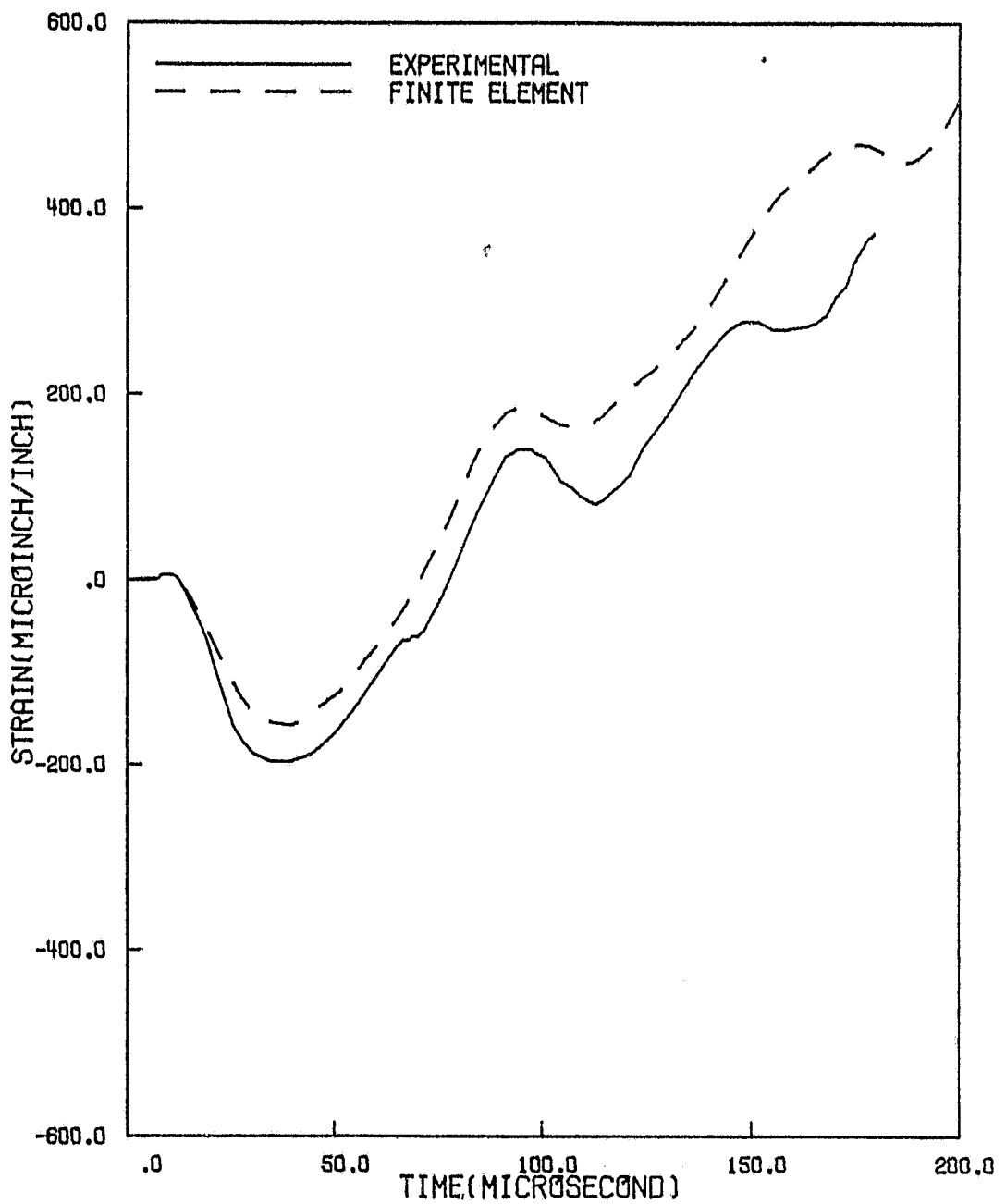


Figure 4.15 Strain response history at gage No.4

ORIGINAL PAGE IS
OF POOR QUALITY

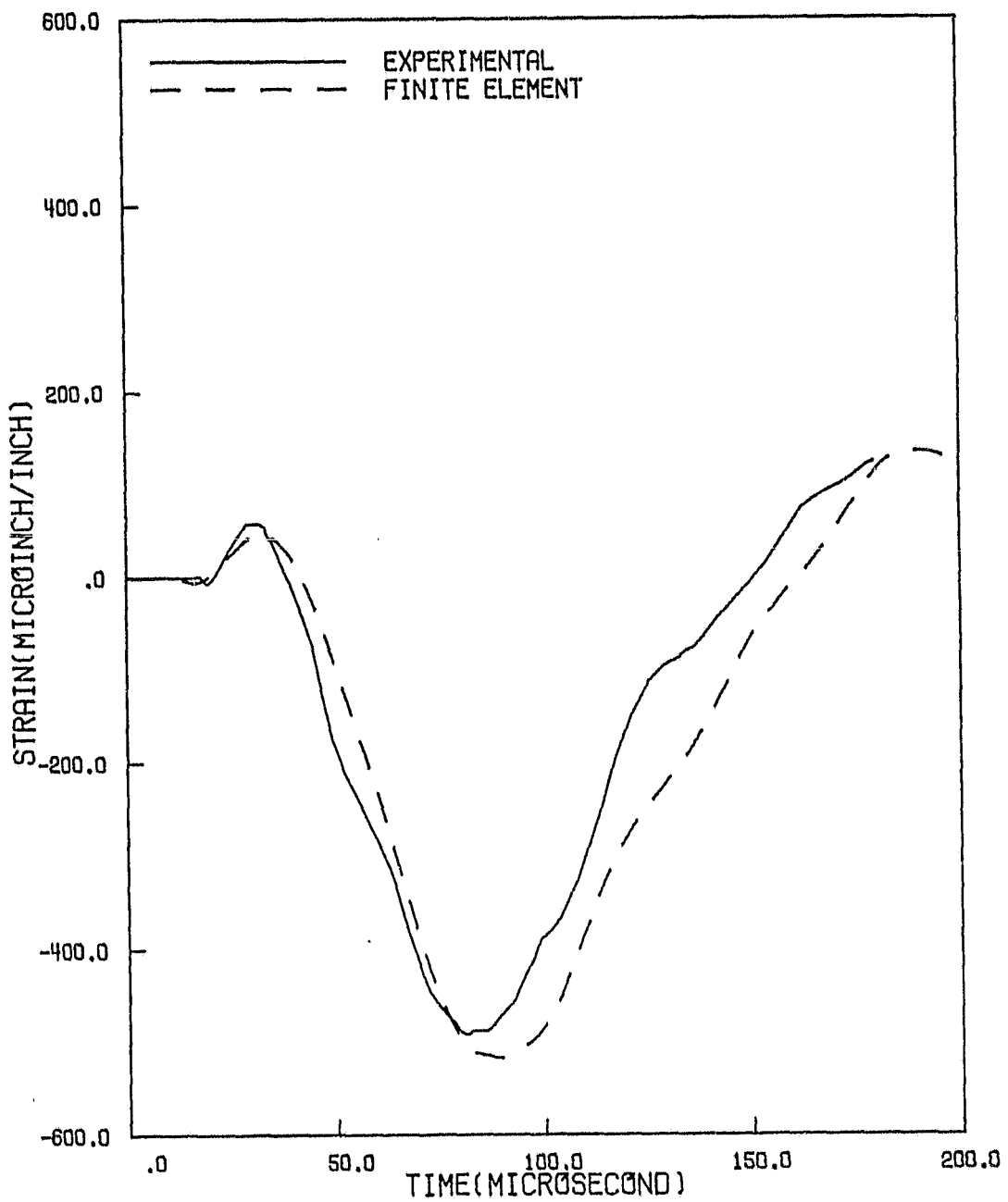


Figure 4.16 Strain response history at gage No.5

ORIGINAL PAGE IS
OF POOR QUALITY

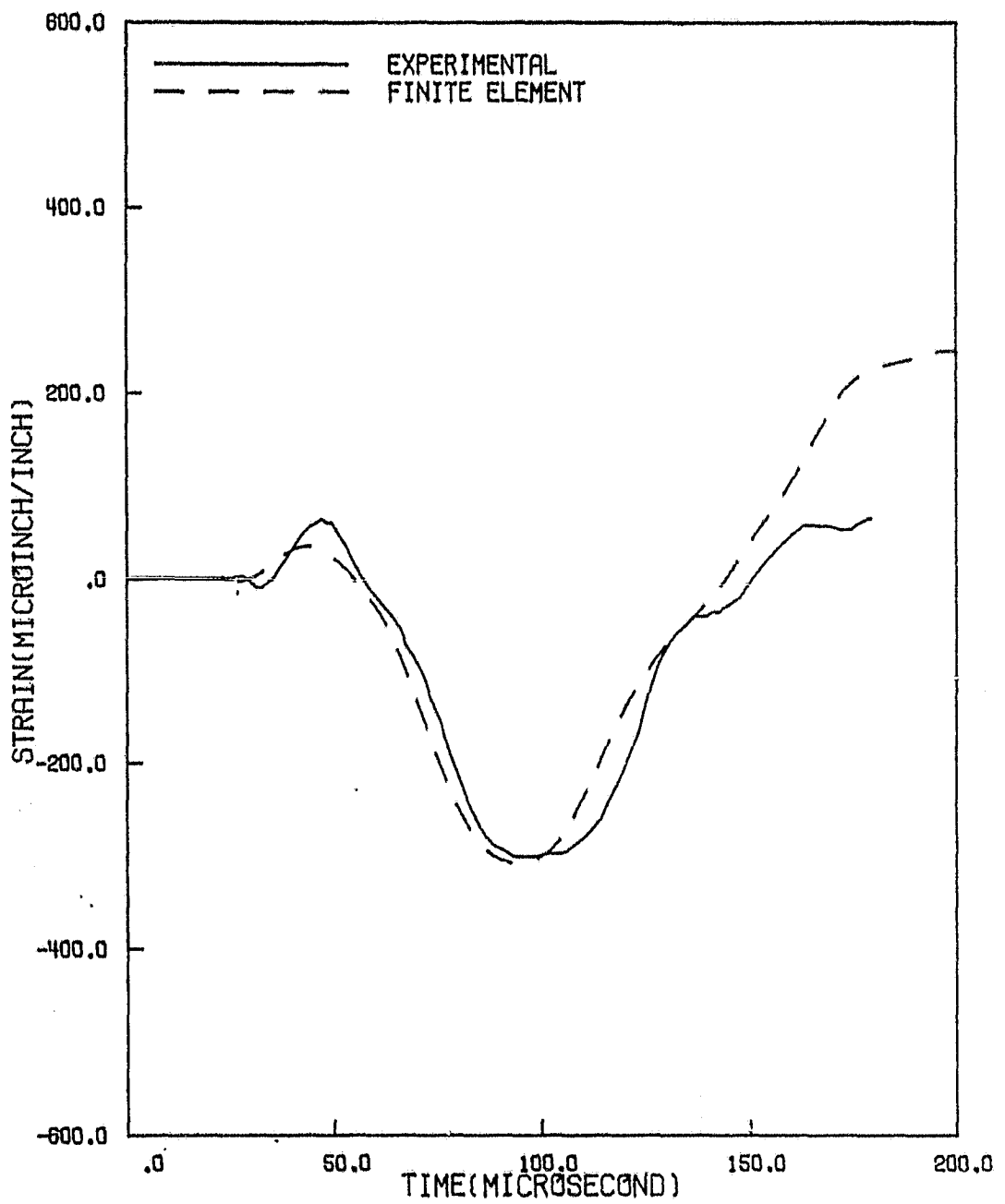


Figure 4.17 Strain response history at gage No.6

ORIGINAL PAGE IS
OF POOR QUALITY

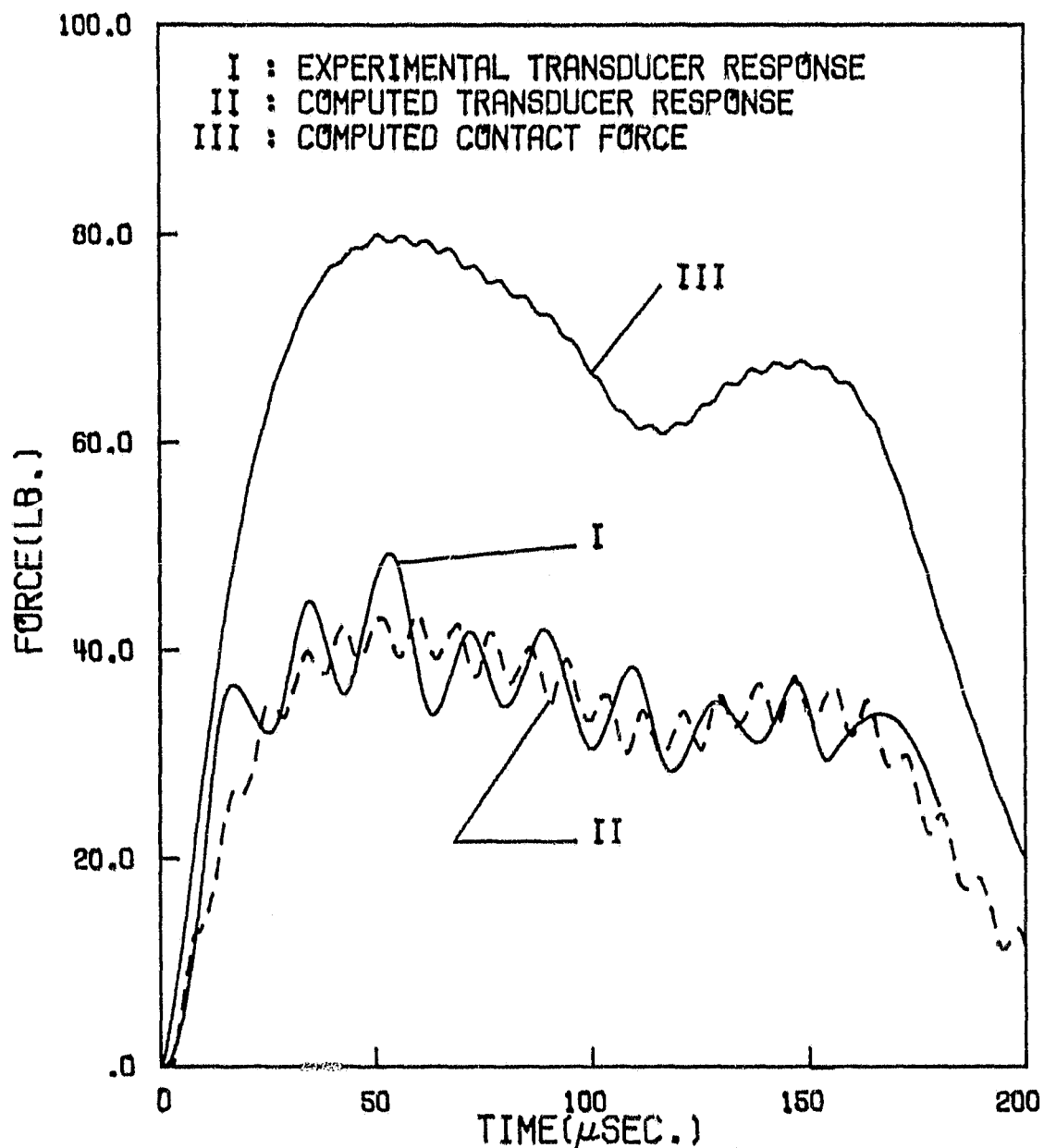


Figure 4.18 Transducer response and contact force histories from experimental and finite element results

least 20 microseconds. This might explain the lower frequency of ringing in the output voltage from the transducer.

The total duration of contact for this impact test is about 800 microseconds, and multiple contact is also observed from the test data. Figure 4.19 shows the experimental transducer responses and the computed transducer responses up to 800 microseconds. Although these two results do not matched very well after the end of the first contact, it is evident that the finite element analysis does predict the multiple contact phenomenon, and the calculated total duration of contact is also approximately the same as the test result.

Figure 4.20 presents a number of deformed configurations of the laminated plate after impact. It is seen that at the point of impact, there is a strong discontinuity in slope of the transverse displacement indicating the presence of a significant transverse shear deformation.

ORIGINAL PAGE IS
OF POOR QUALITY

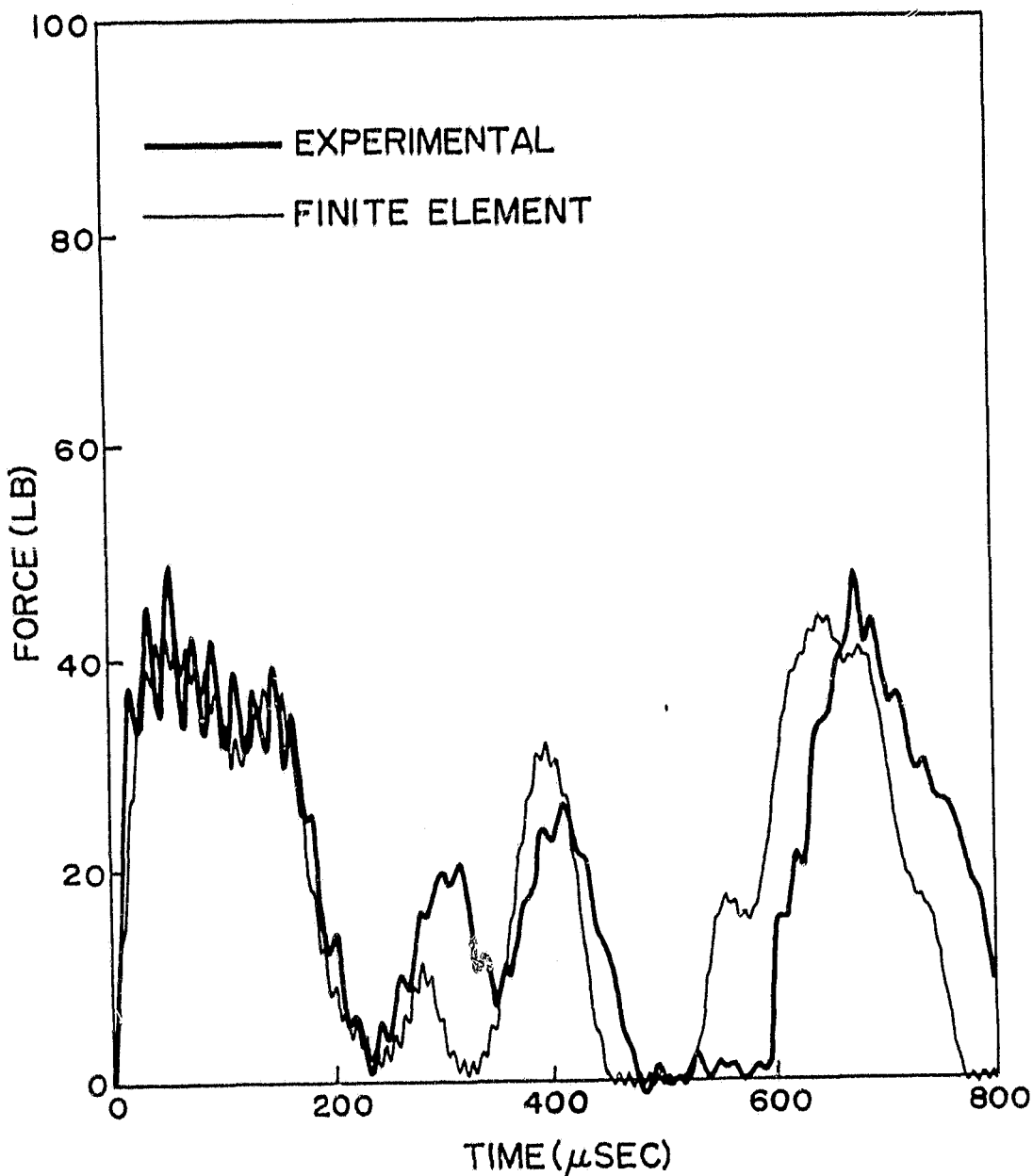


Figure 4.19 Transducer response histories from experimental and finite element results up to 800 microseconds

ORIGINAL PAGE IS
OF POOR QUALITY

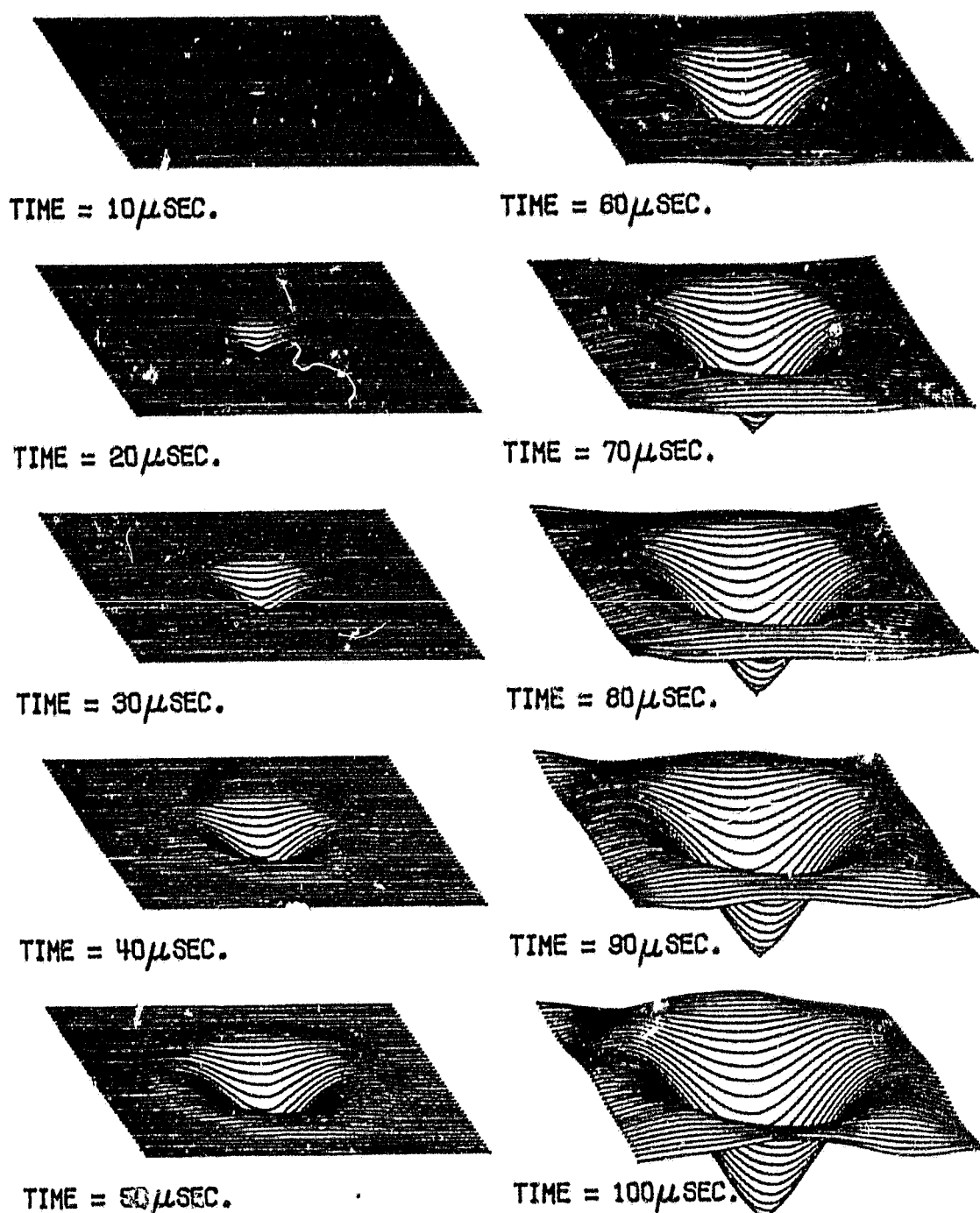


Figure 4.20 Deformed configurations of laminated plate
after impact

ORIGINAL PAGE IS
OF POOR QUALITY

CHAPTER 5

SUMMARY AND CONCLUSION

The laminate theory developed by Whitney and Pagano was employed for studies of harmonic wave and propagation of wave front in a $[0^\circ/45^\circ/0^\circ/-45^\circ/0^\circ]_S$ graphite/epoxy laminate. The dispersion properties of flexural waves were investigated. The wave front surface was constructed using ray theory. It was shown that due to the anisotropic properties of composite laminate, the transient wave would propagate with different velocities in different directions. The growth and decay of the wave front strength were also discussed.

The contact laws between 0.5 inch and 0.75 inch spherical steel indenters and the graphite/epoxy laminate were determined experimentally by means of a statical indentation test. Loading, unloading and reloading curves were fitted into power equations. Linear relation was found between the permanent indentation and the maximum indentation at unloading, which is seen to be independent of the size of indenters. This relation was then used to determine the coefficient of the unloading law. It was demonstrated that there was no need to perform reloading experiments once the loading and unloading laws were established. Test results

showed loading and reloading curves followed the power laws with power indices of 1.5 very well, while the power indices for unloading curves varied from 1.5 to 2.5.

The statically determined contact laws were incorporated into an existing 9-node isoparametric plate finite element program to study the dynamic response of a graphite/epoxy laminated plate subjected to impact of a hard object. An impact experiment was conducted to verify the validity of statical contact laws in the dynamical impact analysis. It was shown that the strain responses predicted using the finite element method agreed with the test results very well. The contact force history of the impact test was measured by an impact-force transducer, which was also seen to match the finite element result in magnitude as well as contact duration.

The indentation tests have been used ever since the beginning of the century to determine the static and dynamic hardnesses of metals in terms of the applied loading, the size of the indenter, and the chordal diameter of the permanent indentation [33]. If similar systematic indentation tests are performed on the laminated composite materials, then the relations between contact coefficients and the sizes of the indenters could be determined more rigorously, and the usefulness of the contact laws could be further extended.

ORIGINAL PAGE IS
OF POOR QUALITY

As the verification of the contact laws has been limited to low velocity impacts in this study, their accuracy under high velocity impact conditions is not clear. Besides the contact behavior which may be significantly different from the static one, the damage induced by waves could be quite extensive which needs to be included in the analysis. While the present study tried to establish experimentally contact laws which can be used in the analysis of low velocity impact, the damage of laminate due to impact loading has not been discussed. It is apparent that more work needs to be done so that the failure mechanism in laminated composites due to impact can be better understood. Stress waves propagating in thickness direction, which may be responsible for the delamination of laminates, is one of the important subjects that should be investigated. Strength and fatigue life degradations of laminates after impact, which have been examined briefly by Wang [15], also need more extensive study.

ORIGINAL PAGE IS
OF POOR QUALITY

LIST OF REFERENCES

- [1] Moon, F.C., "A Critical Survey of Wave Propagation and Impact in Composite Material", NASA CR-121226, 1973.
- [2] Sun, C.T., "Propagation of Shock Waves in Anisotropic Composite Plates", Journal of Composite Materials, Vol.7, 1973, pp.366-382.
- [3] Moon, F.C., "Wave Surfaces Due to Impact on Anisotropic Plates", Journal of Composite Materials, Vol.6, 1972, pp.62-79.
- [4] Chow, T.S., "On the Propagation of Flexural Waves in an Orthotropic Laminated Plate and Its Response to an Impulsive Load", Journal of Composite Materials, Vol.5, 1971, pp.306-319.
- [5] Greszczuk, L.B., "Response of Isotropic and Composite to Particle Impact", Foreign Object Impact Damage to Composite, ASTM STP 568, American Society for Testing and Materials, 1975, pp.183-211.
- [6] Sun, C.T. and Huang, S.N., "Transverse Impact Problems by Higher Order Beam Finite Element", Computers & Structures, Vol.5, 1975, pp.297-303.
- [7] Kim, B.S. and Moon, F.C., "Impact Induced Stress Waves in an Anisotropic Plate", AIAA Journal, Vol.17, No.10, 1979, pp.1126-1133.
- [8] Daniel, I.M., Liber, T. and LaBedz, R.H., "Wave Propagation in Transversely Impacted Composite Laminates", Experimental Mechanics, January 1979, pp.9-16.
- [9] Dally, J.W., Link, J.A. and Prabhakaran, R., "A Photoelastic Study of Stress Waves in Fiber Reinforced Composites", Developments in Mechanics, Vol.6, Proceedings of the 12th Midwestern Mechanics Conference, 1971, pp.937-949.

- [10] Takeda, N., Sierakowski, R.L. and Malvern, L.E., "Wave Propagation Experiments On Ballistically Impacted Composite Laminates", Journal of Composite Materials, Vol.15, 1981, pp.157-174.
- [11] Hertz, H., "Über die Berührung fester elastischer Körper", Journal Reine Angew Math, (Crelle), Vol.92, 1881, p.155.
- [12] Goldsmith, W., Impact, Edward Arnold, London, 1960.
- [13] Sun, C.T., "An Analytical Method for Evaluation of Impact Damage Energy of Laminated Composites", ASTM STP 617, American Society for Testing and Materials, 1977, pp.427-440.
- [14] Yang, S.H. and Sun, C.T., "Indentation Law for Composite Laminates", NASA CR-165460, July 1981, also to appear in ASTM STP series, American Society for Testing and Materials.
- [15] Wang, T., "Dynamic Response and Damage of Hard Object Impact on a Graphite/Epoxy Laminate", Ph.D. Dissertation, Purdue University, 1982.
- [16] Yang, P.C., Norris, C.H. and Stavsky, Y., "Elastic Wave Propagation In Heterogeneous Plates", International Journal of Solids and Structures, Vol.2, 1966, pp.665-683.
- [17] Mindlin, R.D., "Influence of Rotatory Inertia and Shear on Flexural Motions of Isotropic, Elastic Plates", Journal of Applied Mechanics, Vol.18, 1951, pp.31-38.
- [18] Whitney, J.M. and Pagano, N.J., "Shear Deformation in Heterogeneous Anisotropic Plates", Journal of Applied Mechanics, Vol.37, 1970, pp.1031-1036.
- [19] Sun, C.T. and Whitney, J.M., "On Theories for the Dynamic Response of Laminated Plates", Proceedings AIAA/ASME/SAE 13th Structures, Structural Dynamics, and Materials Conference, 1972, AIAA Paper No.72-398.
- [20] Kraut, E., "Advances in the Theory of Anisotropic Elastic Wave Propagation", Review of Geophysics, Vol.1, No.3, 1963, pp.401-448.
- [21] Keller, H.B., "Propagation of Stress Discontinuities in Inhomogeneous Elastic Media", SIAM Review, Vol.6, No.4, 1964, pp.356-382.

ORIGINAL PAGE IS
OF POOR QUALITY

- [22] Vlaar, N.J., "Ray Theory for an Anisotropic Inhomogeneous Elastic Medium", Bulletin of the Seismological Society of America, Vol.58, No.6, 1968, pp.2053-2072.
- [23] Thomas, T.Y., Plastic Flow and Fracture in Solids, Academic Press, 1961, p.10.
- [24] Courant, R. and Hilbert, D., Methods of Mathematical Physics, Vol.II, Interscience Publishers, 1962.
- [25] Foreign Object Impact Damage to Composite, ASTM STP 568, American Society for Testing and Materials, 1973.
- [26] Willis, J.R., "Hertzian Contact of Anisotropic Bodies", Journal of Mechanics and Physics of Solids, Vol.14, 1966, pp.163-176.
- [27] Sun, C.T. and Chattopadhyay, S., "Dynamic Response of Anisotropic Laminated Plates Under Initial Stress to Impact of a Mass", Journal of Applied Mechanics, Vol.42, 1975, pp.693-698.
- [28] Crook, A.W., "A Study of Some Impacts Between Metal Bodies by a Piezoelectric Method", Proceedings of Royal Society, London, A 212, 1952, p.377.
- [29] Sun, C.T., Sankar, B.V. and Tan, T.M., "Dynamic Response of SMC to Impact of a Steel Ball", Advances in Aerospace Structures and Materials, The Winter Annual Meeting of the American Society of Mechanical Engineers, Washington,D.C., 1981.
- [30] Operating Instructions, Model No. 200A05 Transducer, PCB Piezotronics, INC.
- [31] Yang, S.H., "Static and Dynamic Contact Behavior of Composite Laminates", Ph.D. Dissertation, Purdue University, 1981.
- [32] Yang, T.Y. and Sun, C.T., "Finite Elements for the Vibration of Framed Shear Walls", Journal of Sound and Vibration, Vol.27, No.3, 1973, pp.297-311.
- [33] Tabor, D., The Hardness of Metal, Oxford University Press, 1951.
- [34] Zienkiewicz, O.C., The Finite Element Method, 3rd edition, McGraw-Hill, 1977, Chapter 24, pp.677-757

ORIGINAL PAGE IS
OF POOR QUALITY

APPENDIX

COMPUTER PROGRAM AND USER INSTRUCTIONS

The computer program used in this research was written following the program by Professor R. L. Taylor [34] with some necessary modification in order to solve the impact problems of laminated plates. A brief instruction of the input data for solving the impact problem specified in Chapter 4 of this report is given in this appendix. The detailed descriptions of data input as well as the macro instructions for solving various types of problems can be found in [34]. The listing of input is shown at the end of this appendix, followed by the listing of program.

I. Title and control information:

1. Title card-Format(20A4)

Columns Description

1-4 Must contain FECM

5-80 Alphanumeric information to be printed with output as page header.

2. Control information card-Format(6I5)

Columns Description

1-5 Number of nodes (NUMNP)

6-10 Number of elements (NUMEL)

ORIGINAL PAGE IS
OF POOR QUALITY

- 11-15 Number of layers (LAYER)
- 16-20 Spatial dimension (NDM)
- 21-25 Number of unknowns per node (NDF)
- 26-30 Number of nodes per element (NEN)

II. Mesh and initial information:

The input of each segment in this part of data is controlled by the alphanumeric value of macros, which must be followed immediately by the appropriate data. Except for the END card which must be the last card of this part, the data segments can be in any order. Each segment is terminated with blank card(s). The meaning of each macro is given by the following:

<u>Macro</u>	<u>Data to be Input</u>
COOR	Coordinate data
ELEM	Element data
BOUN	Boundary condition data
MATE	Material data
ROD	Initial condition of the projectile
EXPE	Experimental indentation laws data
END	Must be the last card of this part, terminates mesh and initial information input.

1. Coordinate data-Format(2I5,2F10.0)

Columns Description

- 1-5 Nodal number
- 6-10 Generation increment

ORIGINAL PAGE IS
OF POOR QUALITY

11-20	X-coordinate
21-30	Y-coordinate

2. Element data-Format(11I5)

<u>Columns</u>	<u>Description</u>
1-5	Element number
6-10	Node 1 number
11-15	Node 2 number
etc.	.
46-50	Node 9 number
51-55	Generation increment

3. Boundary condition data-Format(7I5)

<u>Columns</u>	<u>Description</u>
1-5	Node number
6-10	Generation increment
11-15	DOF 1 boundary code
16-20	DOF 2 boundary code
21-25	DOF 3 boundary code
26-30	DOF 4 boundary code
31-35	DOF 5 boundary code

4. Initial condition of the projectile-Format(2I5,F10.0)

<u>Columns</u>	<u>Description</u>
1-5	The node at which the projectile hits
6-10	DOF corresponding to the direction of impact
11-20	Initial impact velocity

5. Experimental Indentation laws data-Format(4F10.0)

Columns Description

1-10 Contact coefficient k
11-20 Critical Indentation α_p
21-30 Constant s_p of Equation 3-9
31-40 Power Index q of the unloading law

6. Material data

Card 1-format(3I5,F10.0)

Columns Description

1-5 Order of Gauss quadrature for the numerical integration of the bending energy
6-10 Order of Gauss quadrature for the numerical integration of the transverse shear energy
11-15 Order of Gauss quadrature for strain outputs
at Gauss points if >0
at nodal points if <0
16-25 Total thickness of the laminate

Card 2-Format(7F10.0)

Columns Description

1-10 Mass density
11-20 Poisson's ratio ν_{12}
21-30 Longitudinal Young's modulus E_1
31-40 Transverse Young's modulus E_2
41-50 Shear modulus G_{12}
11-20 Shear modulus G_{13}
11-20 Shear modulus G_{23}

Card 3,4,... Format(I5,F5.0,F10.0)

<u>Columns</u>	<u>Description</u>	ORIGINAL PAGE IS OF POOR QUALITY
1-5	Layer number	
6-10	Fiber angle	
11-20	Thickness of the layer	

III. Macro Instructions:

The first instruction must be a card with MACR in columns 1 to 4. The macro instructions needed to solve the problem specified in Chapter 4 of this report are shown in the listing of input. Cards must be input in the precise order. The following is the explanation of each macro:

<u>Columns</u>	<u>Columns</u>	<u>Columns</u>	<u>Description</u>
1-4	5-10	11-15	
LMAS			Lumped mass formulation
DT	V		Set time increment to value V
LOOP	N		Execute N times the instructions between this macro and macro NEXT
TIME			Advance time by DT value
RODP	N		Integration of the equations of motion using the finite difference method. Contact force, indentation and element strain will be stored stored every N steps in loop
DISP	N		Nodal displacements will be stored every N steps in loop
NEXT			End of loop instructions

END

End of macro program Instructions

IV. Termination of program execution

A card with STOP in columns 1 to 4 must be supplied at the end of the input data in order to properly terminate the execution.

The values of contact force, indentation, element strain, nodal displacement and the response of the projectile at each requested output time step are stored in program files which can be saved (say, copy to a magnetic tape) at the end of execution. Three program files, i.e.; tape3, tape8 and tape9 are used for data saving:

Tape3: Nodal displacement - Format(6E12.4)

Nodal displacements, from node 1 to node NUMNP, are saved on tape3 at each requested output time step according to the format.

Tape8: Element strain - Format(2I6,5E12.4)

Element strains, from element 1 to element NUMEL, and then from node 1 to node NEN of each element, are saved on tape8 at each requested output time step.

Columns Data saved

1-6 Element number

7-12 Node number of element

13-24 Bending strain κ_x

25-36 Bending strain κ_y

- 37-48 Bending strain κ_{xy}
- 49-60 Transverse shearing strain γ_{yz}
- 49-60 Transverse shearing strain γ_{xz}

Tape9: Contact force, Indentation and the response of the projectile - Format(6E12.4)

The following information is saved on tape9 at each requested output time step:

Columns Data saved

- 1-12 Contact force
- 13-24 Indentation
- 25-36 'Transducer' response (see Chapter 4)
- 37-48 Displacement of the projectile at the impacted end
- 37-48 Velocity of the projectile at the impacted end
- 37-48 Acceleration of the projectile at the impacted end

ORIGINAL PAGE IS
OF POOR QUALITY

LISTING OF INPUT DATA

FECM **LOW VELOCITY IMPACT OF LAMINATED PLATE**
 609 140 20 2 5 9

COOR					
1	1	0.0	0.0000		
7	1	1.5	0.0000		
23	1	4.5	0.0000		
29	0	6.0	0.0000		
30	1	0.0	0.2500		
36	1	1.5	0.2500		
52	1	4.5	0.2500		
58	0	6.0	0.2500		
59	1	0.0	0.5000		
65	1	1.5	0.5000		
81	1	4.5	0.5000		
87	0	6.0	0.5000		
88	1	0.0	0.6875		
94	1	1.5	0.6875		
110	1	4.5	0.6875		
116	0	6.0	0.6875		
117	1	0.0	0.8750		
123	1	1.5	0.8750		
139	1	4.5	0.8750		
145	0	6.0	0.8750		
146	1	0.0	1.0625		
152	1	1.5	1.0625		
168	1	4.5	1.0625		
174	0	6.0	1.0625		
175	1	0.0	1.2500		
181	1	1.5	1.2500		
197	1	4.5	1.2500		
203	0	6.0	1.2500		
204	1	0.0	1.4375		
210	1	1.5	1.4375		
226	1	4.5	1.4375		
232	0	6.0	1.4375		
233	1	0.0	1.6250		
239	1	1.5	1.6250		
255	1	4.5	1.6250		
261	0	6.0	1.6250		
262	1	0.0	1.8125		
268	1	1.5	1.8125		
284	1	4.5	1.8125		
290	0	6.0	1.8125		
291	1	0.0	2.0000		
297	1	1.5	2.0000		
313	1	4.5	2.0000		
319	0	6.0	2.0000		
320	1	0.0	2.1875		
326	1	1.5	2.1875		
342	1	4.5	2.1875		
348	0	6.0	2.1875		
349	1	0.0	2.3750		
355	1	1.5	2.3750		
371	1	4.5	2.3750		
377	0	6.0	2.3750		
378	1	0.0	2.5625		
384	1	1.5	2.5625		
400	1	4.5	2.5625		
406	0	6.0	2.5625		
407	1	0.0	2.7500		
413	1	1.5	2.7500		
429	1	4.5	2.7500		
435	0	6.0	2.7500		
436	1	0.0	2.9375		
442	1	1.5	2.9375		

ORIGINAL PAGE IS
OF POOR QUALITY

127

458	1	4.5	2.9375
464	0	6.0	2.9375
465	1	0.0	3.1250
471	1	1.5	3.1250
487	1	4.5	3.1250
493	0	6.0	3.1250
494	1	0.0	3.3125
500	1	1.5	3.3125
516	1	4.5	3.3125
522	0	6.0	3.3125
523	1	0.0	3.5000
529	1	1.5	3.5000
545	1	4.5	3.5000
551	0	6.0	3.5000
552	1	0.0	3.7500
558	1	1.5	3.7500
574	1	4.5	3.7500
580	0	6.0	3.7500
581	1	0.0	4.0000
587	1	1.5	4.0000
603	1	4.5	4.0000
609	0	6.0	4.0000

ELEM

1	1	3	61	59	2	32	60	30	31
15	59	61	119	117	60	90	118	88	89
29	117	119	177	175	118	148	176	146	147
43	175	177	235	233	176	206	234	204	205
57	233	235	293	291	234	264	292	262	263
71	291	293	351	349	292	322	350	320	321
85	349	351	409	407	350	380	408	378	379
99	407	409	467	465	408	438	466	436	437
113	465	467	525	523	466	496	524	494	495
127	523	525	583	581	524	554	582	552	553

1 2 3 4 5 6 7 8 9 10 11 12 13 14 15 16 17 18 19 20

BOUN

1	1	-1	-1	0	0	0
609	0	1	1	0	0	0

ROD

305	3	115.0
-----	---	-------

EXPE

1912000.	0.0006564	0.094	2.0
----------	-----------	-------	-----

MATE

3	3	-3	.106						
0.000148			0.3	17500000.	1150000.	800000.	800000.	800000.	
1	0.		0.0053						
2	45.		0.0053						
3	0.		0.0053						
4	-45.		0.0053						
5	0.		0.0053						
6	0.		0.0053						
7	45.		0.0053						
8	0.		0.0053						
9	-45.		0.0053						
10	0.		0.0053						
11	0.		0.0053						
12	-45.		0.0053						
13	0.		0.0053						
14	45.		0.0053						
15	0.		0.0053						
16	0.		0.0053						
17	-45.		0.0053						
18	0.		0.0053						
19	45.		0.0053						
20	0.		0.0053						

END

MACR
LMAS
DT .2E-6
LOOP 10
TIME
RODP
DISP 5
NEXT
END
STOP

ORIGINAL PAGE IS
OF POOR QUALITY

ORIGINAL PAGE IS
OF POOR QUALITY

LISTING OF PROGRAM

```

PROGRAM MAIN(INPUT,OUTPUT,TAPE5=INPUT,TAPE6=OUTPUT,TAPE2,TAPE3,
1           TAPE8,TAPE9)                                MAIN  1
C*****  MAIN PROGRAM                                MAIN  2
      LOGICAL PCOMP                                MAIN  3
      COMMON /PRSIZE/ MAX                            MAIN  4
      COMMON /CTDATA/ O,HEAD(20),NUMNP,NUMEL,LAYER,NEQ,IPR
      COMMON /LABELS/ PDIS(6),A(6),BC(2),DI(6),CD(3),FD(3)
      COMMON /LODATA/ NDF,NDM,NEN,NST,NKM
      COMMON /PARATS/ NPAR(14),NEND
      DIMENSION TITL(20),WD(3)
      COMMON G(39000)
      DIMENSION M(39000)
      EQUIVALENCE (G(1),M(1))
      MAX=39000
      WD(1)=4HFECK
      WD(2)=4HMACR
      WD(3)=4HSTOP
999  READ(5,1000) TITL
      IF(PCOMP(TITL(1),WD(1))) GO TO 100
      IF(PCOMP(TITL(1),WD(2))) GO TO 200
      IF(PCOMP(TITL(1),WD(3))) STOP
      GO TO 999
100  DO 101 I=1,20
101  HEAD(I)=TITL(I)
      READ(5,1001) NUMNP,NUMEL,LAYER,NDM,NDF,NEN
      WRITE(6,2000) HEAD,NUMNP,NUMEL,LAYER,NDM,NDF,NEN
      PDIS(2)=A(NDM)
      NST=NEN*NDF
      DO 110 I=1,14
110  NPAR(I)=1
      NPAR(1)=1
      NPAR(2)=NPAR(1)+3*NST*IPR
      NPAR(3)=NPAR(2)+NDM*NEN*IPR
      NPAR(4)=NPAR(3)+NST
      NPAR(5)=NPAR(4)+NST*IPR
      NPAR(6)=NPAR(5)+NEN*NUMEL
      NPAR(7)=NPAR(6)+NDF*NUMNP
      NPAR(8)=NPAR(7)+NDM*NUMNP*IPR
      NPAR(9)=NPAR(8)+NDF*NUMNP*IPR
      NPAR(10)=NPAR(9)+NDF*NUMNP
      CALL SETMEM(NPAR(9))
      CALL PZERO(G(1),NPAR(9))
      CALL PMESH(M(NPAR(3)),G(NPAR(2)),M(NPAR(5)),M(NPAR(6)),
1      G(NPAR(7)),G(NPAR(8)),M(NPAR(9)),NDF,NDM,NEN,NKM)
      NPAR(10)=NPAR(9)+NEQ
      NPAR(11)=NPAR(10)+NDF*NUMNP*IPR
      NEND=NPAR(11)+NEQ*IPR
      NE=NEND
      CALL SETMEM(NE)
      CALL PZERO(G(NPAR(10)),NE-NPAR(10))
      GO TO 999
200  CALL PMACR(G(NPAR(1)),G(NPAR(2)),M(NPAR(3)),G(NPAR(4)),
1      M(NPAR(5)),M(NPAR(6)),G(NPAR(7)),G(NPAR(8)),M(NPAR(9)),
2      G(NPAR(10)),G(NPAR(11)),G(NE),NDF,NDM,NEN,NST)
      CALL PZERO(G,MAX)
      GO TO 999
1000 FORMAT(20A4)
1001 FORMAT(16I5)
2000 FORMAT(1H1,20A4//)
1      5X,F0.0 N T R O L L   I N F O R M A T I O N S///
2      10X,35HNUMBER OF NODAL POINTS      =,I6/
3      10X,35HNUMBER OF ELEMENTS        =,I6/
4      10X,35HNUMBER OF MATERIAL LAYERS =,I6/
5      10X,35HDIMENSION OF COORDINATE SPACE =,I6/
6      10X,35HDEGREES OF FREEDOM FOR EACH NODE =,I6/
7      10X,35HNODES PER ELEMENT (MAXIMUM)    =,I6/
      END

```

ORIGINAL PAGE IS
OF POOR QUALITY

```

C      BLOCK DATA
C*** BLOCK DATA
COMMON /CTDATA/ O,HEAD(20),NUMNP,NUMEL,LAYER,NEQ,IPR
COMMON /LABELS/ PDIS(6),A(6),BC(2),DI(6),CD(3),FD(3)
DATA O/1H1/,IPR/1/
DATA PDIS/4H(I10,2H,,4HF13.,4H4,,4HGE13,4H.4) /
DATA A/2H,1,2H,2,2H,3,2H,4,2H,5,2H,6/
DATA BC/4H B.C.2H. /
DATA DI/4H DIS,2HPL,4H VEL,2HOC,4H ACC,2HEL/
DATA CD/4H COO,4HRDIN,4HATES/
DATA FD/4H FOR,4HCE/D,4HISPL/
END

C      SUBROUTINE PMACR(UL,XL,LD,P,IX,ID,X,F,JDIAG,DR,B,CT,NDF,NDM,
NEN,NST)
C*** MACRO INSTRUCTION ROUTINE
LOGICAL PCMP
COMMON G(1)
DIMENSION M(1)
EQUIVALENCE (G(1),M(1))
COMMON /CTDATA/ O,HEAD(20),NUMNP,NUMEL,LAYER,NEQ,IPR
COMMON /PROLOD/ PROP
COMMON /TMDATA/ TIME,DT,DDT,FORCE,ALPHA
COMMON /ISWIDX/ ISW
COMMON /PARATS/ NPAR(14),NEND
COMMON /RODPT/ UR,IQ,NDS
DIMENSION UL(1),XL(1),LD(1),P(1),IX(1),ID(1),X(1),F(1),
^ JDIAG(1),DR(1),B(1)
DIMENSION WD(9),CT(4,16),LUE(9)
DATA WD/4HLOOP,4HNEXT,4HDT,,4HPROP,4HLMAS,4HRODP,
1     4HSTRE,4HDISP,4HCHEC/
DATA NWD/9/,ENDM/4HEND /

C....  INITIALIZATION
DT = 0.0
PROP = 1.0
TIME = 0.0
NNEQ = NDF*NUMNP
NPLD = 0
FORCE= 0.
ALPHA= 0.
WRITE(6,2001) O,HEAD
LL = 1
LMAX = 16
CALL SETMEM(NEND+LMAX*4*IPR)
CT(1,1) = WD(1)
CT(3,1) = 1.0
100 LL = LL + 1
IF(LL.LT.LMAX) GO TO 110
LMAX = LMAX + 16
CALL SETMEM(NEND+LMAX*4*IPR)
110 READ(5,1000) (CT(J,LL),J=1,4)
WRITE(6,2000) (CT(J,LL),J=1,4)
IF(.NOT.PCOMP(CT(1,LL),ENDM)) GO TO 100
CT(1,LL) = WD(2)
NEND = NEND +LMAX*4*IPR
LX = LL - 1
DO 230 L=1,LX
IF(.NOT.PCOMP(CT(1,L),WD(1))) GO TO 230
J = 1
K = L + 1
DO 210 I=K,LL
IF(PCOMP(CT(1,I),WD(1))) J = J + 1
IF(J .GT. 9) GO TO 401
IF(PCOMP(CT(1,I),WD(2))) J = J - 1
210 IF(J.EQ.0) GO TO 220
GO TO 400
220 CT(4,I) = L
CT(4,L) = I
230 CONTINUE

```

BLOC 1
BLOC 2
BLOC 3
BLOC 4
BLOC 5
BLOC 6
BLOC 7
BLOC 8
BLOC 9
BLOC 10
BLOC 11
BLOC 12

PMAC 1
PMAC 2
PMAC 3
PMAC 4
PMAC 5
PMAC 6
PMAC 7
PMAC 8
PMAC 9
PMAC 10
PMAC 11
PMAC 12
PMAC 13
PMAC 14
PMAC 15
PMAC 16
PMAC 17
PMAC 18
PMAC 19
PMAC 20
PMAC 21
PMAC 22
PMAC 23
PMAC 24
PMAC 25
PMAC 26
PMAC 27
PMAC 28
PMAC 29
PMAC 30
PMAC 31
PMAC 32
PMAC 33
PMAC 34
PMAC 35
PMAC 36
PMAC 37
PMAC 38
PMAC 39
PMAC 40
PMAC 41
PMAC 42
PMAC 43
PMAC 44
PMAC 45
PMAC 46
PMAC 47
PMAC 48
PMAC 49
PMAC 50
PMAC 51
PMAC 52
PMAC 53
PMAC 54
PMAC 55
PMAC 56

ORIGINAL PAGE IS
OF POOR QUALITY

```

J = 0
DO 240 L=1,LL
IF(PCOMP(CT(1,L),WD(1))) J = J + 1
240 IF(PCOMP(CT(1,L),WD(2))) J = J - 1
IF(J,NE.0) GO TO 400
LU = 0
L = 1
299 DO 300 J=1,NWD
300 IF(PCOMP(CT(1,L),WD(J))) GO TO 310
GO TO 330
310 I = L - 1
GO TO (1,2,3,4,5,6,7,8,9),J
C.... SET LOOP START INDICATORS
1 LU = LU + 1
LX = CT(4,L)
LUE(LU) = LX
CT(3,LX) = 1.
GO TO 330
C.... LOOP TERMINATOR CONTROL
2 N = CT(4,L)
CT(3+L) = CT(3,L) + 1.0
IF(CT(3,L).GT.CT(3,N)) LU = LU - 1
IF(CT(3,L).LE.CT(3,N)) L = N
GO TO 330
C.... SET TIME INCREMENT
3 DT = CT(3,L)
DDT= DT*DT
GO TO 330
C.... INPUT PROPORTIONAL LOAD TABLE
4 NPLD = CT(3,L)
PROP = PROPLD(0.,NPLD)
GO TO 330
C.... FORM LUMPED MASS MATRIX
5 ISW=3
CALL KMLIB
GO TO 330
C.... IMPACT
6 NDS=CT(3,L)
IF(NDS.EQ.0) NDS=1
CALL RODIPCT
GO TO 330
C.... PRINT STRESS/STRAIN VALUE
7 ISW=4
LX = LUE(LU)
IF(ANMOD(CT(3,LX),AMAX1(CT(3,L),1.))) 330,71,330
71 CALL FSTRLA(UL,XL,LD,P,IX, ID,X,F,JDIAG,DR,B,NDF,NDM,NEM,NST,NNEQ)
GO TO 330
C.... PRINT DISPLACEMENTS
8 LX = LUE(LU)
IF(ANMOD(CT(3,LX),AMAX1(CT(3,L),1.))) 330,81,330
81 CALL FRDIS(UL, ID,X,B,F,DR,NDM,NDF)
GO TO 330
C.... CHECK
9 WRITE(G,5001) NEND,JDIAG(NEQ)
RETURN
330 L=L+1
IF(L.GT.LL) RETURN
GO TO 299
C.... PRINT ERROR FORMATS
400 WRITE(G,4000)
RETURN
401 WRITE(S,4001)
RETURN
C.... INPUT/OUTPUT FORMATS
1000 FORMAT(A4,1X,A4,1X,2F5.0)
2000 FORMAT(10X,A4,1X,A4,1X,2G15.5)
2001 FORMAT(A1,20A4//,5X,18HMACRO INSTRUCTIONS//5X,15HMACRO STATEMENT
      ^ ,5X,10H VARIABLE 1,5X,10H VARIABLE 2)
4000 FORMAT(5X,4G15.5//PMACR ERROR 01** UNBALANCED LOOP//NEXT MACROS )
4001 FORMAT(5X,4G15.5//PMACR ERROR 02** LOOPS NESTED DEEPER THAN 8)

```

```

5001 FORMAT(1H1,///5X,32HCHECK MESH DATA AND MEMORY SPACE//  

^ 10X,12H      NEND =,I10//10X,12HJDIAG(NEQ) =,I10)  

END

C      SUBROUTINE PZERO(V,NN)          PMAC127  

C****  ZERO REAL ARRAY            PMAC128  

DIMENSION V(NN)                  PMAC129  

DO 100 N=1,NN  

100 V(N) = 0.0  

RETURN  

END

C      SUBROUTINE SETMEM(J)          PEER   1  

C****  MONITOR AVAIABLE MEMORY IN BLANK COMMON  

COMMON /PRSIZE/ MAX             PEER   2  

K = J                            PEER   3  

IF(K.LE.MAX) RETURN              PEER   4  

WRITE(G,1000) K,MAX              PEER   5  

STOP                            PEER   6  

1000 FORMAT(5X,49H**SETMEM ERROR 01** INSUFFICIENT STORAGE IN BLANK,  

^ 8H COMMON //17X,11HREQUIRED =,I8/17X,11HAVAILABLE =,I8)  

END                                PEER   7  

SETM   8  

SETM   9  

SETM  10

C      LOGICAL FUNCTION PCOMP(A,B)    PCOM   1  

C****  LOGICAL COMPARISON          PCOM   2  

IF(A-B) 10,20,10                PCOM   3  

10 PCOMP = .FALSE.               PCOM   4  

RETURN                          PCOM   5  

20 PCOMP = .TRUE.                PCOM   6  

RETURN                          PCOM   7  

END                                PCOM   8

C      SUBROUTINE ACTCOL(A,B,JDIAG,NEQ,AFAC,BACK,ISS)    ACTC   1  

C****  ACTIVE COLUMN PROFILE SYMMETRIC EQUATION SOLVER  

LOGICAL AFAC,BACK,FLAG           ACTC   2  

DIMENSION A(1),B(1),JDIAG(1)     ACTC   3  

C....  FACTOR A TO UT*D*U, REDUCE B                 ACTC   4  

FLAG=.FALSE.                     ACTC   5  

JR = 0                           ACTC   6  

DO 600 J=1,NEQ                  ACTC   7  

JD = JDIAG(J)                   ACTC   8  

JH = JD - JR                   ACTC   9  

IS = J - JH + 2                 ACTC  10  

IF(JH-2) 600,300,100             ACTC  11  

100 IF(.NOT.AFAC) GO TO 500     ACTC  12  

IE = J - 1                       ACTC  13  

K = JR + 2                       ACTC  14  

ID = JDIAG(IS-1)                 ACTC  15  

C....  REDUCE ALL EQUATIONS EXCEPT DIAGONAL          ACTC  16  

DO 200 I=IS,IE                  ACTC  17  

IR = ID                          ACTC  18  

ID = JDIAG(I)                   ACTC  19  

IH = MINO(ID-IR-1,I-IS+1)       ACTC  20  

IF(IH.GT.0) A(K)=A(K)-DOT(A(K-IH),A(ID-IH),IH)  

200 K = K + 1                   ACTC  21  

C....  REDUCE DIGONAL TERM          ACTC  22  

300 IF(.NOT.AFAC) GO TO 500     ACTC  23  

IR = JR + 1                     ACTC  24  

IE = JB - 1                     ACTC  25  

K = J - JD                      ACTC  26  

DO 400 I=IR,IE                  ACTC  27  

ID = JDIAG(K+I)                 ACTC  28  

IF(A(ID)) 301,400,301           ACTC  29  

301 D = A(I)                     ACTC  30  

A(I) = A(I)/A(ID)               ACTC  31  

A(JD) = A(JD) - D*A(I)         ACTC  32  

400 CONTINUE                     ACTC  33  

IF(A(JD)) 450,450,500           ACTC  34  

450 IF(ISS.NE.0) GO TO 500      ACTC  35  

IF(FLAG) GO TO 465              ACTC  36  

ACTC  37  

ACTC  38

```

ORIGINAL PAGE IS
OF POOR QUALITY

133

```

        WRITE(6,460)
460  FORMAT(//50H**ACTCOL ERROR 01** STIFFNESS MATRIX NOT POSITIVE ,
1      8HDEFINITE)
      FLAG=.TRUE.
465  WRITE(6,466) J,A(JD)
466  FORMAT(32H NONPOSITIVE PIVOT FOR EQUATION ,I4,5X,7HPOVIT =,
^      E20.10)
C....    REDUCE RHS
500  IF(BACK) B(J) = B(J) - DOT(A(JR+1),B(IS-1),JH-1)
600  JR = JD
      IF(FLAG) STOP
      IF(.NOT.BACK) RETURN
C....    DIVIDED BY DIAGONAL PIVOTS
DO 700 I=1,NEQ
ID = JDIAG(I)
IF(A(ID)) 650,700,650
650 B(I) = B(I)/A(ID)
700 CONTINUE
C....    BACK SUBSTITUTE
      J = NEQ
      JD = JD1AG(J)
800 D = B(J)
      J = J - 1
      IF(J.LE.0) RETURN
      JR = JDIAG(J)
      IF(JD-JR.LE.1) GO TO 1000
      IS = J - JD + JR + 2
      K = JR - IS + 1
      DO 900 I=IS,J
900 B(I) = B(I) - A(I+K)*D
1000 JD = JR
      GO TO 800
END
C
SUBROUTINE ADDSTF(A,S,P,JDIAG,LD,NST,NEL,FLG)
C****  ASSEMBLE GLOBAL ARRAYS
      LOGICAL FLG
      DIMENSION A(1),S(NST,1),P(1),JDIAG(1),LD(1)
      DO 200 J=1,NEL
      K = LD(J)
      IF(K.EQ.0) GO TO 200
      IF(FLG) GO TO 50
      A(K)=A(K)+P(J)
      GO TO 200
50 L = JDIAG(K) - K
      DO 100 I=1,NEL
      M = LD(I)
      IF(M.GT.K .OR. M.EQ.0) GO TO 100
      M = L + M
      A(M)=A(M)+S(I,J)
100 CONTINUE
200 CONTINUE
      RETURN
END
C
FUNCTION DOT(A,B,N)
C****  VECTOR DOT PRODUCT
      DIMENSION A(1),B(1)
      DOT = 0.0
      DO 100 I=1,N
100 DOT = DOT + A(I)*B(I)
      RETURN
END
C
SUBROUTINE PLOAD(ID,F,B,NN,P)
C****  FORM LOAD VECTOR IN COMPACT FORM
      DIMENSION ID(1),F(1),B(1)
      DO 100 N=1,NN
      J=ID(N)
100 IF(J.GT.0) B(J)=F(N)*P
      ACTC 39
      ACTC 40
      ACTC 41
      ACTC 42
      ACTC 43
      ACTC 44
      ACTC 45
      ACTC 46
      ACTC 47
      ACTC 48
      ACTC 49
      ACTC 50
      ACTC 51
      ACTC 52
      ACTC 53
      ACTC 54
      ACTC 55
      ACTC 56
      ACTC 57
      ACTC 58
      ACTC 59
      ACTC 60
      ACTC 61
      ACTC 62
      ACTC 63
      ACTC 64
      ACTC 65
      ACTC 66
      ACTC 67
      ACTC 68
      ACTC 69
      ACTC 70
      ACTC 71
      ADDS  1
      ADDS  2
      ADDS  3
      ADDS  4
      ADDS  5
      ADDS  6
      ADDS  7
      ADDS  8
      ADDS  9
      ADDS 10
      ADDS 11
      ADDS 12
      ADDS 13
      ADDS 14
      ADDS 15
      ADDS 16
      ADDS 17
      ADDS 18
      ADDS 19
      ADDS 20
      DOT   1
      DOT   2
      DOT   3
      DOT   4
      DOT   5
      DOT   6
      DOT   7
      DOT   8
      PLOA  1
      PLOA  2
      PLOA  3
      PLOA  4
      PLOA  5
      PLOA  6
      PLOA  7
      PLOA  8
      PLOA  9
      PLOA 10
      PLOA 11
      PLOA 12
      PLOA 13
      PLOA 14
      PLOA 15
      PLOA 16
      PLOA 17
      PLOA 18
      PLOA 19
      PLOA 20
      PLOA 21
      PLOA 22
      PLOA 23
      PLOA 24
      PLOA 25
      PLOA 26
      PLOA 27
      PLOA 28
      PLOA 29
      PLOA 30
      PLOA 31
      PLOA 32
      PLOA 33
      PLOA 34
      PLOA 35
      PLOA 36
      PLOA 37
      PLOA 38
      PLOA 39
      PLOA 40
      PLOA 41
      PLOA 42
      PLOA 43
      PLOA 44
      PLOA 45
      PLOA 46
      PLOA 47
      PLOA 48
      PLOA 49
      PLOA 50
      PLOA 51
      PLOA 52
      PLOA 53
      PLOA 54
      PLOA 55
      PLOA 56
      PLOA 57
      PLOA 58
      PLOA 59
      PLOA 60
      PLOA 61
      PLOA 62
      PLOA 63
      PLOA 64
      PLOA 65
      PLOA 66
      PLOA 67
      PLOA 68
      PLOA 69
      PLOA 70
      PLOA 71
      PLOA 72
      PLOA 73
      PLOA 74
      PLOA 75
      PLOA 76
      PLOA 77
      PLOA 78
      PLOA 79
      PLOA 80
      PLOA 81
      PLOA 82
      PLOA 83
      PLOA 84
      PLOA 85
      PLOA 86
      PLOA 87
      PLOA 88
      PLOA 89
      PLOA 90
      PLOA 91
      PLOA 92
      PLOA 93
      PLOA 94
      PLOA 95
      PLOA 96
      PLOA 97
      PLOA 98
      PLOA 99
      PLOA 100
      PLOA 101
      PLOA 102
      PLOA 103
      PLOA 104
      PLOA 105
      PLOA 106
      PLOA 107
      PLOA 108
      PLOA 109
      PLOA 110
      PLOA 111
      PLOA 112
      PLOA 113
      PLOA 114
      PLOA 115
      PLOA 116
      PLOA 117
      PLOA 118
      PLOA 119
      PLOA 120
      PLOA 121
      PLOA 122
      PLOA 123
      PLOA 124
      PLOA 125
      PLOA 126
      PLOA 127
      PLOA 128
      PLOA 129
      PLOA 130
      PLOA 131
      PLOA 132
      PLOA 133
      PLOA 134
      PLOA 135
      PLOA 136
      PLOA 137
      PLOA 138
      PLOA 139
      PLOA 140
      PLOA 141
      PLOA 142
      PLOA 143
      PLOA 144
      PLOA 145
      PLOA 146
      PLOA 147
      PLOA 148
      PLOA 149
      PLOA 150
      PLOA 151
      PLOA 152
      PLOA 153
      PLOA 154
      PLOA 155
      PLOA 156
      PLOA 157
      PLOA 158
      PLOA 159
      PLOA 160
      PLOA 161
      PLOA 162
      PLOA 163
      PLOA 164
      PLOA 165
      PLOA 166
      PLOA 167
      PLOA 168
      PLOA 169
      PLOA 170
      PLOA 171
      PLOA 172
      PLOA 173
      PLOA 174
      PLOA 175
      PLOA 176
      PLOA 177
      PLOA 178
      PLOA 179
      PLOA 180
      PLOA 181
      PLOA 182
      PLOA 183
      PLOA 184
      PLOA 185
      PLOA 186
      PLOA 187
      PLOA 188
      PLOA 189
      PLOA 190
      PLOA 191
      PLOA 192
      PLOA 193
      PLOA 194
      PLOA 195
      PLOA 196
      PLOA 197
      PLOA 198
      PLOA 199
      PLOA 200
      PLOA 201
      PLOA 202
      PLOA 203
      PLOA 204
      PLOA 205
      PLOA 206
      PLOA 207
      PLOA 208
      PLOA 209
      PLOA 210
      PLOA 211
      PLOA 212
      PLOA 213
      PLOA 214
      PLOA 215
      PLOA 216
      PLOA 217
      PLOA 218
      PLOA 219
      PLOA 220
      PLOA 221
      PLOA 222
      PLOA 223
      PLOA 224
      PLOA 225
      PLOA 226
      PLOA 227
      PLOA 228
      PLOA 229
      PLOA 230
      PLOA 231
      PLOA 232
      PLOA 233
      PLOA 234
      PLOA 235
      PLOA 236
      PLOA 237
      PLOA 238
      PLOA 239
      PLOA 240
      PLOA 241
      PLOA 242
      PLOA 243
      PLOA 244
      PLOA 245
      PLOA 246
      PLOA 247
      PLOA 248
      PLOA 249
      PLOA 250
      PLOA 251
      PLOA 252
      PLOA 253
      PLOA 254
      PLOA 255
      PLOA 256
      PLOA 257
      PLOA 258
      PLOA 259
      PLOA 260
      PLOA 261
      PLOA 262
      PLOA 263
      PLOA 264
      PLOA 265
      PLOA 266
      PLOA 267
      PLOA 268
      PLOA 269
      PLOA 270
      PLOA 271
      PLOA 272
      PLOA 273
      PLOA 274
      PLOA 275
      PLOA 276
      PLOA 277
      PLOA 278
      PLOA 279
      PLOA 280
      PLOA 281
      PLOA 282
      PLOA 283
      PLOA 284
      PLOA 285
      PLOA 286
      PLOA 287
      PLOA 288
      PLOA 289
      PLOA 290
      PLOA 291
      PLOA 292
      PLOA 293
      PLOA 294
      PLOA 295
      PLOA 296
      PLOA 297
      PLOA 298
      PLOA 299
      PLOA 300
      PLOA 301
      PLOA 302
      PLOA 303
      PLOA 304
      PLOA 305
      PLOA 306
      PLOA 307
      PLOA 308
      PLOA 309
      PLOA 310
      PLOA 311
      PLOA 312
      PLOA 313
      PLOA 314
      PLOA 315
      PLOA 316
      PLOA 317
      PLOA 318
      PLOA 319
      PLOA 320
      PLOA 321
      PLOA 322
      PLOA 323
      PLOA 324
      PLOA 325
      PLOA 326
      PLOA 327
      PLOA 328
      PLOA 329
      PLOA 330
      PLOA 331
      PLOA 332
      PLOA 333
      PLOA 334
      PLOA 335
      PLOA 336
      PLOA 337
      PLOA 338
      PLOA 339
      PLOA 340
      PLOA 341
      PLOA 342
      PLOA 343
      PLOA 344
      PLOA 345
      PLOA 346
      PLOA 347
      PLOA 348
      PLOA 349
      PLOA 350
      PLOA 351
      PLOA 352
      PLOA 353
      PLOA 354
      PLOA 355
      PLOA 356
      PLOA 357
      PLOA 358
      PLOA 359
      PLOA 360
      PLOA 361
      PLOA 362
      PLOA 363
      PLOA 364
      PLOA 365
      PLOA 366
      PLOA 367
      PLOA 368
      PLOA 369
      PLOA 370
      PLOA 371
      PLOA 372
      PLOA 373
      PLOA 374
      PLOA 375
      PLOA 376
      PLOA 377
      PLOA 378
      PLOA 379
      PLOA 380
      PLOA 381
      PLOA 382
      PLOA 383
      PLOA 384
      PLOA 385
      PLOA 386
      PLOA 387
      PLOA 388
      PLOA 389
      PLOA 390
      PLOA 391
      PLOA 392
      PLOA 393
      PLOA 394
      PLOA 395
      PLOA 396
      PLOA 397
      PLOA 398
      PLOA 399
      PLOA 400
      PLOA 401
      PLOA 402
      PLOA 403
      PLOA 404
      PLOA 405
      PLOA 406
      PLOA 407
      PLOA 408
      PLOA 409
      PLOA 410
      PLOA 411
      PLOA 412
      PLOA 413
      PLOA 414
      PLOA 415
      PLOA 416
      PLOA 417
      PLOA 418
      PLOA 419
      PLOA 420
      PLOA 421
      PLOA 422
      PLOA 423
      PLOA 424
      PLOA 425
      PLOA 426
      PLOA 427
      PLOA 428
      PLOA 429
      PLOA 430
      PLOA 431
      PLOA 432
      PLOA 433
      PLOA 434
      PLOA 435
      PLOA 436
      PLOA 437
      PLOA 438
      PLOA 439
      PLOA 440
      PLOA 441
      PLOA 442
      PLOA 443
      PLOA 444
      PLOA 445
      PLOA 446
      PLOA 447
      PLOA 448
      PLOA 449
      PLOA 450
      PLOA 451
      PLOA 452
      PLOA 453
      PLOA 454
      PLOA 455
      PLOA 456
      PLOA 457
      PLOA 458
      PLOA 459
      PLOA 460
      PLOA 461
      PLOA 462
      PLOA 463
      PLOA 464
      PLOA 465
      PLOA 466
      PLOA 467
      PLOA 468
      PLOA 469
      PLOA 470
      PLOA 471
      PLOA 472
      PLOA 473
      PLOA 474
      PLOA 475
      PLOA 476
      PLOA 477
      PLOA 478
      PLOA 479
      PLOA 480
      PLOA 481
      PLOA 482
      PLOA 483
      PLOA 484
      PLOA 485
      PLOA 486
      PLOA 487
      PLOA 488
      PLOA 489
      PLOA 490
      PLOA 491
      PLOA 492
      PLOA 493
      PLOA 494
      PLOA 495
      PLOA 496
      PLOA 497
      PLOA 498
      PLOA 499
      PLOA 500
      PLOA 501
      PLOA 502
      PLOA 503
      PLOA 504
      PLOA 505
      PLOA 506
      PLOA 507
      PLOA 508
      PLOA 509
      PLOA 510
      PLOA 511
      PLOA 512
      PLOA 513
      PLOA 514
      PLOA 515
      PLOA 516
      PLOA 517
      PLOA 518
      PLOA 519
      PLOA 520
      PLOA 521
      PLOA 522
      PLOA 523
      PLOA 524
      PLOA 525
      PLOA 526
      PLOA 527
      PLOA 528
      PLOA 529
      PLOA 530
      PLOA 531
      PLOA 532
      PLOA 533
      PLOA 534
      PLOA 535
      PLOA 536
      PLOA 537
      PLOA 538
      PLOA 539
      PLOA 540
      PLOA 541
      PLOA 542
      PLOA 543
      PLOA 544
      PLOA 545
      PLOA 546
      PLOA 547
      PLOA 548
      PLOA 549
      PLOA 550
      PLOA 551
      PLOA 552
      PLOA 553
      PLOA 554
      PLOA 555
      PLOA 556
      PLOA 557
      PLOA 558
      PLOA 559
      PLOA 560
      PLOA 561
      PLOA 562
      PLOA 563
      PLOA 564
      PLOA 565
      PLOA 566
      PLOA 567
      PLOA 568
      PLOA 569
      PLOA 570
      PLOA 571
      PLOA 572
      PLOA 573
      PLOA 574
      PLOA 575
      PLOA 576
      PLOA 577
      PLOA 578
      PLOA 579
      PLOA 580
      PLOA 581
      PLOA 582
      PLOA 583
      PLOA 584
      PLOA 585
      PLOA 586
      PLOA 587
      PLOA 588
      PLOA 589
      PLOA 590
      PLOA 591
      PLOA 592
      PLOA 593
      PLOA 594
      PLOA 595
      PLOA 596
      PLOA 597
      PLOA 598
      PLOA 599
      PLOA 600
      PLOA 601
      PLOA 602
      PLOA 603
      PLOA 604
      PLOA 605
      PLOA 606
      PLOA 607
      PLOA 608
      PLOA 609
      PLOA 610
      PLOA 611
      PLOA 612
      PLOA 613
      PLOA 614
      PLOA 615
      PLOA 616
      PLOA 617
      PLOA 618
      PLOA 619
      PLOA 620
      PLOA 621
      PLOA 622
      PLOA 623
      PLOA 624
      PLOA 625
      PLOA 626
      PLOA 627
      PLOA 628
      PLOA 629
      PLOA 630
      PLOA 631
      PLOA 632
      PLOA 633
      PLOA 634
      PLOA 635
      PLOA 636
      PLOA 637
      PLOA 638
      PLOA 639
      PLOA 640
      PLOA 641
      PLOA 642
      PLOA 643
      PLOA 644
      PLOA 645
      PLOA 646
      PLOA 647
      PLOA 648
      PLOA 649
      PLOA 650
      PLOA 651
      PLOA 652
      PLOA 653
      PLOA 654
      PLOA 655
      PLOA 656
      PLOA 657
      PLOA 658
      PLOA 659
      PLOA 660
      PLOA 661
      PLOA 662
      PLOA 663
      PLOA 664
      PLOA 665
      PLOA 666
      PLOA 667
      PLOA 668
      PLOA 669
      PLOA 670
      PLOA 671
      PLOA 672
      PLOA 673
      PLOA 674
      PLOA 675
      PLOA 676
      PLOA 677
      PLOA 678
      PLOA 679
      PLOA 680
      PLOA 681
      PLOA 682
      PLOA 683
      PLOA 684
      PLOA 685
      PLOA 686
      PLOA 687
      PLOA 688
      PLOA 689
      PLOA 690
      PLOA 691
      PLOA 692
      PLOA 693
      PLOA 694
      PLOA 695
      PLOA 696
      PLOA 697
      PLOA 698
      PLOA 699
      PLOA 700
      PLOA 701
      PLOA 702
      PLOA 703
      PLOA 704
      PLOA 705
      PLOA 706
      PLOA 707
      PLOA 708
      PLOA 709
      PLOA 710
      PLOA 711
      PLOA 712
      PLOA 713
      PLOA 714
      PLOA 715
      PLOA 716
      PLOA 717
      PLOA 718
      PLOA 719
      PLOA 720
      PLOA 721
      PLOA 722
      PLOA 723
      PLOA 724
      PLOA 725
      PLOA 726
      PLOA 727
      PLOA 728
      PLOA 729
      PLOA 730
      PLOA 731
      PLOA 732
      PLOA 733
      PLOA 734
      PLOA 735
      PLOA 736
      PLOA 737
      PLOA 738
      PLOA 739
      PLOA 740
      PLOA 741
      PLOA 742
      PLOA 743
      PLOA 744
      PLOA 745
      PLOA 746
      PLOA 747
      PLOA 748
      PLOA 749
      PLOA 750
      PLOA 751
      PLOA 752
      PLOA 753
      PLOA 754
      PLOA 755
      PLOA 756
      PLOA 757
      PLOA 758
      PLOA 759
      PLOA 760
      PLOA 761
      PLOA 762
      PLOA 763
      PLOA 764
      PLOA 765
      PLOA 766
      PLOA 767
      PLOA 768
      PLOA 769
      PLOA 770
      PLOA 771
      PLOA 772
      PLOA 773
      PLOA 774
      PLOA 775
      PLOA 776
      PLOA 777
      PLOA 778
      PLOA 779
      PLOA 780
      PLOA 781
      PLOA 782
      PLOA 783
      PLOA 784
      PLOA 785
      PLOA 786
      PLOA 787
      PLOA 788
      PLOA 789
      PLOA 790
      PLOA 791
      PLOA 792
      PLOA 793
      PLOA 794
      PLOA 795
      PLOA 796
      PLOA 797
      PLOA 798
      PLOA 799
      PLOA 800
      PLOA 801
      PLOA 802
      PLOA 803
      PLOA 804
      PLOA 805
      PLOA 806
      PLOA 807
      PLOA 808
      PLOA 809
      PLOA 810
      PLOA 811
      PLOA 812
      PLOA 813
      PLOA 814
      PLOA 815
      PLOA 816
      PLOA 817
      PLOA 818
      PLOA 819
      PLOA 820
      PLOA 821
      PLOA 822
      PLOA 823
      PLOA 824
      PLOA 825
      PLOA 826
      PLOA 827
      PLOA 828
      PLOA 829
      PLOA 830
      PLOA 831
      PLOA 832
      PLOA 833
      PLOA 834
      PLOA 835
      PLOA 836
      PLOA 837
      PLOA 838
      PLOA 839
      PLOA 840
      PLOA 841
      PLOA 842
      PLOA 843
      PLOA 844
      PLOA 845
      PLOA 846
      PLOA 847
      PLOA 848
      PLOA 849
      PLOA 850
      PLOA 851
      PLOA 852
      PLOA 853
      PLOA 854
      PLOA 855
      PLOA 856
      PLOA 857
      PLOA 858
      PLOA 859
      PLOA 860
      PLOA 861
      PLOA 862
      PLOA 863
      PLOA 864
      PLOA 865
      PLOA 866
      PLOA 867
      PLOA 868
      PLOA 869
      PLOA 870
      PLOA 871
      PLOA 872
      PLOA 873
      PLOA 874
      PLOA 875
      PLOA 876
      PLOA 877
      PLOA 878
      PLOA 879
      PLOA 880
      PLOA 881
      PLOA 882
      PLOA 883
      PLOA 884
      PLOA 885
      PLOA 886
      PLOA 887
      PLOA 888
      PLOA 889
      PLOA 890
      PLOA 891
      PLOA 892
      PLOA 893
      PLOA 894
      PLOA 895
      PLOA 896
      PLOA 897
      PLOA 898
      PLOA 899
      PLOA 900
      PLOA 901
      PLOA 902
      PLOA 903
      PLOA 904
      PLOA 905
      PLOA 906
      PLOA 907
      PLOA 908
      PLOA 909
      PLOA 910
      PLOA 911
      PLOA 912
      PLOA 913
      PLOA 914
      PLOA 915
      PLOA 916
      PLOA 917
      PLOA 918
      PLOA 919
      PLOA 920
      PLOA 921
      PLOA 922
      PLOA 923
      PLOA 924
      PLOA 925
      PLOA 926
      PLOA 927
      PLOA 928
      PLOA 929
      PLOA 930
      PLOA 931
      PLOA 932
      PLOA 933
      PLOA 934
      PLOA 935
      PLOA 936
      PLOA 937
      PLOA 938
      PLOA 939
      PLOA 940
      PLOA 941
      PLOA 942
      PLOA 943
      PLOA 944
      PLOA 945
      PLOA 946
      PLOA 947
      PLOA 948
      PLOA 949
      PLOA 950
      PLOA 951
      PLOA 952
      PLOA 953
      PLOA 954
      PLOA 955
      PLOA 956
      PLOA 957
      PLOA 958
      PLOA 959
      PLOA 960
      PLOA 961
      PLOA 962
      PLOA 963
      PLOA 964
      PLOA 965
      PLOA 966
      PLOA 967
      PLOA 968
      PLOA 969
      PLOA 970
      PLOA 971
      PLOA 972
      PLOA 973
      PLOA 974
      PLOA 975
      PLOA 976
      PLOA 977
      PLOA 978
      PLOA 979
      PLOA 980
      PLOA 981
      PLOA 982
      PLOA 983
      PLOA 984
      PLOA 985
      PLOA 986
      PLOA 987
      PLOA 988
      PLOA 989
      PLOA 990
      PLOA 991
      PLOA 992
      PLOA 993
      PLOA 994
      PLOA 995
      PLOA 996
      PLOA 997
      PLOA 998
      PLOA 999
      PLOA 1000
      PLOA 1001
      PLOA 1002
      PLOA 1003
      PLOA 1004
      PLOA 1005
      PLOA 1006
      PLOA 1007
      PLOA 1008
      PLOA 1009
      PLOA 1010
      PLOA 1011
      PLOA 1012
      PLOA 1013
      PLOA 1014
      PLOA 1015
      PLOA 1016
      PLOA 1017
      PLOA 1018
      PLOA 1019
      PLOA 1020
      PLOA 1021
      PLOA 1022
      PLOA 1023
      PLOA 1024
      PLOA 1025
      PLOA 1026
      PLOA 1027
      PLOA 1028
      PLOA 1029
      PLOA 1030
      PLOA 1031
      PLOA 1032
      PLOA 1033
      PLOA 1034
      PLOA 1035
      PLOA 1036
      PLOA 1037
      PLOA 1038
      PLOA 1039
      PLOA 1040
      PLOA 1041
      PLOA 1042
      PLOA 1043
      PLOA 1044
      PLOA 1045
      PLOA 1046
      PLOA 1047
      PLOA 1048
      PLOA 1049
      PLOA 1050
      PLOA 1051
      PLOA 1052
      PLOA 1053
      PLOA 1054
      PLOA 1055
      PLOA 1056
      PLOA 1057
      PLOA 1058
      PLOA 1059
      PLOA 1060
      PLOA 1061
      PLOA 1062
      PLOA 1063
      PLOA 1064
      PLOA 1065
      PLOA 1066
      PLOA 1067
      PLOA 1068
      PLOA 1069
      PLOA 1070
      PLOA 1071
      PLOA 1072
      PLOA 1073
      PLOA 1074
      PLOA 1075
      PLOA 1076
      PLOA 1077
      PLOA 1078
      PLOA 1079
      PLOA 1080
      PLOA 1081
      PLOA 1082
      PLOA 1083
      PLOA 1084
      PLOA 1085
      PLOA 1086
      PLOA 1087
      PLOA 1088
      PLOA 1089
      PLOA 1090
      PLOA 1091
      PLOA 1092
      PLOA 1093
      PLOA 1094
      PLOA 1095
      PLOA 1096
      PLOA 1097
      PLOA 1098
      PLOA 1099
      PLOA 1100
      PLOA 1101
      PLOA 1102
      PLOA 1103
      PLOA 1104
      PLOA 1105
      PLOA 1106
      PLOA 1107
      PLOA 1108
      PLOA 1109
      PLOA 1110
      PLOA 1111
      PLOA 1112
      PLOA 1113
      PLOA 1114
      PLOA 1115
      PLOA 1116
      PLOA 1117
      PLOA 1118
      PLOA 1119
      PLOA 1120
      PLOA 1121
      PLOA 1122
      PLOA 1123
      PLOA 1124
      PLOA 1125
      PLOA 1126
      PLOA 1127
      PLOA 1128
      PLOA 1129
      PLOA 1130
      PLOA 1131
      PLOA 1132
      PLOA 1133
      PLOA 1134
      PLOA 1135
      PLOA 1136
      PLOA 1137
      PLOA 1138
      PLOA 1139
      PLOA 1140
      PLOA 1141
      PLOA 1142
      PLOA 1143
      PLOA 1144
      PLOA 1145
      PLOA 1146
      PLOA 1147
      PLOA 1148
      PLOA 1149
      PLOA 1150
      PLOA 1151
      PLOA 1152
      PLOA 1153
      PLOA 1154
      PLOA 1155
      PLOA 1156
      PLOA 1157
      PLOA 1158
      PLOA 1159
      PLOA 1160
      PLOA 1161
      PLOA 1162
      PLOA 1163
      PLOA 1164
      PLOA 1165
      PLOA 1166
      PLOA 1167
      PLOA 1168
      PLOA 1169
      PLOA 1170
      PLOA 1171
      PLOA 1172
      PLOA 1173
      PLOA 1174
      PLOA 1175
      PLOA 1176
      PLOA 1177
      PLOA 1178
      PLOA 1179
      PLOA 1180
      PLOA 1181
      PLOA 1182
      PLOA 1183
      PLOA 1184
      PLOA 1185
      PLO
```

```

      RETURN
      END
C
      FUNCTION PROPLD(T,J)
C****  PROPORTIONAL LOAD TABLE (ONE LOAD CARD ONLY)
      COMMON /CTDATA/ O,HEAD(20),NUMNP,NUMEL,LAYER,NEQ,IPR
      DIMENSION A(5)
      IF (J .LE. 0) GO TO 200
C....  INPUT TABLE OF PROPORTIONAL LOADS
      I=1
      READ(5,1000) K,L,TMIN,TMAX,(A(KKK),KKK=1,5)
      WRITE(6,2000) O,HEAD,I,K,L,TMIN,TMAX,(A(KKK),KKK=1,5)
      RETURN
C...  COMPUTE VALUE AT TIME T
200  PROPLD = 0.0
      IF(T.LT.TMIN .OR. T.GT.TMAX) RETURN
      L = MAX0(L,1)
      PROPLD = A(1)+A(2)*T+A(3)*(SIN(A(4)*T+A(5)))*L
      RETURN
1000 FORMAT(2I5,7F10.0)
2000 FORMAT(A1,20A4//5X,23HPROPORTIONAL LOAD TABLE//11H NUMBER ,
1        43H TYPE EXP. MINIMUM TIME MAXIMUM TIME,13X,2HA1,13X,
2        2HA2,13X,2HA3,13X,2HA4,13X,2HA5/(3I8,7G15.5))
      END
C
      SUBROUTINE PRTDIS(UL, ID, X, B, F, T, NDM, NDF)
C****  OUTPUT NODAL VALUES
      LOGICAL PCOMP
      COMMON /PROPLD/ PROP
      COMMON /CTDATA/ O,HEAD(20),NUMNP,NUMEL,LAYER,NEQ,IPR
      COMMON /LABELS/ PDIS(6),A(6),BC(2),DI(6),CD(3),FD(3)
      COMMON /TMDATA/ TIME,DT,DDT,FORCE,ALPHA
      DIMENSION X(NDM,1),B(1),UL(6),ID(NDM,1),F(NDF,1),T(1)
      DATA BL/4HBLAN/
      DO 102 N=1,NUMNP
      IF(PCOMP(X(1,N),BL)) GO TO 101
      DO 100 I=1,NDF
      UL(I) = F(I,N)*PROP
      K = IAABS(ID(I,N))
100   IF(K.GT.0) UL(I)=B(K)
      T(N)=UL(3)
101   CONTINUE
102   CONTINUE
      WRITE(3,2001) (T(I),I=1,NUMNP)
      RETURN
2001 FORMAT(6E12.4)
      END
C
      SUBROUTINE FSTREA(UL,XL,LD,P,IX, ID, X, F, JDIAG, DR, B, NDF, NDM, NEN,
^          NST, NNEQ)
C****  ELEMENT ROUTINE
      COMMON /CTDATA/ O,HEAD(20),NUMNP,NUMEL,LAYER,NEQ,IPR
      COMMON /ELDATA/ N,NEL,MCT
      COMMON /ISWIDX/ ISW
      COMMON /PROPLD/ PROP
      DIMENSION UL(NDF,1),XL(NDM,1),LD(NDF,1),P(1),IX(NEN,1),
1      ID(NDF,1),X(NDM,1),F(NDF,1),JDIAG(1),DR(1),B(1),S(1)
      IF(ISW.EQ.5) CALL PLOAD(ID,F,DR,NNEQ,PROP)
      MCT=0
      DO 110 N=1,NUMEL
      CALL PFORM(UL,XL,LD,IX, ID, X, F, B, NDF, NDM, NEN, ISW)
      CALL ELMT01(UL,XL,IX(1,N),P,NDF,NDM,NST,ISW)
      IF(ISW.NE.4) CALL ADDSTF(DR,S,P,JDIAG,LD,1,NEL*NDF,.FALSE.)
110   CONTINUE
      RETURN
      END
C
      SUBROUTINE PFORM(UL,XL,LD,IX, ID, X, F, U, NDF, NDM, NEN, ISW)
C****  FORM LOCAL ARRAYS
      COMMON /ELDATA/ N,NEL,MCT
      PLOA  7
      PLOA  8
      PROP  1
      PROP  2
      PROP  3
      PROP  4
      PROP  5
      PROP  6
      PROP  7
      PROP  8
      PROP  9
      PROP 10
      PROP 11
      PROP 12
      PROP 13
      PROP 14
      PROP 15
      PROP 16
      PROP 17
      PROP 18
      PROP 19
      PROP 20
      PROP 21
      PRTU  1
      PRTD  2
      PRTD  3
      PRTD  4
      PRTD  5
      PRTD  6
      PRTD  7
      PRTD  8
      PRTD  9
      PRTD 10
      PRTD 11
      PRTD 12
      PRTD 13
      PRTD 14
      PRTD 15
      PRTD 16
      PRTD 17
      PRTD 18
      PRTD 19
      PRTD 20
      PRTD 21
      PRTD 22
      FSTR  1
      FSTR  2
      FSTR  3
      FSTR  4
      FSTR  5
      FSTR  6
      FSTR  7
      FSTR  8
      FSTR  9
      FSTR 10
      FSTR 11
      FSTR 12
      FSTR 13
      FSTR 14
      FSTR 15
      FSTR 16
      FSTR 17
      FSTR 18
      PFOR  1
      PFOR  2
      PFOR  3

```

```

COMMON /PROLUD/ PROP
DIMENSION UL(NDF,1),XL(NDM,1),LD(NDF,1),IX(NEN,1),ID(NDF,1),
^ X(NDM,1),F(NDF,1),U(1)
DO 108 I=1,NEN
II = IX(I,N)
IF(II .NE. 0) GO TO 105
DO 103 J=1,NDN
XL(J,I) = 0.
DO 104 J=1,NDF
UL(J,I) = 0.
104 LD(J,I) = 0
GO TO 108
105 IID = II*NDF - NDF
NEL = I
DO 106 J=1,NDM
106 XL(J,I) = X(J,II)
DO 107 J=1,NDF
K = IAABS(ID(J,II))
UL(J,I) = F(J,II)*PROP
IF(K.GT.0) UL(J,I)=U(K)
IF(ISW.EQ.6) K=IID+J
107 LD(J,I) = K
108 CONTINUE
RETURN
END
C
C      SUBROUTINE ELMTO1(UL,XL,IX,P,NDF,NDM,NST,ISW)
C****   LINEAR ELASTIC IN-PLANE ^ BENDING ELEMENT ROUTINE
LOGICAL TAN
COMMON /ELDATA/ N,NEL,NCT
COMMON /MTDATA/ RHO,UU12,E1,E2,G12,G13,G23,THK,WIDTH
COMMON /COMPST/ ABD(6,6),DS(2,2),QBR(3,3,25),QBS(2,2,25),
^ TH(25),ZK(25)
COMMON /DMATRIX/ D(10),DB(6,6),LINT
COMMON /TMDATA/ TIME,DT,DDT,FORCE,ALPHA
COMMON /GAUSSP/ SG(16),TG(16),WG(16)
COMMON /EXTRAS/ TAN
DIMENSION UL(NDF,1),XL(NDM,1),IX(1),P(1),SHP(3,12),
1 SIGT(3),SIGB(3),SIGS(2),EPT(3),EPB(3),EPS(2)
C
DO 20 L=1,NST
20 P(L) = 0.0
C.... COMPUTE NEUTRAL STRAINS AND STRESS RESULTANTS
L = D(1)
IF(ISW.EQ.4) L=D(3)
CALL PGAUSS(L,LINT)
DO 600 L=1,LINT
C .. COMPUTE ELEMENT SHAPE FUNCTIONS
CALL SHAPE(SG(L),TG(L),XL,SHP,XSJ,NDM,NEL,IX,.FALSE.)
C .. COMPUTE STRAINS AND COORDINATES
DO 410 I=1,3
EPT(I) = 0.0
410 EPB(I) = 0.0
DO 420 I=1,2
420 EPS(I) = 0.0
XX = 0.0
YY = 0.0
DO 430 J=1,NEL
XX = XX + SHP(3,J)*XL(1,J)
YY = YY + SHP(3,J)*XL(2,J)
C .. IN-PLANE STRAINS
EPT(1) = EPT(1) + SHP(1,J)*UL(1,J)
EPT(2) = EPT(2) + SHP(2,J)*UL(2,J)
EPT(3) = EPT(3) + SHP(1,J)*UL(2,J) + SHP(2,J)*UL(1,J)
C .. BENDING CURVATURES
EPB(1) = EPB(1) - SHP(1,J)*UL(4,J)
EPB(2) = EPB(2) - SHP(2,J)*UL(5,J)
EPB(3) = EPB(3) - SHP(1,J)*UL(5,J) - SHP(2,J)*UL(4,J)
C .. SHEARING STRAINS
EPS(1) = EPS(1) + SHP(1,J)*UL(3,J) - SHP(3,J)*UL(4,J)
PFOR 4
PFOR 5
PFOR 6
PFOR 7
PFOR 8
PFOR 9
PFOR 10
PFOR 11
PFOR 12
PFOR 13
PFOR 14
PFOR 15
PFOR 16
PFOR 17
PFOR 18
PFOR 19
PFOR 20
PFOR 21
PFOR 22
PFOR 23
PFOR 24
PFOR 25
PFOR 26
PFOR 27
PFOR 28
ELMT 1
ELMT 2
ELMT 3
ELMT 4
ELMT 5
ELMT 6
ELMT 7
ELMT 8
ELMT 9
ELMT 10
ELMT 11
ELMT 12
ELMT 13
ELMT 14
ELMT 15
ELMT 16
ELMT 17
ELMT 18
ELMT 19
ELMT 20
ELMT 21
ELMT 22
ELMT 23
ELMT 24
ELMT 25
ELMT 26
ELMT 27
ELMT 28
ELMT 29
ELMT 30
ELMT 31
ELMT 32
ELMT 33
ELMT 34
ELMT 35
ELMT 36
ELMT 37
ELMT 38
ELMT 39
ELMT 40
ELMT 41
ELMT 42
ELMT 43
ELMT 44

```

```

430 EPS(2) = EPS(2) + SHP(2,J)*UL(3,J) - SHP(3,J)*UL(2,J)
    IF(ISW.EQ.5.AND.TAN)
    ^ WRITE(9,9001) N,L,(EPB(IJ),IJ=1,3),(EPS(IJ),IJ=1,2)
9001 FORMAT(2I6,5E12.4)
C .. COMPUTE STRESS RESULTANTS
DO 440 I=1,3
SIGT(I) = 0.
SIGB(I) = 0.
DO 440 J=1,3
SIGT(I) = SIGT(I) + ABD(I,J)*EPT(J) + ABD(I,J+3)*EPB(J)
440 SIGB(I) = SIGB(I) + ABD(I+3,J)*EPT(J) + ABD(I+3,J+3)*EPB(J)
DO 450 I=1,2
SIGS(I) = 0.
DO 450 J=1,2
450 SIGS(I) = SIGS(I) + DS(I,J)*EPS(J)
IF(ISW.GT.4) GO TO G20
C .. OUTPUT STRESS RESULTANTS AND STRAINS
MCT = MCT - 2
IF(MCT.GT.0) GO TO 470
WRITE(6,2001) TIME
MCT = 50
470 WRITE(6,2002) N,XX,YY,EPT,EPB,EPS,SIGT,SIGB,SIGS
GO TO 600
C.... COMPUTE INTERAL FORCES
620 DU = XSJ*WG(L)
J1 = 1
DO 610 J=1,NEL
P(J1) = P(J1) - (SHP(1,J)*SIGT(1)+SHP(2,J)*SIGT(3))*DU
P(J1+1) = P(J1+1) - (SHP(2,J)*SIGT(2)+SHP(1,J)*SIGT(3))*DU
P(J1+2) = P(J1+2) - (SHP(1,J)*SIGS(1)+SHP(2,J)*SIGS(2))*DU
P(J1+3) = P(J1+3) + (SHP(1,J)*SIGB(1)+SHP(2,J)*SIGB(3)+SHP(3,J)
    *SIGS(1))*DU
    ^ P(J1+4) = P(J1+4) + (SHP(2,J)*SIGB(2)+SHP(1,J)*SIGB(3)+SHP(3,J)
    *SIGS(2))*DU
    ^
610 J1 = J1 + NDF
600 CONTINUE
RETURN
C
2001 FORMAT(1H1//
    ^ 5X,6HTIME =,E12.3//5X,33HELEMENT STRAINS/STRESS RESULTANTS//,
    1 8H ELEMENT,3X,7H1-COORD,3X,7H2-COORD,4X,9HXX-STRAIN,4X,
    2 9HY-STRAIN,4X,9HXY-STRAIN,3X,10HKXX-STRAIN,3X,
    3 10HKYY-STRAIN,3X,10HKXY-STRAIN,4X,9HSX-STRAIN,4X,
    4 9HSY-STRAIN/28X,8(6X,7H-STRESS)//)
2002 FORMAT(I8,2F10.4,8E13.4/28X,8E13.4)
END
C
SUBROUTINE PGAUSS(LL,LINT)
***** GAUSSIAN POINTS AND WEIGHTS FOR TWO DIMENSIONS
COMMON /GAUSSP/ SG(16),TG(16),WG(16)
DIMENSION LR(9),LZ(9),LW(9),WR(2),GR(2),GC(2)
DATA LR/-1,1,-1,0,1,0,-1,0/,LZ/-1,-1,1,1,-1,0,1,0,0/
DATA LW/4*25,4*40,64/
DATA GR/0.861136311594053,0.339981043584856/
DATA GC/1.0,0.3333333333/
DATA WR/0.347854845137454,0.652145154862546/
LINT = LL*LL
L=IABS(LL)
GO TO (1,2,3,4),L
C.... 1X1 INTEGRATION
1 SG(1) = 0.
TG(1) = 0.
WG(1) = 4.
RETURN
C.... 2X2 INTEGRATION
2 G = 1./SQRT(3.)
IF(LL.LT.0) G=1.
DO 21 I=1,4
SG(I) = G*LR(I)
TG(I) = G*LZ(I)
PGAU 1
PGAU 2
PGAU 3
PGAU 4
PGAU 5
PGAU 6
PGAU 7
PGAU 8
PGAU 9
PGAU 10
PGAU 11
PGAU 12
PGAU 13
PGAU 14
PGAU 15
PGAU 16
PGAU 17
PGAU 18
PGAU 19
PGAU 20
PGAU 21
PGAU 22
PGAU 23

```

```

21 WG(I) = 1.
      RETURN
C.... 3X3 INTEGRATION
3 G = SORT(0.6)
      IF(LL.LT.0) G=1.
      H = 1./81.
      DO 31 I=1,9
      SG(I) = G*LR(I)
      TG(I) = G*LZ(I)
31 WG(I) = H*LNK(I)
      RETURN
C.... 4X4 INTEGRATION
4 DO 41 I=1,4
      I1 = 1+MOD(I+1,2)
      I2 = 1
      IF(I.GT.2) I2 = 2
      DO 41 J=1,4
      JJ = (I-1)*4+J
      SG(JJ) = LR(J)*GR(I1)
      IF(LL.LT.0) SG(JJ) = LR(J)*GC(I1)
      TG(JJ) = LZ(J)*GR(I2)
      IF(LL.LT.0) TG(JJ) = LZ(J)*GC(I2)
41 WG(JJ) = WR(I1)*WR(I2)
      RETURN
      END
C
C SUBROUTINE SHAPE(SS,TT,X,SHP,XSJ,NDM,NEL,IX,FLG)
C**** SHAPE FUNCTION ROUTINE FOR TWO DIMENSIONAL ELEMENTS
      LOGICAL FLG
      DIMENSION SHP(3,4),X(NDM,1),S(4),T(4),XS(2,2),SX(2,2),IX(9)
      DATA S/-0.5,0.5,0.5,-0.5/,T/-0.5,-0.5,0.5,0.5/
C.... FORM 4-NODE QUADRILATERAL SHAPE FUNCTIONS
      DO 100 I=1,4
      SHP(3,I) = (0.5+S(I)*SS)*(0.5+T(I)*TT)
      SHP(1,I) = S(I)*(0.5+T(I)*TT)
100 SHP(2,I) = T(I)*(0.5+S(I)*SS)
      IF(NEL.GE.4) GO TO 120
C.... FORM TRIANGLE BY ADDING THIRD AND FOURTH TOGETHER
      DO 110 I=1,3
110 SHP(I,3) = SHP(I,3)+SHP(I,4)
C.... ADD QUADRATIC TERMS IF NECESSARY
120 IF(NEL.GT.4 .AND. NEL.LT.10) CALL SHAP2(SS,TT,SHP,IX,NEL)
C.... ADD CUBIC TERMS IF NECESSARY
125 IF(NEL.GT.9) CALL SHAP3(SS,TT,SHP,IX,NEL)
C.... CONSTRUCT JACOBIAN AND ITS INVERSE
      DO 130 I=1,NDM
      DO 130 J=1,2
      XS(I,J) = 0.0
      DO 130 K=1,NEL
130 XS(I,J) = XS(I,J)+ X(J,K)*SHP(I,K)
      XSJ = XS(1,1)*XS(2,2)-XS(1,2)*XS(2,1)
      IF(XSJ .GT. 0.00000001) GO TO 135
      WRITE(6,2000) IX
      STOP
135 IF(FLG) RETURN
      SX(1,1) = XS(2,2)/XSJ
      SX(2,2) = XS(1,1)/XSJ
      SX(1,2) = -XS(1,2)/XSJ
      SX(2,1) = -XS(2,1)/XSJ
C.... FORM GLOBAL DERIVATIVES
      DO 140 I=1,NEL
      TP      = SHP(1,I)*SX(1,1)+SHP(2,I)*SX(2,1)
      SHP(2,I) = SHP(1,I)*SX(1,2)+SHP(2,I)*SX(2,2)
140 SHP(1,I) = TP
      RETURN
2000 FORMAT(5X,67H***SHAPE ERROR 01*** ZERO OR NEGATIVE JACOBIAN DET. FOR
      ^ELEMENT NODES:/20X,12I4)
      END
C
C SUBROUTINE SHAP2(S,T,SHP,IX,NEL)

```

```

***** ADD QUADRATIC FUNCTIONS AS NECESSARY
      DIMENSION IX(9),SHP(3,12)
      S2 = (1.-S*T)/2.
      T2 = (1.-T*T)/2.
      DO 100 I=5,NEL
      DO 100 J=1,3
 100  SHP(J,I) = 0.0
C....  MIDSIDE NODES (SERENDIPITY)
      IF(IX(5).EQ.0) GO TO 101
      SHP(1,5) = -S*(1.-T)
      SHP(2,5) = -S2
      SHP(3,5) = S2*(1.-T)
 101  IF(NEL.LT.6) GO TO 107
      IF(IX(6).EQ.0) GO TO 102
      SHP(1,6) = T2
      SHP(2,6) = -T*(1.+S)
      SHP(3,6) = T2*(1.+S)
 102  IF(NEL.LT.7) GO TO 107
      IF(IX(7).EQ.0) GO TO 103
      SHP(1,7) = -S*(1.+T)
      SHP(2,7) = S2
      SHP(3,7) = S2*(1.+T)
 103  IF(NEL.LT.8) GO TO 107
      IF(IX(8).EQ.0) GO TO 104
      SHP(1,8) = -T2
      SHP(2,8) = -T*(1.-S)
      SHP(3,8) = T2*(1.-S)
C...  INTERIOR NODE (LAGRANGIAN)
 104  IF(NEL.LT.9) GO TO 107
      IF(IX(9).EQ.0) GO TO 107
      SHP(1,9) = -4.*S*T2
      SHP(2,9) = -4.*T*S2
      SHP(3,9) = 4.*S2*T2
C....  CORRECT EDGE NODES FOR INTERIOR NODE(LAGRANGIAN)
      DO 106 J=1,3
      DO 105 I=1,4
 105  SHP(J,I) = SHP(J,I) - 0.25*SHP(J,9)
      DO 106 I=5,8
 106  IF(IX(I).NE.0) SHP(J,I) = SHP(J,I) - 0.5*SHP(J,9)
C...  CORRECT CORNER NODES FOR PRESENCE OF MIDSIDE NODES
 107  K = 8
      DO 109 I=1,4
      L = I + 4
      DO 108 J=1,3
 108  SHP(J,I) = SHP(J,I) - 0.5*(SHP(J,K)+SHP(J,L))
 109  K = L
      RETURN
      END

C
      SUBROUTINE SHAP3(S,T,SHP,IX,NEL)
***** ADD CUBIC FUNCTION AS NECESSARY (SERENDIPITY)
      DIMENSION IX(12),SHP(3,12)
      DO 100 I=5,NEL
      DO 100 J=1,3
 100  SHP(J,I)=0.0
      IF(IX(5).EQ.0) GO TO 101
      S1=-1./3.
      T1=-1.
      CALL CSHAPE(S,T,S1,T1,SHP,1,5)
 101  IF(IX(6).EQ.0) GO TO 102
      S1=1.
      T1=-1./3.
      CALL CSHAPE(S,T,S1,T1,SHP,2,6)
 102  IF(IX(7).EQ.0) GO TO 103
      S1=1./3.
      T1=1.
      CALL CSHAPE(S,T,S1,T1,SHP,1,7)
 103  IF(IX(8).EQ.0) GO TO 104
      S1=-1.
      T1=1./3.

```

```

104 CALL CSHAPE(S,T,S1,T1,SHP,2,8) SHAP 22
IF(IX(9).EQ.0) GO TO 105 SHAP 23
S1=-1. SHAP 24
T1=-1./3. SHAP 25
CALL CSHAPE(S,T,S1,T1,SHP,2,9) SHAP 26
105 IF(NEL.LT.10) GO TO 200 SHAP 27
IF(IX(10).EQ.0) GO TO 106 SHAP 28
S1=1./3. SHAP 29
T1=-1. SHAP 30
CALL CSHAPE(S,T,S1,T1,SHP,1,10) SHAP 31
106 IF(NEL.LT.11) GO TO 200 SHAP 32
IF(IX(11).EQ.0) GO TO 107 SHAP 33
S1=1. SHAP 34
T1=1./3. SHAP 35
CALL CSHAPE(S,T,S1,T1,SHP,2,11) SHAP 36
107 IF(NEL.LT.12) GO TO 200 SHAP 37
IF(IX(12).EQ.0) GO TO 200 SHAP 38
S1=-1./3. SHAP 39
T1=1. SHAP 40
CALL CSHAPE(S,T,S1,T1,SHP,1,12) SHAP 41
C.... CORRECT CORNER NODES SHAP 42
200 DO 210 I=1,4 SHAP 43
I1=I+4 SHAP 44
I2=I+8 SHAP 45
IF(I.EQ.1) I3=I+7 SHAP 46
IF(I.GT.1) I3=I+3 SHAP 47
IF(I.LT.4) I4=I+9 SHAP 48
IF(I.EQ.4) I4=I+5 SHAP 49
DO 210 J=1,3 SHAP 50
210 SHP(J,I)=SHP(J,I)-2./3.*((SHP(J,I1)+SHP(J,I2))-1./3.*((SHP(J,I3)
^ +SHP(J,I4))) SHAP 51
RETURN SHAP 52
END SHAP 53
SHAP 54
C
SUBROUTINE CSHAPE(S,T,S1,T1,SHP,K,L) CSHA 1
C**** SUPPLEMENTAL ROUTINE FOR THE SHAPE FUNCTIONS CSHA 2
DIMENSION SHP(3,12) CSHA 3
C=9./32. CSHA 4
GO TO (1,2),K CSHA 5
1 SHP(1,L)=C*(1.+T1*T)*(9.*S1-2.*S-27.*S1*S*S) CSHA 6
SHP(2,L)=C*T1*(1.-S*S)*(1.+9.*S1*S) CSHA 7
SHP(3,L)=C*(1.+T1*T)*(1.-S*S)*(1.+9.*S1*S) CSHA 8
RETURN CSHA 9
2 SHP(1,L)=C*S1*(1.-T*T)*(1.+9.*T1*T) CSHA 10
SHP(2,L)=C*(1.+S1*S)*(9.*T1-2.*T-27.*T1*T*T) CSHA 11
SHP(3,L)=C*(1.+S1*S)*(1.-T*T)*(1.+9.*T1*T) CSHA 12
RETURN CSHA 13
END CSHA 14
C
SUBROUTINE PMESH(IDL,XL,IX,ID,X,F,JDIAG,NDF,NDM,NEN,NKM) PMES 1
C**** I N P U T M E S H D A T A PMES 2
LOGICAL PRT,ERR,PCOMP PMES 3
COMMON /CTDATAL/ O,HEAD(20),NUMNP,NUMEL,LAYER,NEQ,IPR PMES 4
COMMON /MTDATAL/ RHO,VU12,E1,E2,G12,G13,G23,THK,WIDTH PMES 5
COMMON /LABELS/ PDIS(6),A(6),BC(2),DI(6),CD(3),FD(3) PMES 6
COMMON /EXIDATA/ QLAW(4) PMES 7
COMMON /RODATA/ VR,IQ,NDS PMES 8
DIMENSION IDL(6),XL(7),IX(NEN,1),ID(NDF,1),X(NDM,1), PMES 9
F(NDF,1),DUM(1),WD(13),JDIAG(1) PMES 10
DATA WD/4HCOOR,4HELEM,4HMATE,4HBOUN,4HFORC,4HROD , PMES 11
^ 4HEND ,4HPRIN,4HNOPR,4HPAGE,4HEXP/ PMES 12
DATA BL/4HBLAN/,LIST/11/,PRT/.TRUE./ PMES 13
C.... INITIALIZE ARRAYS PMES 14
ERR = .FALSE. PMES 15
DO 501 I=1,4 PMES 16
501 QLAW(I)=0. PMES 17
DO 502 N=1,NUMNP PMES 18
DO 502 I=1,NDF PMES 19
ID(I,N)=0 PMES 20
F(I,N)=0. PMES 21

```

502 CONTINUE

C.... READ A CARD AND COMPARE WITH MACRO LIST

10 READ(5,1000) CC

DO 20 I=1,LIST

20 IF(PCOMP(CC,WD(I))) GO TO 30

GO TO 10

30 GO TO (1,2,3,4,5,6,7,8,9,11,12),I

C.... NODAL COORDINATE DATA INPUT

1 DO 102 N=1,NUMNP

102 X(1,N)= BL

CALL GENVEC(NDM,XL,X,CD,PRT,ERR)

GO TO 10

C.... ELEMENT DATA INPUT

2 L=0

DO 206 I=1,NUMEL,50

IF(PRT) WRITE(6,2001) 0,HEAD, (K,K=1,NEN)

J = MIN0(NUMEL,I+49)

DO 206 N=1,J

IF(L-N) 200,202,203

200 READ(5,1001) L,(IDL(K),K=1,NEN),LX

IF(L.EQ.0) L=NUMEL+1

IF(LX.EQ.0) LX=1

IF(L-N) 201,202,203

201 WRITE(6,3001) L,N

ERR = .TRUE.

GO TO 206

202 NX = LX

DO 207 K=1,NEN

207 IX(K,L) = IDL(K)

GO TO 205

203 IX(NEN,N) = IX(NEN,N-1)

DO 204 K=1,NEN

IX(K,N) = IX(K,N-1) + NX

204 IF(IX(K,N-1).EQ.0) IX(K,N) = 0

205 IF(PRT) WRITE(6,2002) N,(IX(K,N),K=1,NEN)

206 CONTINUE

GO TO 10

C.... MATERIAL DATA INPUT

3 WRITE(6,2004) 0,HEAD

CALL MATLIB

GO TO 10

C.... READ IN THE RESTRAINT CONDITIONS FOR EACH NODE

4 IF(PRT) WRITE(6,2000) 0,HEAD,(I,BC,I=1,NDF)

N = 0

NG = 0

420 L = N

LG = NG

READ(5,1001) N,NG,IDL

IF(N.LE.0 .OR. N.GT.NUMNP) GO TO 50

DO 41 I=1,NDF

ID(I,N) = IDL(I)

41 IF(L.NE.0 .AND. IDL(I).EQ.0 .AND. ID(I,L).LT.0) ID(I,N)=-1

LG = ISIGN(LG,N-L)

42 L = L+LG

IF((N-L)*LG .LE. 0) GO TO 420

DO 43 I=1,NDF

43 IF(ID(I,L-LG) .LT. 0) ID(I,L) = -1

GO TO 42

50 DO 48 N=1,NUMNP

DO 46 I=1,NDF

46 IF(ID(I,N) .NE. 0) GO TO 47

GO TO 48

47 IF(PRT) WRITE(6,2007) N,(ID(I,N),I=1,NDF)

48 CONTINUE

GO TO 10

C.... FORCE/DISPL DATA INPUT

5 CALL GENVEC(NDF,XL,F,FD,PRT,ERR)

GO TO 10

C.... END OF MESH DATA INPUT

C.... COMPUTE THE PROFILE OF GLOBLE ARRAYS

PMES 22

PMES 23

PMES 24

PMES 25

PMES 26

PMES 27

PMES 28

PMES 29

PMES 30

PMES 31

PMES 32

PMES 33

PMES 34

PMES 35

PMES 36

PMES 37

PMES 38

PMES 39

PMES 40

PMES 41

PMES 42

PMES 43

PMES 44

PMES 45

PMES 46

PMES 47

PMES 48

PMES 49

PMES 50

PMES 51

PMES 52

PMES 53

PMES 54

PMES 55

PMES 56

PMES 57

PMES 58

PMES 59

PMES 60

PMES 61

PMES 62

PMES 63

PMES 64

PMES 65

PMES 66

PMES 67

PMES 68

PMES 69

PMES 70

PMES 71

PMES 72

PMES 73

PMES 74

PMES 75

PMES 76

PMES 77

PMES 78

PMES 79

PMES 80

PMES 81

PMES 82

PMES 83

PMES 84

PMES 85

PMES 86

PMES 87

PMES 88

PMES 89

PMES 90

PMES 91

```

? IF(ERR) STOP
CALL PROFIL(JDIAG, ID, IX, NDF, NEN, NKM, PRT)
RETURN
C... PRINT OPTION
8 PRT = .TRUE.
GO TO 10
C... NOPRINT OPTION
9 PRT = .FALSE.
GO TO 10
C... READ IN PAPER EJECTION OPTION
11 READ(5,1000) O
GO TO 16
C... INPUT EXPERIMENTAL INDENTATION LAW
12 READ(5,1007) (QLAW(I), I=1,4)
WRITE(6,2008) O, HEAD, (QLAW(I), I=1,4)
GO TO 10
C... INPUT INITIAL IMPACT CONDITION
6 WRITE(6,2009) O, HEAD
READ(5,1002) NO, INDF, UR
WRITE(6,2010) NO, INDF, UR
F(INDF, NO)=1.0
IO=ID(INDF, NO)
GO TO 10
C... INPUT/OUTPUT FORMATS
1000 FORMAT(A4,7SX,A1)
1001 FORMAT(1G15)
1002 FORMAT(2IS,F10.0)
1007 FORMAT(4F10.0)
2000 FORMAT(A1,20A4//5X,10HNODAL B.C.,7X//GX,SHNODE, ,9(I7,A4,A2)/1X)
2001 FORMAT(A1,20A4//5X,8HELEMENTS//3X,7HELEMENT,
           ^ 14(I3,5H NODE)/(20X,14(I3,5H NODE)))
2002 FORMAT(I10,14I8/(10X,14I8))
2004 FORMAT(A1,20A4//5X,19HMATERIAL PROPERTIES)
2007 FORMAT(I10,9I13)
2008 FORMAT(A1,20A4//5X,*EXPERIMENTAL INDENTATION LAW*/
           1 10X,*CONTACT COEFFICIENT:      *,E12.4/
           2 10X,*CRITICAL INDENTATION:    *,E12.4/
           3 10X,*CONSTANT S:            *,E12.4/
           4 10X,*POWER INDEX OF UNLOADING LAW: * F12.3)
3001 FORMAT(5X,2GH**PMESH ERROR 01** ELEMENT,IS,
           ^ 22H APPEARS AFTER ELEMENT,IS)
2009 FORMAT(A1,20A4//5X,*IMPACT OF LAMINATED PLATE*)
2010 FORMAT(//10X,*IMPACT NODAL POINT:      *,110/
           ^          10X,*IMPACT D.O.F.:        *,110/
           ^          10X,*INITIAL IMPACT VELOCITY:*,E12.4)
END
C
C***** SUBROUTINE GENUCC(NDM, XL, X, CD, PRT, ERR)
C***** GENERATE REAL DATA ARRAYS BY LINEAR INTERPOLATION
LOGICAL PRT, ERR, PCOMP
COMMON /CTDATA/ O, HEAD(20), NUMNP, NUMEL, LAYER, NEQ, IPR
DIMENSION X(NDM, 1), XL(7), CD(3)
DATA BL/4HBLAN/
N=0
NG=0
102 LN
LG=NG
READ(5,1000) N, NG, XL
IF(N.LE.0 .OR. N.GT.NUMNP) GO TO 108
DO 103 I=1, NDM
103 X(I,N)=XL(I)
IF(LG) 104, 102, 104
104 LG=ISIGN(LG, N-L)
LI=(IABS(N-L+LG)-1)/IABS(LG)
DO 105 I=1, NDM
105 XL(I)=(X(I,N)-X(I,L))/LI
106 L=L+LG
IF((N-L)*LG .LE. 0) GO TO 102
IF(L.LE.0 .OR. L.GT.NUMNP) GO TO 110
DO 107 I=1, NDM
107

```

PMES 92
PMES 93
PMES 94
PMES 95
PMES 96
PMES 97
PMES 98
PMES 99
PMES100
PMES101
PMES102
PMES103
PMES104
PMES105
PMES106
PMES107
PMES108
PMES109
PMES110
PMES111
PMES112
PMES113
PMES114
PMES115
PMES116
PMES117
PMES118
PMES119
PMES120
PMES121
PMES122
PMES123
PMES124
PMES125
PMES126
PMES127
PMES128
PMES129
PMES130
PMES131
PMES132
PMES133
PMES134
PMES135
PMES136
PMES137

GENU 1
GENU 2
GENU 3
GENU 4
GENU 5
GENU 6
GENU 7
GENU 8
GENU 9
GENU 10
GENU 11
GENU 12
GENU 13
GENU 14
GENU 15
GENU 16
GENU 17
GENU 18
GENU 19
GENU 20
GENU 21
GENU 22
GENU 23

```

107 X(I,L)=X(I,L-LG)+XL(I)
110 WRITE(6,3000) L,(CD(I),I=1,3)
ERR = .TRUE.
GO TO 102
108 DO 109 I=1,NUMNP,50
IF(FRT) WRITE(6,2000) 0,HEAD,(CD(L),L=1,3),(L,CD(1),CD(2),L=1,NDM)
N = NINO(NUMNP,I+49)
DO 109 J=I,N
IF(PCOMP(X(1,J),BL),.AND.,PRT) WRITE(6,2008) N
109 IF(.NOT.PCOMP(X(1,J),BL).AND.PRT) WRITE(6,2009) J,(X(L,J),L=1,NDM)
RETURN
1000 FORMAT(2I5,7F10.0)
2000 FORMAT(A1,20A4//5X, 5HNODEL,3A4//6X,4HNODE,9(I7,A4,A2))
2008 FORMAT(5X,21H**GENVEC WARNING 01**,I10,
^ 32H HAS NOT BEEN INPUT OR GENERATED)
2009 FORMAT(I10,9F13.4)
3000 FORMAT(5X,44H**GENVEC ERROR 01**ATTEMPT TO GENETATE NODE,I5,
1 3H IN,3A4)
END
C
C***** SUBROUTINE PROFIL(JDIAG, ID, IX, NDF, NEN, NKM, PRT)
C***** COMPUTE PROFILE OF GLOBAL ARRAYS
LOGICAL PRT
COMMON /CTDATAL/ 0,HEAD(20),NUMNP,NUMEL,LAYER,NEQ,IPR
DIMENSION JDIAG(1),ID(NDF,1),IX(NEN,1),EQ(2)
DATA EQ/4H DOF,2H/
C.... SET UP THE EQUATION NUMBERS
NEQ = 0
DO 50 N=1,NUMNP
DO 40 I=1,NDF
J = ID(I,N)
IF(J) 30,20,30
20 NEQ = NEQ + 1
ID(I,N) = NEQ
JDIAG(NEQ) = 0
GO TO 40
30 ID(I,N) = 0
40 CONTINUE
50 CONTINUE
IF(.NOT.PRT) GO TO 70
WRITE(6,2000) 0,HEAD,(I,EQ,I=1,NDF)
DO 60 I=1,NUMNP
60 WRITE(6,2001) I,(ID(K,I),K=1,NDF)
C... COMPUTE COLUMN HEIGHTS
70 DO 500 N=1,NUMEL
DO 400 I=1,NEN
II = IX(I,N)
IF(II.EQ.0) GO TO 400
DO 300 K=1,NDF
KK = ID(K,II)
IF(KK.EQ.0) GO TO 300
DO 200 J=I,NEN
JJ = IX(J,N)
IF(JJ.EQ.0) GO TO 200
DO 100 L=1,NDF
LL = ID(L,JJ)
IF(LL.EQ.0) GO TO 100
M = MAX0(KK,LL)
JDIAG(M) = MAX0(JDIAG(M),IAbs(KK-LL))
100 CONTINUE
200 CONTINUE
300 CONTINUE
400 CONTINUE
500 CONTINUE
C.... COMPUTE DIAGONAL POINTERS FOR PROFILE
NKM = 1
JDIAG(1) = 1
IF(NEQ.EQ.1) RETURN
DO 600 N=2,NEQ

```

GENU 24
GENU 25
GENU 26
GENU 27
GENU 28
GENU 29
GENU 30
GENU 31
GENU 32
GENU 33
GENU 34
GENU 35
GENU 36
GENU 37
GENU 38
GENU 39
GENU 40
GENU 41
GENU 42
GENU 43

PROF 1
PROF 2
PROF 3
PROF 4
PROF 5
PROF 6
PROF 7
PROF 8
PROF 9
PROF 10
PROF 11
PROF 12
PROF 13
PROF 14
PROF 15
PROF 16
PROF 17
PROF 18
PROF 19
PROF 20
PROF 21
PROF 22
PROF 23
PROF 24
PROF 25
PROF 26
PROF 27
PROF 28
PROF 29
PROF 30
PROF 31
PROF 32
PROF 33
PROF 34
PROF 35
PROF 36
PROF 37
PROF 38
PROF 39
PROF 40
PROF 41
PROF 42
PROF 43
PROF 44
PROF 45
PROF 46
PROF 47
PROF 48
PROF 49

ORIGINAL PAGE IS
OF POOR QUALITY

```

600 JDIAG(N) = JDIAG(N) + JDIAG(N-1) + 1 PROF 50
      NKM = JDIAG(NEQ) PROF 51
2000 FORMAT(A1,20A4//5X,1GHEQUATION NUMBERS//GX,5HNODE , PROF 52
      ^ 9(I5,A4,A2)/1X) PROF 53
2001 FORMAT(I10,9I11) PROF 54
      RETURN PROF 55
      END PROF 56
C
C***** SUBROUTINE MATLID NATL 1
C***** MATERIAL PROPERTIES ROUTINE NATL 2
COMMON /CTDATA/ O,HEAD(20),NUMNP,NUMEL,LAYER,NEQ,IPR NATL 3
COMMON /MTDATA/ RHO,UU12,E1,E2,G12,G13,G23,THK,WIDTH NATL 4
COMMON /COMPST/ ABD(G,G),DS(2,2),QBR(3,3,25),QBS(2,2,25), NATL 5
      ^ TH(25),2K(25) NATL 6
COMMON /DMATIX/ D(10),DB(6,6),LINT NATL 7
DIMENSION WD(S) NATL 8
DATA WD/GH ISO-,GH ORTHO,GHTROPIC,GH COMP,GHOSITE / NATL 9
C.... INPUT MATERIAL PROPERTIES NATL 10
READ(S,1000) L1,L2,K,THK,WIDTH NATL 11
READ(S,1001) RHO,UU12,E1,E2,G12,G13,G23 NATL 12
DO 150 J=1,3 NATL 13
DO 150 I=1,3 NATL 14
IF(I.EQ.3 .OR. J.EQ.3) GO TO 150 NATL 15
DS(J,I) = 0. NATL 16
150 ABD(J,I) = ABD(J+3,I) = ABD(J,I+3) = ABD(J+3,I+3) = 0, NATL 17
      L1 = MIN0(4,MAX0(1,L1)) NATL 18
      D(1) = L1 NATL 19
      L2 = MIN0(4,MAX0(1,L2)) NATL 20
      D(2) = L2 NATL 21
      D(3) = K NATL 22
      LINT=0 NATL 23
      IF(E1-E2) 120,110,120 NATL 24
110 G12=E1/(2.**(1.+UU12)) NATL 25
      J1=1 $ J2=3 NATL 26
      GO TO 200 NATL 27
120 J1=4 $ J2=5 NATL 28
      IF(LAYER.EQ.1) J1=2 $ J2=3 NATL 29
200 WRITE(G,2000) LAYER,WD(J1),WD(J2),THK,E1,E2,G12,G13,G23,UU12, NATL 30
      ^ RHO,L1,L2," NATL 31
      CALL CMRD NATL 32
      RETURN NATL 33
C... FORMAT FOR INPUT-OUTPUT NATL 34
1000 FORMAT(3I5,2F10.0) NATL 35
1001 FORMAT(7F10.0) NATL 36
2000 FORMAT(/5X,I2,12H LAYER(S) OF,2AG,21H PLATE WITH THICKNESS, NATL 37
      1 F10.4//10X,15HYOUNG*S MODULUS,10X,*E1=*E,E10.4,10X,*E2=*E,E10.4// NATL 38
      2 10X,15HSHEAR MODULUS,9X,*G12=*E,E10.4,9X,*G13=*E,E10.4,9X, NATL 39
      3 *G23=*E,E10.4/10X,15HPOISSON RATIO,8X,*UU12=*E,F5.3/10X, NATL 40
      4 ?HDENSITY,17X,*RHO=*E,E10.4/10X,13HGAUSS PTS/DIR,12X,*L1=*E,I5, NATL 41
      5 5X,*L2=*E,I5/10X,12HSTRESS POINT,14X,*K=*E,I5/) NATL 42
      END NATL 43
C
C***** SUBROUTINE CMRD CMPD 1
C***** COMPUTE #ABD# MATRIX AND #DS# MATRIX CMPD 2
COMMON /CTDATA/ O,HEAD(20),NUMNP,NUMEL,LAYER,NEQ,IPR CMPD 3
COMMON /MTDATA/ RHO,UU12,E1,E2,G12,G13,G23,THK,WIDTH CMPD 4
COMMON /COMPST/ ABD(G,G),DS(2,2),QBR(3,3,25),QBS(2,2,25), CMPD 5
      ^ TH(25),2K(25) CMPD 6
DIMENSION Q(3,3),DS(2,2),TK(25) CMPD 7
LL=AYER CMPD 8
11=LL+1 CMPD 9
READ(S,1000) (L,TH(L),TK(L),I=1,LL) CMPD 10
2K(1)=TTK=0.0 CMPD 11
DO 15 I=1,LL CMPD 12
    TTK=TTK+TK(I) CMPD 13
    2K(I+1)=TK(I)+2K(I) CMPD 14
15 CONTINUE CMPD 15
DO 25 I=1,NM CMPD 16
    ZK(I)=ZK(I)-TTK/2. CMPD 17
25 CONTINUE CMPD 18

```

```

DEL=4.*ATAN(1.)/180.
DEN = 1. - E2*UU12**2/E1
Q(1,1) = E1/DEN
Q(2,2) = E2/DEN
Q(1,2) = Q(2,1) = UU12*Q(2,2)
Q(3,3) = G12
Q(1,3) = Q(2,3) = Q(3,1) = Q(3,2) = 0.0
QS(1,1) = G13
QS(2,2) = G23
QS(1,2) = QS(2,1) = 0.0
DO 40 I=1,LL
ANGL=TH(I)*DEL
C=COS(ANGL)
W=SIN(ANGL)
QBR(1,1,I)=Q(1,1)*C**4+2.*(Q(1,2)+2.*Q(3,3))*(C*W)**2+Q(2,2)*W**4
QBR(1,2,I)=QBR(2,1,I)=(Q(1,1)+Q(2,2)-4.*Q(3,3))*(C*W)**2
$           +Q(1,2)*(W**4+C**4)
QBR(2,2,I)=Q(1,1)*W**4+2.*(Q(1,2)+2.*Q(3,3))*(C*W)**2+Q(2,2)*C**4
QBR(1,3,I)=QBR(3,1,I)=(Q(1,1)-Q(1,2)-2.*Q(3,3))*W*C**3 +
$           (Q(1,2)-Q(2,2)+2.*Q(3,3))*C*W**3
QBR(2,3,I)=QBR(3,2,I)=(Q(1,1)-Q(1,2)-2.*Q(3,3))*W**3+C*
$           (Q(1,2)-Q(2,2)+2.*Q(3,3))*W*C**3
QBR(3,3,I)=(Q(1,1)+Q(2,2)-2.*Q(1,2)-2.*Q(3,3))*(W*C)**2+
$           Q(3,3)*(W**4+C**4)
QBS(1,1,I) = QS(1,1)*C**2 + QS(2,2)*W**2
QBS(2,2,I) = QS(1,1)*W**2 + QS(2,2)*C**2
QBS(1,2,I) = QBS(2,1,I) = (QS(1,1)-QS(2,2))*C*W
40 CONTINUE
DO 50 J=1,3
DO 50 K=1,3
DO 50 I=1,LL
ABD(J ,K )= ABD(J ,K )+QBR(J,K,I)*(ZK(I+1)-ZK(I))
ABD(J+3,K )= ABD(J ,K+3)= ABD(J+3,K)+QBR(J,K,I)*
$           (ZK(I+1)**2-ZK(I)**2)/2.
ABD(J+3,K+3)= ABD(J+3,K+3)+QBR(J,K,I)*(ZK(I+1)**3-ZK(I)**3)/3.
50 CONTINUE
DO 55 I=1,6
DO 55 J=1,6
IF(I.GE.3 .OR. J.GE.3) GO TO 55
IF(ABS(DS(I,J)) .LT. 1.E-06) DS(I,J)=0.0
55 IF(ABS(ABD(I,J)) .LT. 1.E-06) ABD(I,J)=0.0
WRITE(6,2001) ((ABD(I,J),J=1,6),I=1,6)
DO 60 J=1,2
DO 60 K=1,2
DO 60 I=1,LL
60 DS(J,K) = DS(J,K) + QBS(J,K,I)*(ZK(I+1)-ZK(I))
WRITE(6,2002) ((DS(I,J),J=1,2),I=1,2)
1000 FORMAT(1S,F5.0,F10.0)
2001 FORMAT(//,1X,10HABD MATRIX//6(2X,6E13.4/))
2002 FORMAT(//,1X,9HDS MATRIX//2(2X,2E13.4/))
RETURN
END
C
SUBROUTINE KMLIB
***** ASSEMBLE GLOBLE ARRAY
COMMON G(1)
DIMENSION M(1)
EQUIVALENCE (G(1),M(1))
COMMON /ISWIDX/ ISW
COMMON /CTDATAL/ O,HEAD(20),NUMNP,NUMEL,LAYER,NEQ,IPR
COMMON /LODATA/ NDF,NDM,NEN,NST,NKM
COMMON /PARATS/ NPAR(14),NEND
N1=NEND
N2=N1+NST*NST*IPR
IF(ISW.LE.2) NE=N2+NKM*IPR
IF(ISW.GT.2) NE=N2+NEQ*IPR
CALL SETMEM(NE)
CALL PZERO(G(NEND),NE-NEND)
CALL MASS01(G(NPAR(1)),G(NPAR(2)),M(NPAR(3)),G(NPAR(4)),
1   M(NPAR(5)),M(NPAR(6)),G(NPAR(7)),G(NPAR(8)),M(NPAR(9))),
```

CMPD	19
CMPD	20
CMPD	21
CMPD	22
CMPD	23
CMPD	24
CMPD	25
CMPD	26
CMPD	27
CMPD	28
CMPD	29
CMPD	30
CMPD	31
CMPD	32
CMPD	33
CMPD	34
CMPD	35
CMPD	36
CMPD	37
CMPD	38
CMPD	39
CMPD	40
CMPD	41
CMPD	42
CMPD	43
CMPD	44
CMPD	45
CMPD	46
CMPD	47
CMPD	48
CMPD	49
CMPD	50
CMPD	51
CMPD	52
CMPD	53
CMPD	54
CMPD	55
CMPD	56
CMPD	57
CMPD	58
CMPD	59
CMPD	60
CMPD	61
CMPD	62
CMPD	63
CMPD	64
CMPD	65
CMPD	66
CMPD	67
CMPD	68
CMPD	69
CMPD	70
KMLI	1
KMLI	2
KMLI	3
KMLI	4
KMLI	5
KMLI	6
KMLI	7
KMLI	8
KMLI	9
KMLI	10
KMLI	11
KMLI	12
KMLI	13
KMLI	14
KMLI	15
KMLI	16
KMLI	17

```

2 G(NPAR(11)),G(N1),G(N2),NDF,NDM,NEN,NST,NKM)          KMLI 18
  RETURN                                                 KMLI 19
  END                                                 KMLI 20
C
C      SUBROUTINE MASS01(UL,XL,LD,P,IX, ID,X,F,JDIAG,B,S,A,NDF,NDM,NEN,
^      NST,NKM)                                         MASS 1
C****  FORM MASS MATRIX                               MASS 2
COMMON /CTDATA/ O,HEAD(20),NUMNP,NUMEL,LAYER,NEQ,IPR   MASS 3
COMMON /MTDATA/ RHO,VU12,E1,E2,G12,G13,G23,THK,WIDTH  MASS 4
COMMON /DMATRIX/ D(10),DB(6,6),LINT                  MASS 5
COMMON /ELDATA/ N,NEL,MCT                            MASS 6
COMMON /ISWIDX/ ISW                                MASS 7
COMMON /GAUSSP/ SG(16),TG(16),WG(16)                MASS 8
DIMENSION UL(1),XL(NDM,1),LD(NDF,1),P(1),IX(NEN,1),ID(NDF,1),
1 X(NDM,1),F(1),JDIAG(1),B(1),S(NST,1),A(1),SHP(3,12)  MASS 9
C....  LOOP ON ELEMENTS                           MASS 10
DO 110 N=1,NUMEL                                 MASS 11
DO 10 I=1,NST                                    MASS 12
DO 10 J=1,NST                                    MASS 13
10 S(I,J)=0.                                     MASS 14
C....  SET UP LOCAL ARRAYS                         MASS 15
CALL PFORM(UL,XL,LD,IX, ID,X,F,B,NDF,NDM,NEN,ISW)  MASS 16
C....  COMPUTE CONSISTENT MASS MATRIX             MASS 17
      L = D(1)                                     MASS 18
      CALL PGAUSS(L,LINT)                          MASS 19
      DO 500 L=1,LINT                            MASS 20
      DU = WG(L)*XSJ*RHO*THK                     MASS 21
C ..  COMPUTE SHAPE FUNCTIONS                   MASS 22
      CALL SHAPE(SG(L),TG(L),XL,SHP,XSJ,NDM,NEL,IX,.FALSE.)
      DV = WG(L)*XSJ*RHO*THK                     MASS 23
C ..  FOR EACH NODE J COMPUTE DB=RHO*SHAPE*DU    MASS 24
      K1 = 1                                       MASS 25
      DO 500 J=1,NEL                             MASS 26
      W11 = SHP(3,J)*DU                          MASS 27
      W33 = W11*THK**2/12.                        MASS 28
C ..  FOR EACH NODE K COMPUTE MASS MATRIX (UPPER TRIANGULAR PART)  MASS 29
      J1 = K1                                     MASS 30
      DO 510 K=J,NEL                            MASS 31
      S(J1 ,K1 ) = S(J1 ,K1 ) + SHP(3,K)*W11  MASS 32
      S(J1+3,K1+3) = S(J1+3,K1+3) + SHP(3,K)*W33  MASS 33
      510 J1 = J1 + NDF                          MASS 34
      500 K1 = K1 + NDF                          MASS 35
C ..  COMPUTE MISSING PARTS AND LOWER PART BY SYMMETRY  MASS 36
      NSL = NEL*NDF                            MASS 37
      DO 530 K=1,NSL,NDF                      MASS 38
      DO 520 J=K,NSL,NDF                      MASS 39
      S(J+2,K+2) = S(J+1,K+1) = S(J ,K )       MASS 40
      S(J+4,K+4) = S(J+3,K+3)                   MASS 41
      S(K ,J ) = S(J ,K )                       MASS 42
      S(K+3,J+3) = S(J+3,K+3)                   MASS 43
      S(K+2,J+2) = S(K+1,J+1) = S(J ,K )       MASS 44
      520 S(K+4,J+4) = S(J+3,K+3)               MASS 45
      530 CONTINUE                                MASS 46
      IF(ISW.EQ.2) GO TO 100                    MASS 47
C....  LUMPED MASS MATRIX                      MASS 48
      SUM1 = 0.0                                  MASS 49
      SUM2 = 0.0                                  MASS 50
      SUMD1 = 0.0                                 MASS 51
      SUMD2 = 0.0                                 MASS 52
      DO 540 I=1,NSL,NDF                      MASS 53
      SUMD1 = SUMD1 + S(I,I)                   MASS 54
      SUMD2 = SUMD2 + S(I+3,I+3)               MASS 55
      DO 540 J=1,NSL,NDF                      MASS 56
      SUM1 = SUM1 + S(I,J)                   MASS 57
      540 SUM2 = SUM2 + S(I+3,J+3)               MASS 58
      DO 550 I=1,NSL,NDF                      MASS 59
      P(I) = S(I,I)*SUM1/SUMD1                 MASS 60
      P(I+2) = P(I+1) = P(I)                   MASS 61
      P(I+3) = S(I+3,I+3)*SUM2/SUMD2           MASS 62
      550 P(I+4) = P(I+3)                   MASS 63
C....  ADD TO TOTAL ARRAY                      MASS 64

```

```

100 CALL ADDSTF(A,S,P,JDIAG,LD,NST,NEL*NDF,.FALSE.)
110 CONTINUE
      REWIND 2
      IF(ISW.EQ.2) WRITE(2) (A(I),I=1,NKM)
      IF(ISW.EQ.3) WRITE(2) (A(I),I=1,NEQ)
      RETURN
      END
C
C SUBROUTINE RODIPCT
C*****
LOGICAL FLAG
COMMON G(1)
DIMENSION M(1)
EQUIVALENCE (G(1),M(1))
COMMON /CTDATA/ O,HEAD(20),NUMNP,NUMEL,LAYER,NEQ,IPR
COMMON /LODATA/ NDF,NDM,NEN,NST,NKM
COMMON /PARATS/ NPAR(14),NEND
COMMON /RODATA/ UR,IQ,NDS
COMMON /ROELEM/ NER,NEQR,ER
DATA FLAG/.FALSE./,NER/20/,ER/30000000./
IF(FLAG) GO TO 50
NEQR=2*(NER+1)
NKMR=7*NER+3
N1=NEND
N2=N1+NEQ*IPR
N3=N2+NEQ*IPR
N4=N3+NEQ*IPR
N5=N4+NKMR*IPR
N6=N5+NEQR*IPR
N7=N6+NEQR
N8=N7+NEQR*IPR
N9=N8+NEQR*IPR
N10=N9+NEQR*IPR
N11=N10+NEQR*IPR
NE=N11+NEQR*IPR
CALL SETMEM(NE)
CALL PZERO(G(NEND),NE-NEND)
FLAG=.TRUE.
50 CALL WIMPCT(G(NPAR(1)),G(NPAR(2)),M(NPAR(3)),G(NPAR(4)),
1           M(NPAR(5)),M(NPAR(6)),G(NPAR(7)),G(NPAR(8)),
2           M(NPAR(9)),G(NPAR(10)),G(NPAR(11)),G(N1),G(N2),
3           G(N3),G(N4),G(N5),M(N6),G(N7),G(N8),G(N9),G(N10),
4           G(N11))
      RETURN
      END
C
C SUBROUTINE WIMPCT(UL,XL,LD,P,IX,ID,X,F,JDIAG,DR,U,B,V,A,RK,RM,
^          JDR,RU,RV,RA,RB,FR)
C*****
SOLVE IMPACT PROBLEM
LOGICAL FLAG,TAN
COMMON G(1)
DIMENSION M(1)
EQUIVALENCE (G(1),M(1))
COMMON /CTDATA/ O,HEAD(20),NUMNP,NUMEL,LAYER,NEQ,IPR
COMMON /TMDATA/ TIME,DT,DDT,FORCE,ALPHA
COMMON /LODATA/ NDF,NDM,NEN,NST,NKM
COMMON /NITERS/ ITR
COMMON /PARATS/ NPAR(14),NEND
COMMON /RODATA/ UR,IQ,NDS
COMMON /ROELEM/ NER,NEQR,ER
COMMON /CONSTS/ A0,A2,A4,A5,A6,A7,A8,AREA
COMMON /PROLOD/ PROP
COMMON /ISWIDX/ ISW
COMMON /EXTRAS/ TAN
DIMENSION UL(1),XL(1),LD(1),P(1),IX(1),ID(1),X(1),F(1),JDIAG(1),
1           DR(1),U(1),B(1),V(1),A(1),RK(1),RM(1),JDR(1),RU(1),
2           RV(1),RA(1),RB(1),FR(1),Q(3),QP(3)
DATA ITR/5/,FLAG/.FALSE./,WIL/1.4/,INTE/24/
IF(FLAG) GO TO 50
DO 1 I=1,3
      
```

MASS	67
MASS	68
MASS	69
MASS	70
MASS	71
MASS	72
MASS	73
RODI	1
RODI	2
RODI	3
RODI	4
RODI	5
RODI	6
RODI	7
RODI	8
RODI	9
RODI	10
RODI	11
RODI	12
RODI	13
RODI	14
RODI	15
RODI	16
RODI	17
RODI	18
RODI	19
RODI	20
RODI	21
RODI	22
RODI	23
RODI	24
RODI	25
RODI	26
RODI	27
RODI	28
RODI	29
RODI	30
RODI	31
RODI	32
RODI	33
RODI	34
RODI	35
RODI	36
RODI	37
WIMP	1
WIMP	2
WIMP	3
WIMP	4
WIMP	5
WIMP	6
WIMP	7
WIMP	8
WIMP	9
WIMP	10
WIMP	11
WIMP	12
WIMP	13
WIMP	14
WIMP	15
WIMP	16
WIMP	17
WIMP	18
WIMP	19
WIMP	20
WIMP	21
WIMP	22
WIMP	23
WIMP	24

```

Q(I)=0.0          WIMP 25
QP(I)=0.0         WIMP 26
1 CONTINUE        WIMP 27
IJS=1             WIMP 28
TAN=.FALSE.       WIMP 29
REWIND 2           WIMP 30
READ(2) (B(I),I=1,NEQ) WIMP 31
FORCE=0.0          WIMP 32
ALPHA=0.0          WIMP 33
PROP=0.0           WIMP 34
NNEQ=NDF*NUMNP    WIMP 35
A0=6./(WIL*DT)**2 WIMP 36
A2=6./(WIL*DT)    WIMP 37
A4=A0/WIL          WIMP 38
A5=-A2/WIL         WIMP 39
A6=1.-3./WIL       WIMP 40
A7=DT/2.           WIMP 41
A8=DDT/6.          WIMP 42
CALL FORMROD(RK,RM,JDR) WIMP 43
DO 10 I=1,NEQR    WIMP 44
10 RV(I)=-VR      WIMP 45
Q(2)=-VR          WIMP 46
FLAG=.TRUE.        WIMP 47
50 ISW=5           WIMP 48
IF(IDS.EQ.NDS) TAN=.TRUE.   WIMP 49
CALL FSTREA(UL,XL,LD,P,IX, ID,X,F,JDIAG,DR,U,NDF,NDM,NEN,NST,NNEQ) WIMP 50
DO 20 I=1,NEQ     WIMP 51
A(I)=DR(I)/B(I)  WIMP 52
U(I)=U(I)+DT*A(I) WIMP 53
U(I)=U(I)+DT*U(I) WIMP 54
20 CONTINUE        WIMP 55
OP(1)=U(IQ)       WIMP 56
OP(2)=V(IQ)       WIMP 57
OP(3)=A(IQ)       WIMP 58
DO 30 I=1,NEQR    WIMP 59
RB(I)=RM(I)*(A0*RU(I)+A2*RV(I)+2.*RA(I)) WIMP 60
30 CONTINUE        WIMP 61
RBIQ=RU(1)+DT*RU(1)+DDT/3.*RA(1) WIMP 62
ROT=0.000001       WIMP 63
ICOV=0             WIMP 64
DO 100 IT=1,ITR   WIMP 65
RUT=RBIQ+Q(3)*DDT/6.  WIMP 66
AF=-RUT-QP(1)     WIMP 67
CALL RODLOAD(FIQ,AF) WIMP 68
DO 110 I=1,NEQR    WIMP 69
FR(I)=RB(I)        WIMP 70
110 CONTINUE        WIMP 71
FR(1)=FR(1)+(1.-WIL)*FORCE+WIL*FIQ WIMP 72
CALL ACTCOL(RK,FR,JDR,NEQR,.FALSE.,.TRUE.,0) WIMP 73
Q(3)=A4*(FR(1)-RU(1))+A5*RV(1)+A6*RA(1) WIMP 74
RUTT=RBIQ+Q(3)*DDT/6.  WIMP 75
ROTR=ABS((RUTT-RUT)/RUTT) WIMP 76
IF(ROTR.LT.ROT) ICOV=1 WIMP 77
IF(ICOV.GT.0) GO TO 200 WIMP 78
100 CONTINUE        WIMP 79
200 DO 210 I=1,NEQR WIMP 80
FR(I)=A4*(FR(I)-RU(I))+A5*RV(I)+A6*RA(I) WIMP 81
RU(I)=RU(I)+DT*RU(I)+A8*(FR(I)+2.*RA(I)) WIMP 82
RU(I)=RU(I)+A7*(FR(I)+RA(I)) WIMP 83
RA(I)=FR(I)        WIMP 84
210 CONTINUE        WIMP 85
O(1)=RU(1)          WIMP 86
O(2)=RV(1)          WIMP 87
O(3)=RA(1)          WIMP 88
FORCE=FIQ           WIMP 89
PROP=FORCE          WIMP 90
ALPHA=-Q(1)-QP(1)  WIMP 91
RODFR=RU(INTE)*AREA*ER WIMP 92
WRITE(8,8001) FORCE,ALPHA,RODFR,(Q(I),I=1,3) WIMP 93
8001 FORMAT(6E12.4) WIMP 94

```

ORIGINAL PAGE IS
OF POOR QUALITY

```

IDS=IDS+1
IF(IDS.GT.NDS) IDS=1
TAN=.FALSE.
RETURN
END

C
C***** SUBROUTINE FORMROD(RK,RM,JDR)
      FORM 1
      FORM 2
      FORM 3
      FORM 4
      FORM 5
      FORM 6
      FORM 7
      FORM 8
      FORM 9
      FORM 10
      FORM 11
      FORM 12
      FORM 13
      FORM 14
      FORM 15
      FORM 16
      FORM 17
      FORM 18
      FORM 19
      FORM 20
      FORM 21
      FORM 22
      FORM 23
      FORM 24
      FORM 25
      FORM 26
      FORM 27
      FORM 28
      FORM 29
      FORM 30
      FORM 31
      FORM 32
      FORM 33
      FORM 34
      FORM 35
      FORM 36
      FORM 37
      FORM 38
      FORM 39
      FORM 40
      FORM 41
      FORM 42
      FORM 43
      FORM 44
      FORM 45
      FORM 46
      FORM 47
      FORM 48

      FORM 1
      FORM 2
      FORM 3
      FORM 4
      FORM 5
      FORM 6
      FORM 7
      FORM 8
      FORM 9
      FORM 10
      FORM 11
      FORM 12
      FORM 13
      FORM 14
      FORM 15
      FORM 16
      FORM 17
      FORM 18
      FORM 19
      FORM 20
      FORM 21
      FORM 22
      FORM 23
      FORM 24
      FORM 25
      FORM 26
      FORM 27
      FORM 28
      FORM 29
      FORM 30
      FORM 31
      FORM 32
      FORM 33
      FORM 34
      FORM 35
      FORM 36
      FORM 37
      FORM 38
      FORM 39
      FORM 40
      FORM 41
      FORM 42
      FORM 43
      FORM 44
      FORM 45
      FORM 46
      FORM 47
      FORM 48

C***** SUBROUTINE RODLOAD(F,AF)
      RODL 1
      RODL 2
      RODL 3
      RODL 4
      RODL 5
      RODL 6
      RODL 7
      RODL 8
      RODL 9
      RODL 10
      RODL 11
      RODL 12
      RODL 13
      RODL 14
      RODL 15

      RODL 1
      RODL 2
      RODL 3
      RODL 4
      RODL 5
      RODL 6
      RODL 7
      RODL 8
      RODL 9
      RODL 10
      RODL 11
      RODL 12
      RODL 13
      RODL 14
      RODL 15

```

COMMON /RODATA/ VR, IQ, NDS
 COMMON /ROELEM/ NER, NEQR, ER
 COMMON /CONSTS/ A0, A2, A4, A5, A6, A7, AB, AREA
 DIMENSION RK(1), RM(1), JDR(2), D(6)
 DATA RHOR/.0003225/, RL/1.0/
 DATA D/.22,.36,.43,.48,.50,.625/
 EL=RL/NER
 PAI=4.*ATAN(1.)
 JDR(1)=1
 JDR(2)=3
 DO 100 I=1, NER
 IF(I.LT.6) A=PAI*(D(I)/2.)**2
 IF(I.GE.6) A=PAI*(D(6)/2.)**2
 TT=A*ER/30./EL
 J1=2*(I+1)-1
 J2=J1+1
 J1M1=J1-1
 J1M2=J1-2
 JDR(J1)=JDR(J1M1)+3
 JDR(J2)=JDR(J1)+4
 K1=JDR(J1M2)
 K2=JDR(J1M1)-1
 RK(K1)=RK(K1)+TT*36.
 RK(K2)=RK(K2)+TT*3.*EL
 RK(K2+1)=RK(K2+1)+TT*4.*EL**2
 RK(K2+2)=RK(K2+2)-TT*36.
 RK(K2+3)=RK(K2+3)-TT*3.*EL
 RK(K2+4)=RK(K2+4)+TT*36.
 RK(K2+5)=RK(K2+5)+TT*3.*EL
 RK(K2+6)=RK(K2+6)-TT*EL**2
 RK(K2+7)=RK(K2+7)-TT*3.*EL
 RK(K2+8)=RK(K2+8)+TT*4.*EL**2
 TT=RHOR*A*EL
 L1=2*I-1
 RM(L1)=RM(L1)+TT/2.
 RM(L1+1)=RM(L1+1)+TT*EL**2/420.
 RM(L1+2)=RM(L1+2)+TT/2.
 RM(L1+3)=RM(L1+3)+TT*EL**2/420.
 100 CONTINUE
 AREA=A
 DO 20 I=1, NEQR
 J=JDR(I)
 20 RK(J)=RK(J)+A0*RM(I)
 CALL ACTCOL(RK, RM, JDR, NEQR, .TRUE., .FALSE., 0)
 RETURN
 END

C
C***** SUBROUTINE CONTACTLOADING
 LOGICAL RELD, UNLD, PIL
 COMMON /TMDDATA/ TIME, DT, DDT, FORCE, ALPHA
 COMMON /EXDATA/ Q(4)
 DATA UNLD/.FALSE./, PIL/.FALSE./, RELD/.FALSE./
 IF(PIL) GO TO 10
 AMAX=AMIN=FMAX=0.0
 PIL=.TRUE.

 10 IF(RELD) GO TO 50
 IF(UNLD) GO TO 20
 F=Q(1)*AF**1.5
 IF(F.GE.FFORCE) RETURN
 UNLD=.TRUE.
 AMAX=ALPHA

```
FMAX=FORCE
IF(AMAX.GT.Q(2)) UK=FMAX/((1.-Q(3))*AMAX+Q(2)*Q(3)**Q(4))
IF(AMAX.LE.Q(2)) UK=FMAX/AMAX**Q(4)
AMIN=Q(3)*(AMAX-Q(2))
IF(AMIN.LT.0.) AMIN=0.0
20 IF(AF.LE.AMIN) GO TO 30
F=UK*(AF-AMIN)**Q(4)
IF(F.LT.FORCE) RETURN
RELD=.TRUE.
RK=FMAX/(AMAX-AMIN)**1.5
50 IF(AF.LE.AMIN) GO TO 30
F=RK*(AF-AMIN)**1.5
RETURN
30 F=0.0
RETURN
END
```

RODL 16
RODL 17
RODL 18
RODL 19
RODL 20
RODL 21
RODL 22
RODL 23
RODL 24
RODL 25
RODL 26
RODL 27
RODL 28
RODL 29
RODL 30
RODL 31

INTERIM REPORT

ORIGINAL PAGE IS
OF POOR QUALITY

NSG 3185

WAVE PROPAGATION IN GRAPHITE/EPOXY LAMINATES DUE TO IMPACT

NASA CR-168057

Advanced Research Projects Agency
Washington DC 20525
Attn: Library

Advanced Technology Center, Inc.
LTV Aerospace Corporation
P.O. Box 6144
Dallas, TX 75222
Attn: D. H. Petersen
W. J. Renton

Air Force Flight Dynamics Laboratory
Wright-Patterson Air Force Base, OH 45433
Attn: E. E. Baily
G. P. Sendeckyj (FBC)
R. S. Sandhu

Air Force Materials Laboratory
Wright-Patterson Air Force Base, OH 45433
Attn: H. S. Schwartz (LN)
T. J. Reinhart (MBC)
G. P. Peterson (LC)
E. J. Morrisey (LAE)
S. W. Tsai (MBM)
N. J. Pagano
J. M. Whitney (MBM)

Air Force Office of Scientific Research
Washington DC 20333
Attn: J. F. Masi (SREP)

Air Force Office of Scientific Research
1400 Wilson Blvd.
Arlington, VA 22209

AFOSR/NA
Bolling AFB, DC 20332
Attn: A. K. Amos

Air Force Rocket Propulsion Laboratory
Edwards, CA 93523
Attn: Library

Babcock & Wilcox Company
Advanced Composites Department
P.O. Box 419
Alliance, Ohio 44601
Attn: P. M. Leopold

ORIGINAL PAGE IS
OF POOR QUALITY

Bell Helicopter Company
P.O. Box 482
Ft. Worth, TX 76101
Attn: H. Zinberg

The Boeing Company
P. O. Box 3999
Seattle, WA 98124
Attn: J. T. Hoggatt, MS. 88-33
T. R. Porter

The Boeing Company
Vertol Division
Morton, PA 19070
Attn: E. C. Durchlaub

Battelle Memorial Institute
Columbus Laboratories
505 King Avenue
Columbus, OH 43201
Attn: L. E. Hulbert

Bendix Advanced Technology Center
9140 Old Annapolis Rd/Md. 108
Columbia, MD 21045
Attn: O. Hayden Griffin

Brunswick Corporation
Defense Products Division
P. O. Box 4594
43000 Industrial Avenue
Lincoln, NE 68504
Attn: R. Morse

Celanese Research Company
86 Morris Ave.
Summit, NJ 07901
Attn: H. S. Kliger

Commander
Natick Laboratories
U. S. Army
Natick, MA 01762
Attn: Library

ORIGINAL PAGE IS
OF POOR QUALITY

Commander
Naval Air Systems Command
U. S. Navy Department
Washington DC 20360
Attn: M. Stander, AIR-43032D

Commander
Naval Ordnance Systems Command
U.S. Navy Department
Washington DC 20360
Attn: B. Drimmer, ORD-033
M. Kinna, ORD-033A

Cornell University
Dept. Theoretical & Applied Mech.
Thurston Hall
Ithaca, NY 14853
Attn: S. L. Phoenix

Defense Metals Information Center
Battelle Memorial Institute
Columbus Laboratories
505 King Avenue
Columbus, OH 43201

Department of the Army
U.S. Army Aviation Materials Laboratory
Ft. Eustis, VA 23604
Attn: I. E. Figge, Sr.
Library

Department of the Army
U.S. Army Aviation Systems Command
P.O. Box 209
St. Louis, MO 63166
Attn: R. Vollmer, AMSAV-A-UE

Department of the Army
Plastics Technical Evaluation Center
Picatinny Arsenal
Dover, NJ 07801
Attn: H. E. Pebly, Jr.

Department of the Army
Watervliet Arsenal
Watervliet, NY 12189
Attn: G. D'Andrea

Department of the Army
Watertown Arsenal
Watertown, MA 02172
Attn: A. Thomas

ORIGINAL PAGE IS
OF POOR QUALITY

Department of the Army
Redstone Arsenal
Huntsville, AL 35809
Attn: R. J. Thompson, AMSMI-RSS

Department of the Navy
Naval Ordnance Laboratory
White Oak
Silver Spring, MD 20910
Attn: R. Simon

Department of the Navy
U.S. Naval Ship R&D Laboratory
Annapolis, MD 21402
Attn: C. Hersner, Code 2724

Director
Deep Submergence Systems Project
6900 Wisconsin Avenue
Washington DC 20015
Attn: H. Bernstein, DSSP-221

Director
Naval Research Laboratory
Washington DC 20390
Attn: Code 8430
I. Wolock, Code 8433

Drexel University
32nd and Chestnut Streets
Philadelphia, PA 19104
Attn: P. C. Chou

E. I. DuPont DeNemours & Co.
DuPont Experimental Station
Wilmington, DE 19898
Attn: D. L. G. Sturgeon

Fiber Science, Inc.
245 East 157 Street
Gardena, CA 90248
Attn: E. Dunahoo

General Dynamics
P.O. Box 748
Ft. Worth, TX 76100
Attn: D. J. Wilkins
Library

General Dynamics/Convair
P.O. Box 1128
San Diego, CA 92112
Attn: J. L. Christian
R. Adsit

ORIGINAL PAGE IS
OF POOR QUALITY

General Electric Co.
Ervendale, OH 45215
Attn: C. Stotler
R. Ravenhall

General Motors Corporation
Detroit Diesel-Alison Division
Indianapolis, IN 46244
Attn: M. Herman

Georgia Institute of Technology
School of Aerospace Engineering
Atlanta, GA 30332
Attn: L. W. Rehfield

Grumman Aerospace Corporation
Bethpage, Long Island, NY 11714
Attn: S. Dastin
J. B. Whiteside

Hamilton Standard Division
United Aircraft Corporation
Windsor Locks, CT 06096
Attn: W. A. Percival

Hercules, Inc.
Allegheny Ballistics Laboratory
P. O. Box 210
Cumberland, MD 21053
Attn: A. A. Vicario

Hughes Aircraft Company
Culver City, CA 90230
Attn: A. Knoell

Illinois Institute of Technology
10 West 32 Street
Chicago, IL 60616
Attn: L. J. Broutman
I. M. Daniel

Dr. Joseph Wolf, Engineering Mechanics Dept.
General Motors Research Labs.
256 Research Drive
Warren, MI 48090

Jet Propulsion Laboratory
4800 Oak Grove Drive
Pasadena, CA 91103
Attn: Library

Lawrence Livermore Laboratory
P.O. Box 808, L-421
Livermore, CA 94550
Attn: T. T. Chiao
E. M. Wu

ORIGINAL PAGE IS
OF POOR QUALITY

Lehigh University
Institute of Fracture &
Solid Mechanics
Bethlehem, PA 18015
Attn: G. C. Sih

Lockheed Georgia Co.
Advanced Composites Information Center
Dept. 72-14, Zone 402
Marietta, GA 30060
Attn: T. M. Hsu

Lockheed Missiles and Space Co.
P.O. Box 504
Sunnyvale, CA 94087
Attn: R. W. Fenn

Lockheed-California
Burbank, CA 91503
Attn: J. T. Ryder
K. N. Lauraitis
J. C. Ekvall

McDonnell Douglas Aircraft Corporation
P.O. Box 516
Lambert Field, MS 63166
Attn: J. C. Watson

McDonnell Douglas Aircraft Corporation
3855 Lakewood Blvd.
Long Beach, CA 90810
Attn: L. B. Greszczuk

Material Sciences Corporation
1777 Walton Road
Blue Bell, PA 19422
Attn: B. W. Rosen

Massachusetts Institute of Technology
Cambridge, MA 02139
Attn: F. J. McGarry
J. F. Mandell
J. W. Mar

NASA-Ames Research Center
Moffett Field, CA 94035
Attn: Dr. J. Parker
Library

NASA-Flight Research Center
P.O. Box 273
Edwards, CA 93523
Attn: Library

ORIGINAL FILE,
OF POOR QUALITY

NASA-George C. Marshall Space Flight Center
Huntsville, AL 35812
Attn: C. E. Cataldo, S&E-ASTN-MX
Library

NASA-Goddard Space Flight Center
Greenbelt, MD 20771
Attn: Library

NASA-Langley Research Center
Hampton, VA 23365
Attn: J. H. Starnes

J. G. Davis, Jr.
M. C. Card

J. R. Davidson

NASA-Lewis Research Center
21000 Brookpark Road, Cleveland, OH 44135

Attn: Contracting Officer, MS 501-11
Tech. Report Control, MS 5-5
Tech. Utilization, MS 3-16
AFSC Liaison, MS 501-3
S&MTD Contract Files, MS 49-6
L. Berke, MS 49-6
N. T. Saunders, MS 49-1
R. F. Lark, MS 49-6
J. A. Ziemianski, MS 49-6
R. H. Johns, MS 49-6
C. C. Chamis, MS 49-6 (4 copies)
R. L. Thompson, MS 49-6
T. T. Serafini, MS 49-1
Library, MS 60-3 (2 copies)

NASA-Lyndon B. Johnson Space Center
Houston, TX 77001
Attn: S. Glorioso, SMD-ES52
Library

NASA Scientific and Tech. Information Facility
P.O. Box 8757
Balt/Wash International Airport, MD 21240
Attn: Acquisitions Branch (10 copies)

National Aeronautics & Space Administration
Office of Advanced Research & Technology
Washington DC 20546

Attn: L. Harris, Code RTM-5
M. Greenfield, Code RTM-6
C. Bersch, Code RTM-6

National Aeronautics & Space Administration
Office of Technology Utilization
Washington DC 20546

ORIGINAL PAGE IS
OF POOR QUALITY

National Bureau of Standards
Eng. Mech. Section
Washington DC 20234
Attn: R. Mitchell

National Science Foundation
Engineering Division
1800 G. Street, NW
Washington DC 20540
Attn: Library

Northrop Corporation Aircraft Group
3901 West Broadway
Hawthorne, CA 90250
Attn: R. M. Verette
G. C. Grimes

Pratt & Whitney Aircraft
East Hartford, CT 06108
Attn: J. M. Woodward

Raytheon Co., Missile System Division
Mechanical Systems Laboratory
Bedford, MA
Attn: P. R. Digiovanni

Rensselaer Polytechnic Institute
Troy, NY 12181
Attn: R. Loewy

Rockwell International
Los Angeles Division
International Airport
Los Angles, CA 90009
Attn: L. M. Lackman
D. Y. Konishi

Sikorsky Aircraft Division
United Aircraft Corporation
Stratford, CT 06602
Attn: Library

Southern Methodist University
Dallas, TX 75275
Attn: R. M. Jones

Space & Missile Systems Organization
Air Force Unit Post Office
Los Angeles, CA 90045
Attn: Technical Data Center

Structural Composites Industries, Inc.
6344 N. Irwindale Avenue
Azusa, CA 91702
Attn: R. Gordon

ORIGINAL PAGE IS
OF POOR QUALITY

Texas A&M
Mechanics & Materials Research Center
College Station, TX 77843
Attn: R. A. Schapery
Y. Weitsman
TRW, Inc.
23555 Euclid Avenue
Cleveland, OH 44117
Attn: I. J. Toth

Union Carbide Corporation
P. O. Box 6116
Cleveland, OH 44101
Attn: J. C. Bowman

United Technologies Research Center
East Hartford, CT 06108
Attn: R. C. Novak
Dr. A. Dennis

University of Dayton Research Institute
Dayton, OH 45409
Attn: R. W. Kim

University of Delaware
Mechanical & Aerospace Engineering
Newark, DE 19711
Attn: B. R. Pipes

University of Illinois
Department of Theoretical & Applied Mechanics
Urbana, IL 61801
Attn: S. S. Wang

University of Oklahoma
School of Aerospace Mechanical & Nuclear Engineering
Norman, OK 73069
Attn: C. W. Bert

University of Wyoming
College of Engineering
University Station Box 3295
Laramie, WY 82071
Attn: D. F. Adams

U. S. Army Materials & Mechanics Research Center
Watertown Arsenal
Watertown, MA 02172
Attn: E. M. Lence
D. W. Oplinger

V.P. I. and S. U.
Dept. of Eng. Mech.
Blacksburg, VA 24061
Attn: R. H. Heller
H. J. Brinson
C. T. Herakovich
K. L. Reifsnider

ORIGINAL PAGE IS
OF POOR QUALITY